Pathological Lymphangiogenesis Is Regulated by Galectin-8-Dependent Crosstalk among VEGF-C, Podoplanin and Integrin Pathways

A dissertation

submitted by

Wei-Sheng Chen

In partial fulfillment of the requirements

for the degree of

Doctor of Philosophy

In

Cell, Molecular and Developmental Biology

TUFTS UNIVERSITY

Sackler School of Graduate Biomedical Sciences

July, 2015

Advisor: Prof. Noorjahan Panjwani

Abstract

Galectin expression patterns: Although members of the galectin family of carbohydrate-binding proteins are thought to play a role in the immune response and regulation of allograft survival, little is known about the galectin expression signature in diseased corneas. In this study, we compare the galectin expression pattern in normal, chemically injured, *Pseudomonas aeruginosa*-infected, and allograft rejected or accepted mouse corneas.

In normal corneas, galectins-1, -3, -7, -8 and -9 were expressed in normal corneas. Galectin-1 was distributed mainly in the stroma, galectin-3 was localized mainly in epithelium, and galectins-7, -8 and -9 were detected in both corneal epithelium and stroma. Expression levels of the five galectins were drastically altered under pathological conditions. In both infected and cauterized corneas, overall galectin-3 expression was downregulated, whereas overall galectins-8 and -9 were upregulated. Changes in the expression level of galectins-7, -8 and -9 were distinct in the epithelium of infected and cauterized corneas. Expression of these three galectins was upregulated in corneal epithelium of infected corneas but not in cauterized corneas. Consistent with the changes in protein expression: (i) galectins-7, -8 and -9 mRNA expression was upregulated in cauterized corneas and (ii) galectin-3 mRNA was downregulated and galectin-9 mRNA expression was upregulated in infected corneas.

Although in both accepted and rejected grafts, expression levels of the five galectins were upregulated compared to normal corneas, there were distinct differences in the expression levels of galectins-8 and -9 between accepted and

rejected grafts, as both Western blot and immunofluorescence staining revealed galectin-8 is upregulated, whereas galectin-9 is downregulated in rejected grafts compared to accepted grafts.

Our data demonstrate differential regulation of various members of the galectin family in the course of corneal infection, neovascularization and allograft acceptance/rejection. The emerging functionality of the sugar code of cell surface receptors via endogenous galectins reflect to the pertinent roles of the five tested galectins in the diseases of cornea.

Role of galectin-8 in lymphangiogenesis: Lymphangiogenesis is associated with diverse pathological conditions including metastatic dissemination, graft rejection, type 2 diabetes, obesity, hypertension, lymphedema and glaucoma. Despite recent studies have demonstrated that the members of the galectin family play a critical role in hemangiogenesis, the role of galectins in lymphangiogenesis has not been elucidated. In vitro studies have shown that galectin-8 binds podoplanin and that the lectin promotes haptotaxis of lymphatic endothelial cells (LECs). However, the evidence that galectin-8 exerts its biological functions through podoplanin is lacking.

Here, we demonstrate for the first time that a carbohydrate-binding protein, galectin-8, is a potent lymphangiogenic factor. Galectin-8 was markedly upregulated in inflamed human and mouse corneas, and inhibitors of galectin-8 reduced inflammatory lymphangiogenesis. In corneal micropocket assays and 3D sprouting assays, galectin-8 promoted lymphangiogenesis in a carbohydrate-

dependent manner. Galectin-8 was identified as a key mediator of integrin-dependent crosstalk between VEGF-C (vascular endothelial growth factor-C) and podoplanin lymphangiogenic pathways. Galectin-8 inhibitors reduced VEGF-C-induced lymphangiogenesis. Conversely, exogenous galectin-8 markedly enhanced VEGF-C-induced lymphangiogenesis in a carbohydrate-dependent manner. Knockdown of podoplanin attenuated not only galectin-8 but also VEGF-C-mediated LEC sprouting. Also, in corneal micropocket assays, VEGF-C-induced lymphangiogenesis was significantly reduced in the galectin-8$^{-/-}$ and podoplanin$^{-/-}$ mice; likewise, galectin-8-induced lymphangiogenesis was reduced in podoplanin$^{-/-}$ mice. Interestingly, knockdown of VEGFR-3 did not affect galectin-8-mediated LEC sprouting. Instead, inhibiting integrins α1β1 and α5β1 curtailed both galectin-8- and VEGF-C-mediated LEC sprouting. Additionally, podoplanin knockdown in LECs interfered with integrin activation. Immunoprecipitation assays further confirmed galectin-8-dependent interactions between podoplanin and integrins α5 and β1. In summary, this study has uncovered a unique lymphangiogenic pathway in which galectin-8-mediated interactions between podoplanin and integrins α1β1/α5β1 play a key role.

Acknowledgements

I would like to express my sincere gratitude to Prof. Noorjahan Panjwani for her great mentorship throughout this dissertation journey. I also thank members of the Panjwani lab, especially Dr. Zhiyi Cao.

I am thankful to my thesis committee members, Drs. Peter Brooks, Lucy Liaw, and John Castellot, for your time and constructive advice. I also want to thank my outside examiners, Drs. Pedram Hamrah and Pablo Argueso, for your criticism and advice.

Finally I want to thank my family and friends for providing great support throughout this journey.

Tables of Contents

Introduction Page

1.1 Lymphatic system and diseases. …… 1

1.2 Key molecules that regulate lymphangiogenesis. …… 13

1.3 Galectins: classification and functions. …… 20

1.4 Galectin-8: expression pattern. …… 22

1.5 Galectin-8: binding partners. …… 23

1.6 Galectin-8: role in angiogenesis. …… 25

1.7 Objectives of the dissertation. …… 26

Materials and Methods

2.1 Expression and purification of recombinant galectins. …… 28

2.2 Quantitative RT-PCR. …… 38

2.3 Immunofluorescence staining. …… 39

2.4 Corneal mouse micropocket lymphangiogenesis assay. …… 39

2.5 Mouse model of suture-induced inflammatory corneal lymphangiogenesis. …… 41

2.6 Knockdown with siRNA. …… 41

2.7 Lymphatic endothelial cell (LEC) sprouting assay. …… 42

2.8 Affinity precipitation assay. …… 43

2.9 Western blot analysis. …… 44

2.10 LEC chemotaxis assay. …… 47

2.11 LEC haptotaxis assay. …… 47

2.12 Immunoprecipitation assay. …… 48

2.13 Glycosidase treatment. …… 49

2.14 Mice. …… 50

2.15 X-gal staining. …… 50

Results

3.1 Galectin expression pattern in control and inflamed corneas. …… 55

3.2 Galectin-8 promotes lymphangiogenesis in a carbohydrate-

dependent manner. …… 86
3.3 Galectin-8 modulates VEGF-C-induced lymphangiogenesis. …... 97
3.4 Galectin-8 deficiency ameliorates inflammatory lymphangiogenesis. ……..... 101
3.5 VEGF-C binding receptors play little role on galectin-8-induced lymphangiogenesis. ……...105
3.6 Galectin-8 and VEGF-C-induced lymphangiogenesis is dependent on podoplanin. ……...111
3.7 Integrins play a key role in galectin-8-mediated lymphangiogenesis. ……...119
3.8 Galectin-8 inhibitors significantly decrease inflammatory lymphangiogenesis in vivo. ……..…..129

Discussion

4.1 Galectins as PAMPs and DAMPs in corneas. ……..132
4.2 Gal-8N as a dominant negative inhibitor for galectin-8. ……..135
4.3 The interplay among galectin-8, integrins and VEGFR-3. ……..135

Future Directions

5.1 Role of macrophages in galectin-8-mediated lymphangiogenesis. ……..144
5.2 Targeting galectin-8 to treat inflammatory diseases. ……..145

References ……..150

List of Figures

Figure 1. Generation of *Pdpn* floxed and globally inducible *Pdpn*-deficient mice, and confirmation of *Pdpn* null status in corneas. (P. 52)

Figure 2. Galectin-8 knockout construct and confirmation of galectin-8 null status of the knockout mice. (P. 54)

Figure 3. Analysis of galectin expression of normal and P. aeruginosa-infected mouse corneas by Western blot. (P. 65)

Figure 4. Immunofluorescence localization of galectins in normal and P. aeruginosa-infected mouse corneas. (P. 66)

Figure 5. Galectin expression in corneal epithelium and stroma in normal and P. aeruginosa-infected eyes on day 8 pi. (P. 68)

Figure 6. Analysis of mRNA expression levels of galectins in normal and P. aeruginosa-infected corneas by qRT-PCR. (P. 69)

Figure 7. Analysis of galectin expression of normal and cauterized mouse corneas by Western blot. (P. 70)

Figure 8. Immunofluorescence localization of galectins in normal and cauterized mouse corneas. (P. 71)

Figure 9. Galectin expression in corneal epithelium and stroma in normal and cauterized mouse eyes on day 7 post injury. (P. 72)

Figure 10. Analysis of mRNA expression levels of galectins in normal and cauterized mouse corneas by qRT-PCR. (P. 73)

Figure 11. Analysis of galectin expression of normal mouse corneas and mouse corneas with rejected and accepted allografts by Western blot. (P. 74)

Figure 12. Immunofluorescence localization of galectins in normal mouse corneas and mouse corneas with rejected and accepted allografts. (P. 75)

Figure 13. Immunohistochemical localization of galectin-8 in normal and inflamed human corneas. (P. 77)

Figure 14. Immunofluorescence localization of galecin-8 in extracellular matrix and blood/lymphatic vessels in mouse corneas. (P. 78)

Figure 15. Immunofluorescence localization of galecin-8 in infiltrated immune cells in inflamed mouse corneas. (P. 80)

Figure 16. X-gal staining in control and cauterized mouse corneas of galectin-8 KO mice. (P. 82)

Figure 17. Immunofluorescence localization of bacterial β-galactosidase in cauterized mouse corneas of galectin-8 KO mice. (P. 83)

Figure 18. Immunolocalization of galectin-8 using anti-galectin-8 (clone H-80) antibody. (P. 85)

Figure 19. Galectin-8 promotes lymphangiogenesis in vivo in a micropocket assay. (P. 90)

Figure 20. Galectin-8 promotes lymphangiogenesis in vitro in a dose-dependent manner. (P. 91)

Figure 21. Galectin-8 promotes lymphangiogenesis in vitro by recognition of sialylated glycans. (P. 92)

Figure 22. Kinetic characteristics of inhibitory effect of 3'-SL on galectin-8-mediated LEC sprouting. (P. 93)

Figure 23. Gal-8N inhibits galectin-8-mediated LEC sprouting. (P. 94)

Figure 24. Kinetic characteristics of inhibitory effect of Gal-8N on galectin-8-mediated LEC sprouting. (P. 95)

Figure 25. Galectin-8 promotes lymphangiogenesis through AKT and ERK signaling pathways. (P. 96)

Figure 26. Galectin-8 potentiates VEGF-C-induced lymphangiogenesis in vitro. (P. 98)

Figure 27. Galectin-8 potentiates VEGF-C-induced lymphangiogenesis in vivo. (P. 99)

Figure 28. Galectin-8 inhibitors attenuates VEGF-C-induced LEC sprouting. (P. 100)

Figure 29. Galectin-8 deficiency attenuates VEGF-C-induced lymphangiogenesis in vivo. (P. 102)

Figure 30. Galectin-8 deficiency attenuates suture-induced lymphangiogenesis in vivo. (P. 103)

Figure 31. Galectin-8 deficiency attenuates cautery-induced lymphangiogenesis in vivo. (P. 104)

Figure 32. Galectin-8 binds to VEGFR-3 but not VEGF-C or VEGFR-1. (P. 106)

Figure 33. Galectin-8 clusters VEGFR-3 on cell surface. (P. 107)

Figure 34. Galectin-8 retains VEGFR-3 on cell surface. (P. 108)

Figure 35. VEGFR-3 is dispensable for galectin-8-mediated lymphangiogenesis in vitro. (P. 109)

Figure 36. Neuropilin-2 is dispensable for galectin-8-mediated lymphangiogenesis in vitro. (P. 110)

Figure 37. Galectin-8 binds to PDPN in LECs. (P. 113)

Figure 38. Galectin-8 interacts with the α2,3-sialyl glycans of VEGFR-3, PDPN and integrins. (P. 114)

Figure 39. PDPN is required for galectin-8-mediated LEC sprouting. (P. 115)

Figure 40. PDPN knockdown interferes with galectin-8- and VEGF-C-mediated signal. (P. 116)

Figure 41. PDPN is required for VEGF-C-induced lymphangiogenesis in vivo. (P. 117)

Figure 42. PDPN is required for galectin-8-induced lymphangiogenesis in vivo. (P. 118)

Figure 43. Inhibiting integrins α1β1 and α5β1 attenuates both VEGF-C- and galectin-8-mediated LEC sprouting. (P. 122)

Figure 44. Knockdown and functional blocking of PDPN inhibit fibronectin-mediated LEC migration. (P. 123)

Figure 45. Galectin-8 treatment clusters PDPN and integrin β1. (P. 124)

Figure 46. Galectin-8 treatment retains PDPN on cell surface. (P. 126)

Figure 47. PDPN interacts with integrins in a galectin-8-dependent manner. (P. 127)

Figure 48. Knockdown of PDPN impedes extracellular matrix-induced signal. (P. 128)

Figure 49. TDG and Gal-8N inhibit suture-induced lymphangiogenesis. (P. 130)

Figure 50. TDG and Gal-8N inhibit cautery-induced lymphangiogenesis. (P. 131)

Figure 51. Proposed models of galectin-8-mediated lymphangiogenesis. (P. 141)

Figure 52. Macrophage depletion attenuates galectin-8-mediated lymphangiogenesis. (P. 148)

Figure 53. Galectin-8 transdifferentiates macrophages to lymphatic cell-like cells. (P. 149)

List of Abbreviations

Ab	Antibody
AgNO3	Silver nitrate
ANOVA	Analysis of variance
Arg	arginine
bFGF	Basic fibroblast growth factor
BSA	Bovine serum albumin
BV	Blood vessel
CB	Calbindin
CCBE1	Collagen and calcium-binding EGF domain-containing protein 1
CCL	CC chemokine ligands
CCR	CC chemokine receptors
C-CRD	carboxyl-terminal carbohydrate recognition domain
cDNA	complementary DNA
CHO	Chinese hamster ovary
CR	calretinin
CRD	carbohydrate recognition domain
CXCL	chemokine (C-X-C motif) ligand
DAMP	damage-associated molecular patterns
DAPI	4',6-diamidino-2-phenylindole
DNase I	Deoxyribonuclease I
EC	Endothelial cell
EDTA	Ethylenediaminetetraacetic acid
EGF	Epidermal growth factor
EGFP	Enhanced Green Fluorescent Protein
ENA-78	Epithelial-neutrophil activating peptid
Epi	Epithelium
ERK	Extracellular signal-regulated kinases
FAK	Focal Adhesion Kinase
FOXC2	Forkhead box protein C2
Gal	Galectin
Gal-8N	N-CRD of galectin-8
GAPDH	Glyceraldehyde 3-phosphate dehydrogenase
GATA2	GATA binding protein 2
GJC2	Gap junction gamma-2
Gln	Glutamine
GM-CSF	Granulocyte macrophage colony-stimulating factor
GRIFIN	galectin-related inter-fiber protein
GRO-α	Growth-regulated oncogene α
GST	growth related oncogene-alpha
H&E	Hematoxylin and eosin
HDL	High-density lipoprotein

HMG-coA	3-hydroxy-3-methylglutaryl-coenzyme A
HSV	Herpes simplex virus
ICAM-1	Intercellular Adhesion Molecule 1
IgG	Immunoglobulin G
IL	Interleukin
INF-γ	Interferon gamma
IOP	Intraocular pressure
IR	Infrared
K14	keratin-14
Kd	Dissociation constant
Ki	Inhibition constant
KO	Knock out
LAL	Limulus Amebocyte Lysate
LDL	Low-density lipoprotein
LEC	Lymphatic endothelial cell
LPS	Lipopolysaccharide
LV	Lymphatic vessel
LYVE-1	lymphatic vessel endothelial hyaluronan receptor-1
MAA II	Maackia amurensis lectin II
MCP-1	Monocyte chemoattractant protein-1
MDSC	Myeloid-derived suppressor cell
MEK	Mitogen-activated protein kinase kinase
MEM	Minimum essential medium
MFI	Mean fluorescence intensity
MgCl2	Magnesium chloride
MMP	Matrix metalloproteinase
mRNA	Messenger RNA
NaCl	Sodium chloride
N-CRD	Amino terminal carbohyrate recognition domain
nH	Hill coefficient
NK cells	Natural killer cells
Nrp2	Neuropilin 2
OBB	Odyssey® blocking buffer
PAMP	pathogen-associated molecular patterns
PAS	Periodic acid Schiff
PBS	Phosphate buffered saline
PCTA-1	Prostate carcinoma tumor antigen 1
PDPN	Podoplanin
PI3K	Phosphoinositide 3-kinase
pi	Post infection
PKC-α	Protein kinase C alpha
PNGase F	Peptide -N-Glycosidase F
Prox1	Prospero homeobox protein 1

PTPN11	Tyrosine-protein phosphatase non-receptor type 11
qRT-PCR	Real-time reverse transcription-polymerase chain reaction
RAAS	Renin−angiotensin−aldosterone system
RAGE	Receptor of advanced glycation endproducts
RANTES	Regulated on activation, normal T cell expressed and secreted
RGD	Arginylglycylaspartic acid
SC	Schlemm's canal
SDS-PAGE	Sodium dodecyl sulphate-polyacrylamide gel electrophoresis
SEM	Standard error of the mean
siRNA	Small interfering RNA
SL	Sialyl lactose
Str	Stroma
TDG	Thiodigalactoside
TGF-β1	Transforming growth factor beta 1
Th1	T helper type 1
Th17	T helper type 17
TM	Trabecular meshwork
TNFα	Tumor necrosis factor alpha
Tris-HCl	Tris(hydroxymethyl)aminomethane hydrochloride
uPAR	Urokinase-type plasminogen activator receptor
VEGF-C	Vascular endothelial growth factor-C
VEGFR	Vascular endothelial growth factor receptor
WT	Wild type
X-gal	5-bromo-4-chloro-3-indolyl-β-D-galactopyranoside
α2-3 NA	α2-3 Neuraminidase
β-gal	Beta-galactosidase

Introduction

1.1 Lymphatic system and diseases.

The human body has two major circulatory systems: the blood and lymphatic systems. The adult lymphatic system comprises the lymphatic vessels and lymphoid organs such as lymph nodes and mucosal-associated lymphoid tissue (MALT) (tonsils, Peyer's patches, and lymphoid tissues associated to the bronchial and nasal system). Unlike blood vascular system that has been intensively studied, until recently, lymphatic system was considered less important, invisible, and thus largely neglected by scientists and clinicians. Only in recent years, subsequent to the identification of lymphatic-specific markers, it is becoming increasingly clear that lymphatic system does not just serve as passive conduits for interstitial fluid and cells, but is actively involved in the pathogenesis of numerous diseases.

The lymphatic system has three major functions: (1) preservation of fluid balance by restoring interstitial fluid to the cardiovascular system; (2) a nutritional function, as lacteal lymphatic vessels inside the intestinal villi in the digestive tract absorb and transport fat-soluble vitamins and dietary fat; (3) an important part of immune surveillance by carrying antigen presenting cells to prime B and T cells in the lymph nodes. Considering the importance of lymphatic system for normal body functions, it is not surprising that defects of the lymphatic system are implicated in several human diseases including, but are not limited to, lymphedema, tumor metastasis, cardiovascular diseases (myocardial infarction,

hypercholesterolemia, and hypertension), inflammation and immunity, obesity, glaucoma, dry eye disease, and allergic eye disease.

Lymphedema. Lymphatic vascular insufficiency due to developmental lymphatic vascular abnormalities, injury, obstruction or infection results in the accumulation of interstitial fluid and protein in affected tissues—a situation known as lymphedema. Primary or inherited lymphedema syndromes are characterized by gene mutations in *VEGFR-3, FOXC2, PTPN11, GATA2, GJC2, SOX18, CCBE1*, *VEGF-C*, etc.[1,2] The estimated prevalence of primary lymphedema is 1.15 in 100,000 persons under the age of 20.[3] In children, the two main causes are Milroy disease and lymphedema distichiasis.[4]

However, secondary or acquired lymphedema syndromes are the most prevalent form of lymphedema. In tropical countries, more than 120 million people suffer lymphedema due to lymphatic filariasis, commonly known as elephantiasis, which is caused by infection with the mosquito-borne parasites *Wuchereria bancrofti* (which accounts for ~90% of the cases), *Brugia malayi* (which causes most of the rest of the cases), and *B. timori* (http://www.who.int/mediacentre/factsheets/fs102/en/). Treatment with drugs targeting the microfilariae (larval offspring) has been the main approach to treat this disease.

In contrast to the abundance of filariasis-mediated secondary lymphedema in tropical areas, the leading cause of secondary lymphedema in the industrialized world is axillary lymph node excision and radiotherapy that

damages the lymphatic system after breast cancer surgery. About 25% of the patients after receiving the treatment suffer from the secondary lymphedema.[5,6] Unfortunately, there is no cure currently and treatment for the early-stage lymphedema is still based mainly on conservative therapies such as manual drainage, massage, compression garments, and dietary modification (i.e., limiting the consumption of long-chain fatty acids).

Tumor metastasis. Tumor metastases are a leading cause of cancer-related deaths. Lymphatic vessels provide a route for tumor cells to metastasize. Lymphangiogenesis around primary tumors is strongly correlated with lymph node and distant metastases;[7-9] however, intratumoral lymphatic vessels have been considered poorly functional due to high intratumoral pressure.[10,11] Regardless, lymphangiogenesis occurs not only within or around primary tumors, but also in draining lymph nodes (also known as sentinel lymph node lymphangiogenesis).[12-14] The sentinel lymph node lymphangiogenesis occurs "before" tumor metastasis and has been shown to facilitate tumor metastasis by creating a niche for tumor cells.[15]

Lymphatic vessels are not just conduits for tumor cells to metastasize. Accumulating evidence indicates that lymphatic vessels actively interact with tumor cells. Activated lymphatic endothelial cells secrete CCL21 and CXCL12 (stromal-derived factor-1) cytokines to promote tumor cells that express the cognate receptors CCR7 (receptor for CCL21) and CXCR4 (receptor for CXCL12) to migrate toward the lymphatic vessels.[16-19] Disrupting the cytokine−cytokine

receptor axis in conjunction with anti-lymphangiogenesis therapies may have great potential for the development of clinical anti-metastasis therapy.

Cardiovascular diseases. Cardiovascular disease is a class of diseases that involve the heart or blood vessels. Common cardiovascular diseases include ischemic heart disease or coronary artery disease (e.g. heart attack, or myocardial infarction), cerebrovascular disease (e.g. stroke), disease of the aorta and arteries (e.g. peripheral vascular disease), congenital heart disease, rheumatic heart disease, cardiomyopathies, cardiac arrhythmias, etc. Pathogenesis of cardiovascular diseases varies, many of which (the first three conditions) involve a process called atherosclerosis. Atherosclerosis is an inflammatory process affecting the artery walls in which fatty material, cholesterol and inflammatory cells are accumulated. In 2008, out of the 17.3 million cardiovascular deaths, atherosclerosis-related cardiovascular diseases are responsible for over 75% of the deaths; heart attacks account for 7.3 million deaths and strokes account for 6.2 million deaths.[20] There are many risk factors for the development of atherosclerosis, including hypertension, alcohol use, unhealthy diet, diabetes, raised blood lipids (hypercholesterolemia), obesity, genetic disposition and aging. Decreasing the changeable risk factors (life style, diet, blood pressure, blood sugar, blood lipids/lipoproteins, etc.) is estimated to prevent ~90% of cardiovascular diseases.[21]

The emerging concept of the role of lymphatic vessels in cardiovascular diseases is that lymphatic vessels regulate lipoprotein metabolism and play a key

role in resolving atherosclerosis. Atherosclerosis is thought to be initiated by accumulation of cholesterol in and around macrophages in vessel walls by low-density lipoprotein (LDL) that delivers cholesterol in an unregulated manner. Removal of cholesterol, which is largely stored in macrophages, from the vessel walls is a key step to regress atherosclerosis.[22] Removal of cholesterol from peripheral tissues back to the liver, or reverse cholesterol transport, is a multi-step process involving high-density lipoproteins (HDLs). In 2013, Martel and colleagues[23] identified that lymphatic vessels mediate the reverse cholesterol transport by transporting the unesterified cholesterol- and phospholipid-loaded discoidal HDLs in lymph. (The discoidal HDLs are converted from the small, lipid-poor apoA1-containing preβ-HDLs in the interstitial fluid via ABCA1 and ABCG1 transporters of peripheral cells). In human samples, lymphatic vessels are observed within the intima of advanced atherosclerotic plaques.[24] In mouse models of atherosclerosis, disrupting the lymphatic vessels impairs reverse cholesterol transport, elevates plasma cholesterol and promotes atherogenesis.[23,25] Collectively, these studies highlight the importance of lymphatic vessels in the process of atherosclerosis.

Lymphatic vessels have also been demonstrated to play a vital role in regulating hypertension, another risk factor for cardiovascular diseases. The link between high-salt intake and increased blood pressure has been well-established.[26,27] Other than changing lifestyle (e.g. reducing salt intake), many medications target the renin−angiotensin−aldosterone system (RAAS), a hormone system that regulates blood pressure and fluid balance. Over-activated

RAAS results in reduced renal Na^+ excretion, extracellular volume expansion, augmented blood flow, increased systemic vascular resistance, and ultimately hypertension.[28] While this concept is well-accepted, the Titze group proposed an alternative thinking about the regulation of salt retention.[29,30] They observed that salt is primarily stored in the skin interstitium by non-osmotical binding to glycosaminoglycans.[31] The salt storage is dynamic and tightly regulated by monocyte phagocyitc system cells/macrophages and subcutaneous lymphatic vessels.[29,30] Compared to low-salt diet, high-salt diet markedly increases subcutaneous lymphangiogenesis, as the increased interstitial tonicity activates TonEBP (tonicity-responsive enhancer binding protein) of macrophages to generate and secrete more VEGF-C subcutaneously. Depleting the subcutaneous macrophages or blockade of VEGF-C results in faulty salt clearance from skin and salt-sensitive hypertension.[32,33] They also found that hypertensive patients exhibit high levels of Na^+ in the skin as determined by ^{23}Na magnetic resonance imaging.[34] These results suggest that patients with salt-sensitive hypertension may have defective subcutaneous lymphatic vessels and/or macrophages, which may be novel therapeutic targets for hypertension treatment.

In a mouse model of myocardial infarction by permanent ligation of the left descending artery, the ischemic injury markedly increases lymphangiogenesis in the heart.[35] In addition, promoting lymphangiogenesis by administration of recombinant VEGF-C(C156S), which is specific for VEGFR-3 but no other VEGFRs, markedly improves cardiac function post myocardial infarction.[35]

Therefore, increasing lymphangiogenesis in the injured/ischemic heart may be a novel approach to treat myocardial infarction in clinic in the future.

Inflammation and immunity. Inflammation is the normal biological response of tissues to harmful stimuli such as injury, infection, or tumors. Although it is well known that the blood vasculature is an important regulator of the inflammatory process, the role of the lymphatic network in this process is becoming better understood. Upon initiation of inflammation, the lymphatic system is activated and robust lymphangiogenesis occurs not only at peripheral tissues but also inside lymph nodes in response to inflammatory stimuli.[36] In addition, lymphatic vessels as well as blood vessels undergo extensive remodeling during inflammation (e.g. graft rejection, diabetes, asthma, pulmonary disease, rheumatoid arthritis, and inflammatory bowel disease). In recent years, several lines of evidence suggest that inflammation-associated lymphangiogenesis is not just an endpoint phenotype of inflammation, but rather a dynamic and context-dependent reaction that can change the natural course of the inflammatory process and/or tissue repair.[37,38]

In general, activated immune cells such as dendritic cells and macrophages generate high levels of prolymphangiogenic factors to promote lymphangiogenesis. The resulting lymphatic vessels produce chemokines (e.g. CCL21) to attract immune cells (e.g. $CCR7^+$ cells), have enhanced flow of lymph that contains soluble antigens, and facilitate migration of activated antigen-presenting cells. These antigen presenting cells migrate toward lymph nodes

where they prime T and B cells. The primed T and B cells undergo clonal expansion and migrate back to the sites of inflammation via blood vessels.[37]

Therapeutic modulation of inflammatory lymphangiogenesis should be intervened based on the context of inflammation. On the one hand, inhibiting inflammatory lymphangiogenesis helps resolve the pathological conditions in transplantation rejection, diabetes (streptozotocin-induced type II diabetes), herpes simplex virus-1-induced keratitis, etc.[39-42] On the other hand, blocking lymphangiogenesis aggravates inflammation in inflammatory bowel diseases, sterile inflammation mediated by lipopolysaccharide and lipoteichoic acid, chronic airway inflammation, and rheumatoid arthritis;[43-46] therefore, promoting lymphangiogenesis should be introduced in these conditions.

Obesity. Patients with end-stage, pronounced, non-pitting lymphedema are often non-responsive to conservative treatment because of fibrosis and accumulation of adipose tissue, or so-called “wet fat”. Therefore, circumferential suction-assisted lipectomy (liposuction) is now the most commonly performed excisional procedure for the treatment of lymphedema, as it is a less invasive method of removing subcutaneous fat and is associated with fewer complications.[47-49]

Adipose tissue accumulation in mouse models of lymphatic vascular dysfunction has been reported. A Chy mouse mutant characterized by the accumulation of chylous ascites into the abdomen and swelling of the limbs, is a naturally occurring mouse model of primary lymphedema due to heterozygous inactivating mutations in VEGFR-3, and resembles Milroy’s disease (a primary

human lymphedema).[50] The Chy mice have defective lymphatic vessels, and display dermal thickening and adipose tissue accumulation in the edematous subcutaneous adipose layer.[50] While the mechanism of adipose tissue accumulation due to lymphatic vascular dysfunction was not determined in Chy mice, insights into a potential mechanism were recently discovered in mice haploinsufficient for *Prox1*,[51] a gene encoding a homeobox transcription factor crucial for the specification of lymphatic endothelial cell fate.[52] Although many *Prox1*$^{+/-}$ mice die soon after birth, the surviving *Prox1*$^{+/-}$ mice appear grossly normal but have subtle defects in lymphatic endothelial integrity and lymphatic vessel patterning. As the mice aged, they become progressively obese.[51] Notably, the extent of fat deposition correlates with increased leakage of lymph into the surrounding tissues. In conjunction with in vitro assays, the authors concluded that adult onset obesity in the *Prox1*$^{+/-}$ mice is directly related to the adipogenic effects of the lymph.[51,53] Although the factors in the lymph that cause adipogenesis have not been identified, a recent study that analyzed gene expression pattern in human adipose-derived stem cells demonstrated that lymphedema-associated adipose-derived stem cells have stronger adipogenic differentiation potential but lower angiogenic capacity compared to control adipose-derived stem cells from patients undergoing cosmetic procedures.[54] Taken together, impaired lymphatic vessel functions may cause fat accumulation and obesity.

Interestingly, serum levels of prolymphangiogenic factors VEGF-C and -D are elevated in overweight and in obese human subjects.[55-57] In mouse models,

blockade of VEGF-C and -D by soluble VEGFR-3 reduces obesity-associated adipose tissue inflammation; however, body weight of the obese mice is not affected.[58] Clearly, our understandings of the role of lymphatic vessels in the process of obesity are still in the infancy. Further studies are needed in order to treat obesity by manipulating the growth of lymphatic vessels.

Glaucoma. Glaucoma is the second leading cause of blindness, affecting over 60 million adults worldwide.[59,60] More than 3 million Americans age 40 and older, about 2% of this population, have glaucoma. Glaucoma is estimated to account for $US2.9 billion of direct medical costs among US adults annually.[61] Currently, treatment for glaucoma is designed to lower intraocular pressure (IOP), as this is the only modifiable factor that has been shown to slow the progression of glaucoma. IOP is determined by the balance between aqueous production and aqueous outflow. Aqueous drainage through the trabecular meshwork (located at the junction of the cornea/sclera and the iris) and Schlemm's canal (i.e. the conventional outflow pathway) accounts for a large portion of aqueous outflow.[62,63] The inner wall of Schlemm's canal is the final barrier for aqueous humor to cross before returning to systemic circulation. Yet, the vascular identity of endothelial lining of Schlemm's canal has not been determined, as the endothelial cells of Schlemm's canal possess characteristics of both blood and lymphatic vessels.[64] In recent years, several studies have reinforced the concept that the endothelium of Schlemm's canal is blood vessel-like endothelium during embryonic development and transdifferentiates to blood-filled lymphatic vessel-like endothelium postnatally.[65-69] Of note, endothelial cells of inner wall and outer

wall of Schlemm's canal are not the same. Anatomically, aqueous humor crosses the inner wall endothelial cells which are anchored to a fairly deformable substrate (the juxtacanalicular tissue) producing a basal-to-apical pressure gradient, whereas outer wall endothelial cells reside on the relatively inextensible sclera and experience a pressure gradient in the opposite (apical-to-basal) direction. In terms of cellular markers, endothelium of inner wall, but not outer wall, expresses VEGFR-3.[65] The differential expression of VEGFR-3 may partially explain the different response to prolymphangiogenic factors. On the one hand, suture placement-induced corneal inflammatory response dose not induce sprouting of endothelium of Schlemm's canal;[66] on the other hand, intraocular injection of VEGF-C induces an enlargement of Schlemm's canal and a reduction of IOP. (Note that injection of mouse albumin also causes a reduction of IOP despite the effect is less pronounced than VEGF-C treatment).[68]

In addition to Schlemm's canal, it is implied that lymphatic vessels in the anterior chamber may also involve in regulating aqueous drainage. Eyes from mice with induced deletion of Tie2 (Tie2-cKO) or both angiopoietin 1 and 2 (A1A2-cKO) lack both limbal lymphatic vessels and Schlemm's canal, whereas limbal blood vessels are present.[69] As the high IOP observed in A1A2 cKO mice is more severe than that of other models with an abnormal Schlemm's canal, Thomson and colleagues hypothesize that "lymphatic vessels are essential for maintaining aqueous humor flow through the uveoscleral route".[69] The exact role of lymphatic vessels in the anterior chamber during the pathogenesis of glaucoma has not been fully understood. However, considering one of the

functions of lymphatic vessels is to maintain fluid balance, it is reasonable to assume that aqueous drainage through lymphatic vessel-like Schlemm's canal and/or (limbal) lymphatic vessels plays a key role in maintaining IOP, and malfunction of the drainage system in the eye may cause glaucoma.

Dry eye disease. Dry eye disease is a common ocular disorder, affecting 10% to 20% of the adult population.[70] Dry eye disease is defined as "a multifactorial disease of the tears and ocular surface that results in symptoms of discomfort, visual disturbance, and tear film instability with potential damage to the ocular surface. It is accompanied by increased osmolarity of the tear film and inflammation of the ocular surface".[70] Current expenditures for treating dry eye disease surpass $2 billion dollars annually, and because it often affects visual function in working adults, it leads to lost productivity by impacting job performance. The pathogenesis of dry eye disease is not well-characterized; however, ocular surface inflammation is a key feature of dry eye disease, and clinical signs and symptoms are relieved by anti-inflammatory agents such as methylprednisolone and cyclosporine.

In dry eye disease, inflammatory cells (NK cells, T cells, macrophages, etc.) are infiltrated to ocular surface and pro-inflammatory cytokines (IL-1, IL-6, IFN-γ and IL-17) are also increased.[71,72] Among the inflammatory cells, Th1 and Th17 cells have been shown to be responsible for the pathogenic effect in dry eye disease by producing proinflammatory cytokines, chemokines, matrix metalloproteinase, cell adhesion molecules and pro-lymphangiogenic factors

such as VEGF-C, -D and IL-17.[73] Interestingly, lymphangiogenesis without accompanying angiogenesis has been observed in a mouse model of dry eye disease.[74] Alleviating inflammation by methylprednisolone and IL-1Ra also reduces corneal lymphangiogenesis.[75] These findings suggest that in addition to anti-inflammatory therapy, anti-lymphangiogenic therapy could be a new therapeutic option for dry eye diseases.

Allergic eye disease. Allergic eye disease is an inflammatory disease in ocular surface and is driven by Th2, mast cells and eosinophils.[76,77] In a mouse model of allergic eye disease which is induced by ovalbumin, corneas of allergic mice express higher amounts of prolymphangiogenic factors such as VEGF-C and -D.[78] Similar to dry eye disease, the allergic corneas have increased lymphangiogenesis without accompanying angiogenesis.[78] Inhibiting lymphangiogenesis in the mouse model by a small molecule inhibitor, Axitinib, which inhibits VEGFR-1, -2 and -3, markedly improves the clinical signs of allergic eye disease.[78] Thus far, there is only one study regarding the involvement of lymphangiogenesis in the allergic eye disease. Clearly, more studies are needed to be done to understand the role of lymphatic vessels in the allergic eye disease.

1.2 Key molecules that regulate lymphangiogenesis.

VEGF-C and VEGFR-3. Signaling axis of VEGF-C−VEGFR-3 is one of the important pathways for physiological and pathological lymphangiogenesis. In

human, mutations that inactivate VEGFR-3 and VEGF-C cause primary lymphedema (primary congenital lymphedema/Noone-Milroy lymphedema and Milroy-like disease).[1] Genetic manipulations of the pathway in mice also highlight the relevance of VEGF-C and VEGFR-3 in lymphangiogenesis. VEGF-C is required for embryonic lymphangiogenesis, VEGF-$C^{-/-}$ mice are embryonic lethal, and $VEGFC^{+/-}$ mice are not embryonic lethal but suffer from lymphedema.[79] Chy mice have heterozygous inactivating mutations in VEGFR-3, and resemble Milroy's disease (a primary human lymphedema).[50] Mice with overexpression of VEGFR-3−Ig (extracellular domain of VEGFR-3 fused to the Fc domain of immunoglobulin γ chain) that neutralizes VEGF-C/D and inhibits dermal lymphatic vasculature when expressed in epidermis under the keratin-14 (K14) promoter, display features of human lymphedema[80] and have been wildly used to study pathological lymphangiogenesis. Thus, evidence from both human diseases and mouse models indicates that VEGF-C−VEGFR-3 signaling axis is vital for lymphangiogenesis.

Of note, VEGFR-3 is required for developmental angiogenesis[81] but it becomes restricted to lymphatic endothelial cells when development progress.[82] In adults, VEGFR-3 expression is very low or undetectable in most blood vessels, but detectable in high endothelial venules, fenestrated capillaries, inner wall cells of Schlemm's canal, capillaries of normal breast tissue, capillaries of neuroendocrine organs chronic wounds, some tumor-associated blood vessels, and VEGF-C-induced newly formed blood vessels.[65,83-87] Other than endothelial cells, nonvascular VEGFR-3 is also found to be expressed in corneal epithelial

cells,[88] macrophages,[58,89] lipopolysaccharide (LPS)-treated (M1-like) macrophages,[90] corneal but not skin dendritic cells,[91] conjunctival monocytes/macrophages ($CD45^+CD11b^+CD3^-Gr\text{-}1^-$),[92] etc.

Interestingly, while LPS-treated macrophages display M1 phenotype and IL-4-treated macrophages display M2 phenotype, VEGF-C-treated macrophages display a hybrid M1-M2 phenotype and the effect is abolished by an anti-VEGFR-3 neutralizing Ab in vitro and in vivo. These findings indicate VEGF-C/VEGFR-3 signaling axis regulates macrophage plasticity and activation.[93] In addition, the VEGF-C/VEGFR-3 axis in macrophages is important for bacterial antigen clearance and restricts endotoxin shock triggered by TLR-mediated inflammation.[93,94] Therefore, VEGF-C/VEGFR-3 signaling axis is crucial not only for regulating the process of lymphangiogenesis, but also for shaping the proper immune responses.

<u>VEGF-A and VEGFR-2.</u> In addition to VEGFR-3, VEGFR-2 is also expressed in lymphatic endothelial cells (LECs). Results from the genetic ablation of VEGFR-2 expression in lymphatic vessels (*Lyve-1*$^{wt/cre}$*;Vegfr2*$^{flox/flox}$ mice) demonstrate that VEGFR-2 promotes the expansions of the lymphatic network and may not be involved in lymphatic drainage.[95] In addition, activating VEGFR-2 by overexpressing VEGF165 and VEGF-E (a viral-derived VEGF that only activates VEGFR-2) promotes lymphatic vessel enlargement but very little sprouting.[96] On the other hand, VEGF-A−VEGFR-2 signaling can indirectly contribute to lymphangiogenesis by recruiting VEGF-C/D-secreting macrophages to sites of

inflammation,[97-99] which explains VEGF-A-induced lymphangiogenesis in vivo in other studies.[12,100,101] Therefore, the "direct" effect of VEGF-A−VEGFR-2 signaling on lymphangiogenesis may be less important than VEGF-C−VEGFR-3 signaling.

Integrins. The integrin family of cell adhesion receptors mediates the anchoring of cells to the extracellular matrix proteins and some members of the integrin family can interact with certain growth factors.[102] The integrin family exists as heterodimers of unique α and β subunits; mammals express 18 α and 8 β subunits forming 24 distinct αβ integrin dimers.

LECs express integrins α1β1, α2β1, α3β1, α4β1, α5β1, α6β1, αvβ3, αvβ5, and α9β1.[103] Among these integrins, integrin α9β1 is crucial in developmental lymphangiogenesis; mice lacking integrin α9, which only pairs with integrin β1, die postnatally due to defective lymphatic valve development.[104,105] In addition, defective integrin α9 due to missense mutation (G404S) has been linked to severe fetal chylothorax,[106] an accumulation of lymph in the pleural cavity due to disruption or obstruction of the thoracic duct. Other than the extracellular matrix ligands (e.g. tenascin-C, the EDA domain of fibronectin and osteopontin), integrin α9β1 also interacts with several growth factors such as VEGF-A, -C, -D, nerve growth factor, brain-derived neurotrophic factor and neurotrophin-3.[105,107-109] Blocking integrin α9β1 by a neutralizing antibody has been shown to inhibit VEGF-C/D-mediated lymphangiogenesis and VEGF-A-mediated angiogenesis in

vitro.[107,108] However, the anti-lymphangiogenic effect of the anti-integrin α9β1 blocking antibody has yet to be determined in vivo.

While integrin α9β1 is crucial for developmental lymphangiogenesis, integrins α1β1, α2β1, α4β1, α5β1 have been shown to play a role in pathological lymphangiogenesis. Blockade of integrins α1β1 and α2β1 using antibodies reduces inflammatory lymphangiogenesis in cornea and skin.[100,110] Integrin α4β1 is expressed in tumor associated lymphatic vessels and intra-nodal lymphatic vessels in pre-metastatic lymph nodes.[15,111] Treatment with anti-integrin α4β1 blocking antibodies decreases lymphangiogenesis and lymph node metastasis.[15] In addition, functional blocking of integrin α5β1 by neutralizing antibodies or small-molecule inhibitors curtails lymphangiogenesis in mouse models of suture-induced corneal inflammation, corneal graft rejection and lung inflammation.[41,112,113] Together, among the integrins expressed in LECs, integrins α1β1, α2β1, α4β1, α5β1 and α9β1 are considered pro-lymphangiogenic integrins.

Podoplanin. Podoplanin (PDPN) is a 36- to 43-kDa transmembrane glycoprotein. It is expressed by LECs but not blood ECs and promotes blood-lymph separation. Mice lacking PDPN have leaky lymphatic vessels and congenital lymphedema.[114,115] In vitro studies have shown that PDPN expression in LECs is required for lymphatic capillary tube formation in matrigel as well as VEGF-A-induced cell migration in the scratch wound assays.[116,117] That the extracellular domain of PDPN plays a critical role in lymphangiogenesis has been demonstrated by studies showing that PDPN-Fc and the functional blocking

antibody against extracellular domain of PDPN (PMab-1) inhibit LEC migration and tube formation in vitro and suppress lymphangiogenesis but not hemangiogenesis in inflamed mouse corneas in vivo.[118,119] The extracellular domain of PDPN is heavily glycosylated, and *O*-glycosylation as well as sialylation are critical for PDPN-mediated blood-lymph separation and platelet aggregation.[115,120-122] In addition, it is known that sialylated *O*-glycans protect PDPN from metalloprotineases (MMP)-2/9-mediated proteolytic degradation.[122]

While PDPN has been wildly used as a LEC marker, PDPN is also expressed in other types of cells including kidney podocytes, alveolar type I cells, mature osteoblasts, fibroblastic reticular cells of lymphoid organs, thymic epithelial cells, Th17 cells, inflammatory macrophages (thioglycollate-elicited peritoneal macrophages, LPS-stimulated macrophages, TNF-α-stimulated macrophages, TLR2 ligand-stimulated macrophages), skin keratinocytes upon injury, choroid plexus epithelial cells, retinal pigment epithelial cells, activated astrocytes (glial fibrillary acidic protein-positive astrocytes), trabecular meshwork cells, some types of tumor cells, etc.[123-128]

Prox-1. Prox1 is a transcriptional factor that plays a key role in determining the LEC fate specification. The expression of Prox1 in LEC progenitors in the embryonic cardinal veins is the initial step in the formation of the lymphatic vasculature.[129] Prox1 is required for developmental lymphangiogenesis, as embryos of Prox1 KO mice are devoid of lymphatic vessels.[130] In addition, conditional downregulation of Prox1 during development or adulthood is sufficient

to reprogram LECs into blood ECs.[131] Conversely, ectopic overexpression of Prox1 in the differentiated blood ECs is sufficient to induce the lymphatic phenotype; lymphatic vessel-associated genes (e.g. PDPN and VEGFR-3) are upregulated, while blood vessel-associated genes (e.g. ICAM-1, MCP-1, neuropilin-1, thrombomodulin, uPAR) are downregulated.[132] Together, these findings indicate that Prox1 is the master transcriptional factor that is required and sufficient to initiate and maintain the LEC identity.

Although Prox1 is considered the molecular marker to distinguish between LECs and blood ECs, it is also expressed in other types of non-vascular cells. In the eye, “green eyes” are one of the obvious features in the *Prox1*-EGFP reporter mice,[133] as Prox1 is robustly expressed in the developing lens and is required for lens cells (fiber cells) to polarize and elongate.[134] In the retina, Prox1 is primarily expressed in the inner nuclear layer and the immunoreactivity of Prox1 is detected in Muller cells, horizontal cells, some bipolar cells (PKC-α^+ cells), some amacrine cells (paralbumin$^+$ cells and most calbindin (CB)$^+$ cells) and some cells in the ganglion cell layer (some CB$^-$ cells and some calretinin (CR)$^-$ cells).[135,136] In the central nervous system, Prox1 expression leads to differentiation of neural progenitor cells and initiation of neurogenesis.[137] In the liver and pancreas, Prox1 null embryos display smaller liver and pancreas due to failed hepatocyte migration and pancreatic precursor cell differentiation, respectively.[137] In addition, Prox1 expression is altered in several different cancers, and it plays a role in tumor progression, metastasis and stemness of cancer stem cells.[137]

1.3 Galectins: classification and functions.

Galectins are a family of animal lectins which bind β-galactosides.[138,139] Galectins are present both inside and outside cells and function both intracellularly and extracellularly.[140,141] They share a common structural fold and at least one conserved carbohydrate recognition domain (CRD) comprising about 130 amino acids. A total of 15 galectins have now been found in mammals and have been classified into three major groups: (1) the prototypical galectins including galectins-1, -2, -5, -7, -10, -11, -13, -14 and -15, which contain a single CRD and can form homodimers; (2) the unique chimera-type galectin-3, which is characterized by having a single CRD and an amino-terminal domain that contributes to self-association; and (3) the tandem-repeat galectins including galectins-4, -6, -8, -9 and -12, which contain two CRDs separated by a linker peptide. Although it is generally stated there are 15 members of galectin family, the actual number of authentic members of galectin family in mammalian tissues is smaller. Galectin-5 has been found only in rat and is almost identical to the C-terminal CRD of rat galectin-9.[142,143] Galectin-6 is only found in mouse and is almost identical to mouse galectin-4.[144] Galectins-10 and -12 have relatively weak affinity for galactose-containing sugars. In fact, galectin-10 prefers mannose.[145-147] The name galectin-11 has been given to a galectin-related interfiber protein (GRIFIN), which is found in the lens. It too does not have carbohydrate-binding activity.[148] Interestingly, galectin nomenclature has omitted no. 13 and galectins-14 and -15 are found only in ovine and goat. Thus, for the analysis of galectin signature relevant to human tissues, one should include

galectins-1 to 4, and 7 to 9. However, galectins-2 and -4 are either not present or present only in trace amounts in normal or diseased corneas (Cao and Panjwani, unpublished). Therefore, of relevance to the cornea are galectins-1, -3, -7, -8 and -9.

Functions of galectins include, but are not limited to, immune regulation, host-pathogen interactions, angiogenesis, re-epithelialization of wounds and fibrosis. Galectins are expressed in the cells of the innate and adaptive immune system[149] and can have anti- or pro-inflammatory roles depending on the stage of infection and the degree of inflammation.[150,151] Galectins can also function as pattern-recognition receptors either to facilitate or to inhibit attachment/invasion of pathogens, such as virus, bacteria, protista and fungi.[149,152] More recently, galectins have been shown to modulate angiogenic responses. Previous studies have shown that galectins-1, -3, -8 and -9 are involved in modulating angiogenesis. Galectins-1 and -3 activate VEGFR-2,[153-156] Galectin-8 promotes angiogenesis in a CD166-dependent manner,[157] and galectin-9 inhibits angiogenesis by an unknown mechanism.[158] In addition to their direct effect on endothelial cells, Galectins-1, -3 and -8 also activate platelets to release VEGF.[159] Studies aimed at characterization of the role of galectins in wound healing have shown that several members of galectin family, including galectins-2, -3, -4 and -7, promote re-epithelialization of wounds.[160] In addition, it has been demonstrated that experimentally-induced fibrosis is dependent on galectin-3 in a variety of tissues including lung, heart and liver. Specifically, in the context of cornea, galectin-3 has been shown to play a key role in maintaining ocular

surface barrier function through carbohydrate-dependent interactions with cell surface mucins.[161] It has also been demonstrated that galectins-3 and -7, but not galectin-1, promote corneal epithelial cell migration and re-epithelialization of corneal wounds.[162] Studies from our laboratory have also shown that corneal neovascularization is much reduced in galectin-3 knockout mice and that galectin-3 modulates VEGF-mediated angiogenesis by binding via its carbohydrate recognition domain (CRD) to N-glycans of VEGFR-2 and αvβ3 integrin, and subsequently activating the signaling pathways that promote the growth of new blood vessels.[155]

1.4 Galectin-8: expression pattern.

Galectin-8 is also known as prostate carcinoma tumor antigen 1 (PCTA-1) and Po66-carbohydrate binding protein. The human galectin-8 has seven different isoforms; three isoforms belong to the tandem-repeat galectin group and the others belong to the prototype group. The predominant isoform is galectin-8 isoform b (NP_963837) which comprises 317 amino acids (~35 kDa). Galectin-8 isoform a (NP_963839) has 359 amino acids with a longer linker peptide and is susceptible to thrombin cleavage.[163] Galectin-8 was first isolated from rat liver cDNA expression library in 1995.[164] Galectin-8 mRNA is highly expressed in lung and to a lower extent in liver, kidney, spleen, cardiac muscle, spleen and hind limb muscle. Lower levels of expression were detected in brain, and almost no expression was found in whole rat embryos.[164] In pathological conditions, it is reported that in a mouse model of lung cancers, immunoreactivity of galectin-8 is

absent in extracellular matrix of primary tumors, whereas a robust immunoreactivity is detected in the extracellular matrix of lymph node metastasis and distant metastasis.[165] In addition, compared to healthy subjects, serum galectin-8 is also markedly increased in patients with colorectal and breast cancers; patients with metastatic colorectal cancer also has much higher concentration of serum galectin-8.[166] The cellular sources of galectin-8 can be endothelial cells,[167] platelets/megakaryocytes,[168,169] epithelial cells,[170,171] and B cells/plasma cells (galectin-8 expression is higher in $B220^{low}CD138^{+}$ cells).[172] We also observed that galectin-8 is expressed in several different types of cells including RAW264.7 cells (mouse monocytes/macrophages), HaCaT cells (human keratinocyte), primary human corneal epithelial cells, primary human stromal fibrocytes, and mouse $CD4^{+}$ spleen T cells. Interestingly, it was found that the mRNA expression level does not reflect the protein expression level in endothelial cells and B cells/plasma cells.[172,173]

As mentioned above, galectins are present both inside and outside cells.[140,141] Intracellular localization of galectin-8 is in the cytosol and nucleus. Extracellular galectin-8 is found at plasma membrane and in extracellular matrix, presumably due to the unconventional secretion pathway.[174-179] Although the regulation of galectin secretion is not well-understood, inflammatory stimuli such as LPS promote secretion of galectin-8 isoform b,[179] and activation of caspase-1 is linked to secretion of galectins-1 and -3.[180]

1.5 Galectin-8: binding partners.

Galectin-8 has two CRDs, which possess different binding specificity to glycans. The best glycan ligands for galectin-8 N-terminal CRD (N-CRD) are α2,3-sialylated and 3' sulfated β-galactosides.[32,181] Dissociation constant (Kd) of galectin-8 N-CRD to NeuAcα2-3Lac (3'-sialyl lactose) is 50 nM, which is 100-fold higher than the Kd of N-CRD to lactose as determined by a fluorescence polarization assay.[32] Residues Arg^{45}, Gln^{47} and Arg^{59} of the N-CRD are indispensable for the strong binding of Gal-8N to sialylated and sulfated glycans.[32,182,183] Using a Lec2 Chinese hamster ovary (CHO) cell mutant which has almost no sialylated glycoconjugates, it was demonstrated that sialylation of cell surface proteins/lipids is required for galectin-8 N-CRD to bind to cell surface.[184] In addition, unlike the bi-CRD galectin-8, galectin-8 N-CRD strongly binds to Lec1 CHO cell mutant, which has no complex or hybrid *N*-glycans, suggesting that galectin-8 N-CRD binds well to glycans that are not *N*-linked, such as GM3 glycolipid and sialylated *O*-glycans.[184] Considering that the bi-CRD galectin-8 binds well to complex/hybrid *N*-glycans, that the galectin-8 N-CRD has little affinity to complex/hybrid *N*-glycans, and that galectin-8 C-CRD binds better to non-sialylated cells (Lec2) than to CHO parental cells, the Stanley group[184] concluded that galectin-8 C-CRD may be responsible for the high affinity of intact galectin-8 to complex *N*-glycans through the bivalent cooperation whereas N-CRD provides binding to sialylated glycans. Taken together, the two CRDs of galectin-8 have very distinct glycan-binding specificity, and they act together to exert the biological functions of the intact bi-CRD galectin-8.

Galectin-8 binds to glycans of several glycoproteins, including integrins (α1β1, α3β1, α5β1, α6β1, αvβ1, αMβ2, but not α2β1, α4β1 or β3),[185-188] CD44,[189] CD166,[157] fibronectin,[190] MMP-9,[187,191] CD45R (B220, in B cells), CD45RA (in naïve cells), CD45RO (in activated/memory T cells),[191] etc. In vitro studies have shown that galectin-8, but not galectins-1, -2, -3 and -7, binds PDPN and that the lectin promotes adhesion and haptotaxis of LECs.[192] However, the direct evidence that galectin-8 exerts its biological functions through PDPN is lacking. In fact, Cueini and Detmar[192] speculated that contribution of the interaction of galectin-8 with PDPN in the modulation of LEC migration and adhesion is most likely minor. Also, based on the findings that unglycosylated ectodomain of PDPN-Fc was more effective in inhibiting the functions of human LECs in vitro than the extensively glycosylated form of PDPN-Fc, it has been suggested that the interactions with PDPN ligands on the surface of LECs do not depend on PDPN glycosylation.[118] To date, the biological relevance of carbohydrate-dependent galectin-8/PDPN interactions is still elusive and more direct studies involving the use of galectin-8 KO and PDPN KO mice have not been reported.

1.6 Galectin-8: role in angiogenesis.

Galectin-8 promotes angiogenesis in vitro and in vivo.[157] Recombinant galectin-8 promotes tube formation and cell migration of blood endothelial cells (bovine aortic endothelial cells and human microvascular endothelial cells). In addition, recombinant galectin-8 promotes angiogenesis in vivo in a matrigel plug assay. Conversely, galectin-8 knockdown reduces tube formation in vitro.[157]

Mechanistically, it was demonstrated that CD166 is important for galectin-8-mediated angiogenesis in vitro.[157] Furthermore, recombinant galectin-8 stimulate endothelial cells to secrete pro-inflammatory cytokines such as IL-6, monocyte chemotactic protein (MCP-1), growth related oncogene-alpha (GRO-alpha, CXCL1), granulocyte macrophage colony-stimulating factor (GM-CSF) and CCL5 (RANTES),[179] all of which are linked directly or indirectly to promoting angiogenesis. While galectin-8 can directly act on endothelial cells to promote angiogenesis, it has been shown that galectin-8 can indirectly promote angiogenesis by stimulating platelets to release proangiogenic factors such as VEGF-A, EGF, bFGF, epithelial-neutrophil activating peptide (ENA-78), etc.[159] In addition, considering that galectin-8 catalyzes the processing of pro-MMP-9 to MMP-9[187] and that MMP-9 plays a key role in stimulating angiogenesis,[187,193] it is reasonable to speculate that galectin-8 can also promote angiogenesis in a MMP-9-dependent manner. Taken together, galectin-8 has pleiotropic effects in regulating the process of angiogenesis.

1.7 Objectives of the dissertation.

The aims of this dissertation are (1) to assess galectin expression patterns in diseased corneas and (2) to determine which galectin directly promotes lymphangiogenesis. For **Aim 1**, our study using three different mouse models of corneal inflammations (*P. aeruginosa* infection, chemical injury and corneal transplantation), revealed distinct expression patterns of galectins-1, -3, -7, -8 and -9 in the inflamed mouse corneas. For **Aim 2**, using multiple approaches involving the use of galectin-8 mutants lacking carbohydrate-binding activity,

knockout mice, specific sugar inhibitors of galectins, and siRNA knockdown of key players of lymphangiogenesis, I establish a critical role of galectin-8 and carbohydrate-mediated recognition in the process of lymphangiogenesis. Additionally, considering that galectin-8 is not expressed in embryonic stages, that galectin-8 KO mice do not exhibit overt defects, that galectin-8 is upregulated in inflammatory conditions as we demonstrated in this study, and that galectin-8 is crucial for regulating pathological lymphangiogenesis, manipulating the activity of galectin-8 is potentially a great approach to treat diseases related to excessive lymphangiogenesis and/or lymphatic defects.

Materials and Methods

2.1 Expression and purification of recombinant galectins.

Recombinant human galectins were expressed and purified as descried previously.[32,183,194-197] Expected yields for each galectin: galectin-1, ~10 mg/L; galectin-3, ~20 mg/L; galectin-7, ~70 mg/L; galectin-8-GST, ~3 mg/L.

Small-scale expression screening: One colony of transformed *E. coli* was picked and placed into a test tube each containing 5 ml of LB media into the 50 ml culture test tube containing the appropriate antibiotic indicated below for each individual galectin. For each experiment, 5 to 8 individual colonies were picked. The culture was incubated overnight at 37ºC in the rotating incubator (This is a regular incubator in which orbital shaker has been placed) and then 0.5 ml of the overnight culture was diluted into 5 ml of fresh pre-warmed LB media with antibiotic. (Make certain that the tubes are filled less than 25% to ensure adequate aeration). The liquid cultures were grown until the absorbance at 600 nm (OD600) reaches 0.6 - 0.8 with vigorous agitation at 37ºC. LB was used as the blank. (It could take 1 to 3 hours for the growth to reach this absorbance and the time required for the cells to grow to the correct density depends on strain and will vary for each fusion protein). Once the OD600 was correct, 4.0 ml of the culture cells were removed and exchanged the medium to 50% glycerol/LB medium for long-term storage. The 1 ml of the remaining culture was separated in to 2 parts: one was left untreated and the other was induced with IPTG (Sigma, concentration was descried in the protocols of different galectins expression).

After 3 to 4 hour incubation, cell cultures were centrifuged at 5,000 rpm for 10 min and the supernatants were discarded. The pellets were dissolved in lysis buffer (10 mM Tri-Cl, pH 7.2, 300 mM NaCl). Take 30 µl of the suspension, add 6 µl of 6X sample buffer, and boil for 5 to 10 min. The protein lysates were then subjected to electrophoresis in SDS-PAGE gels.

RBC agglutination assay: 25 µl of type A was added to 1 ml of 0.3% BSA/PBS (with Ca^{2+} and Mg^{2+}) and centrifuged at 2,000x g for 1 min. The supernatant was discarded. This step was repeated for 3 more times. The RBC pellets were then resuspended in 1 ml 0.3% BSA/PBS. Galectin solution (40 µl of different concentrations of galectins ranging from 8 to 32 µg/ml) was mixed with the RBC suspension (10 µl). The mixture was placed in a glass slide. Agglutination of RBC indicates that the galectins are functional.

Preparation of lactosyl-sepharose beads. The beads were prepared as described before.[198] Sepharose 4B beads (100 ml, Sigma, 4B200) were washed with 100 ml of 0.5 M Na_2CO_3 three times. The beads were filtered over a Buchner funnel. The drained beads was resuspended in 100 ml of 0.5 M Na_2CO_3, and 10 ml of divinyl sulfone (Sigma) were slowly added. The mixture was stirred gently at 25ºC for 70 min, filtered over a Buchner funnel, and washed five times with 100 ml of 0.5 M Na_2CO_3. The drained beads were then resuspended in 100 ml of 10% lactose in 0.5 M Na_2CO_3. The mixture was gently stirred for 15 hr at 25ºC. The mixture was filtered and washed three times with 100 ml of 0.5 M Na_2CO_3,

once with 100 ml of distilled water, and finally three times with 100 ml of 0.05 M phosphate buffer (pH 7.0). For long-term storage, the beads were resuspended in 100 ml of 0.05 M phosphoate buffer (pH 7.0) supplemented with 0.02% NaN_3 and storage at 4ºC.

Galectin-1 expression and purification: human galectin-1 cDNA was cloned into NcoI/Hind III cut pQE-60 (Qiagen, eliminating 6-his tag sequence residing between NcoI and Hind III), transformed into TG1 competent cells and plated onto LB agar containing ampicillin (50 µg/ml). Small-scale expression screening was performed to select the clones with the highest protein expression. For large scale expression, 100 µl of bacterial stock was spread on LB agar containing ampicillin (50 µg/ml) and incubated at 37ºC overnight (no more than 16 hr). Three loopfuls of bacteria were inoculated into 100 ml of LB solution in I litre flask containing ampicillin (50 µg/ml) and were cultured for 2 hours at 37ºC with vigorous orbital shaking. At the end of culture, the 100 ml culture was diluted with 1 L of LB solution containing ampicillin (50 µg/ml) and was incubated at 37ºC with vigorous orbital shaking until the OD600 is about 0.6. IPTG was added to the culture at final concentration of 1 mM. After 4 hr of induction at 37ºC, cells were harvested by centrifugation at 3,000 rpm for 30 min at 4ºC, supernatants were discarded and the pellets were washed once with cold PBS. The pellets were resuspended in 50 ml of ice-cold lysis buffer (20 mM Tris, pH 7.4, 2 mM EDTA, 150 mM NaCl, 4 mM β-mercaptoethanol and 1 mM PMSF). The resultant suspension was sonicated at 40% output, 30 sec (pulse module: 4 sec on and 2

sec off) per cycle and paused for 1 min. This procedure was repeated 5 more times (6 cycles in total). The cell lysate was centrifuged at 18,000 rpm at 4ºC for 20 min. The supernatant was collected, passed through 0.45 μm filters (Millipore) using a 50 ml syringe, mixed with 3 ml (packed volume) of lactosyl-Sepharose beads, and rotated at 4ºC for 1 hr. The beads-suspension was transferred into a column and settled down. The column was washed with 30 ml of Tris/EDTA/NaCl buffer (TEN buffer: 20 mM Tris, pH7.4, 2 mM EDTA, 150 mM NaCl and 4 mM β-mercaptoethanol) with 0.2 mM PMSF, and again with 10 ml of PBS with 0.2 mM PMSF and 4 mM β-mercaptoethanol. The bound galectin-1 proteins were eluted with 0.1 M lactose in PBS with 0.2 mM PMSF and 4 mM β-mercaptoethanol into 1-ml fractions. Fractions which contained proteins (measured by Bradford method) were collected and combined. The proteins containing 0.1 M lactose were dialyzed against 500 ml of PBS with 2% glycerol and 4 mM β-mercaptoethanol three times at 4ºC. The protein concentration was determined by Bradford method and the activity was assessed by RBC agglutination assay. Proteins were stored as small-amount aliquots at -80ºC freezer.

Galectin-3 expression and purification: human galectin-3 cDNA was cloned into NcoI/Hind III cut pKK233-2, transformed into BL21 Star (DE3) competent cells and plated onto LB agar containing ampicillin (50 μg/ml). The colony that expressed the highest galectin-3 in small-scale expression screening was used for large scale expression. One hundred μl of bacterial stock was spread on LB agar containing ampicillin (50 μg/ml) and incubated at 37ºC overnight (no more

than 16 hr). Three loopfuls of bacteria were inoculated into 100 ml of LB solution containing ampicillin (50 μg/ml) and were cultured for 2 hours at 37ºC with vigorous orbital shaking. At the end of culture, the 100 ml culture was diluted with 1 L of LB solution containing ampicillin (50 μg/ml) and was incubated at 37ºC with vigorous orbital shaking until the OD600 is around 0.8 to 1. IPTG was added to the culture at final concentration of 0.1 mM. After 3 hr of induction at 37ºC, cells were harvest by centrifuging at 3,000 rpm for 30 min at 4ºC, supernatants were discarded and the pellets were washed once with cold PBS. The pellets were resuspended in 80 ml of ice-cold PBS with 2 mM EDTA and 4 mM β-mercaptoethanol. The resultant suspension was sonicated at 40% output, 1 min (pulse module: 4 sec on and 2 sec off) per cycle and paused for 3 min. This procedure was repeated 6 more times (7 cycles in total). The cell lysate was centrifuged at 18,000 rpm at 4ºC for 20 min. The supernatant was collected, passed through 0.45 μm filters, mixed with 4 ml (packed volume) of lactosyl-Sepharose beads, and rotated at 4ºC for 1 hr to overnight. At the end of incubation, the beads-suspension was centrifuged at 1,000 rpm for 2min, supernatants were removed, beads were resuspended in 10 ml PBS and transferred into a column. The column was washed with 50 ml of PBS with with 2 mM EDTA and 4 mM β-mercaptoethanol. The bound galectin-3 proteins were eluted with 150 mM lactose in PBS with with 2 mM EDTA and 4 mM β-mercaptoethanol into 1-ml fractions. Fractions which contained proteins (measured by Bradford method) were collected and combined. The proteins containing 150 mM lactose were dialyzed against 500 ml of PBS with 10%

glycerol three times at 4ºC. The protein concentration was determined by Bradford method and the activity was assessed by RBC agglutination assay. Proteins were stored as small-amount aliquots at -80ºC freezer.

Galectin-7 expression and purification: human galectin-7 cDNA was cloned into NcoI/Hind III cut pQE-60 (Qiagen, eliminating 6-His tag sequence residing between NcoI and Hind III), transformed M15[pREP4] competent cells (Qiagen) and plated onto LB agar containing ampicillin (50 μg/ml) and kanamycin (30 μg/ml).The colony that expressed the highest galectin-7 in small-scale expression was used for large scale expression. One hundred μl of bacterial stock was spread on LB agar containing ampicillin (50 μg/ml) and kanamycin (30 μg/ml) and incubated at 37ºC overnight (no more than 16 hr). Three loopfuls of bacteria were inoculated into 100 ml of LB solution containing ampicillin (50 μg/ml) and kanamycin (30 μg/ml) and were cultured for 2 hours at 37ºC with vigorous orbital shaking. At the end of culture, the 100 ml culture was diluted with 1 L of LB solution containing ampicillin (50 μg/ml) and kanamycin (30 μg/ml) and was incubated at 37ºC with vigorous orbital shaking until the OD600 is around 0.6. IPTG was added to the culture at final concentration of 0.5 mM. After 4 hr of induction at 37ºC, cells were harvest by centrifuging at 7,000 rpm for 20 min at 4ºC, supernatants were discarded and the pellets were washed once with cold PBS. The pellets were resuspended in ice-cold lysis buffer (20 mM Tris, pH 8.0, 5 mM EDTA, 1 mM DTT, 10 μg/ml aprotinin and leupeptine, 1 mM PMSF, 10 mM L-cystein) and lysozyme was added and mixed at 1 mg/ml. After incubation on

ice for 30 min, the suspension was sonicated at 40% output, 30 sec (pulse module: 4 sec on and 2 sec off) per cycle x 4 cycles with 1 min intervals. The lysates were kept on ice all times during the procedure. The cell lysate was centrifuged at 18,000 rpm at 4ºC for 20 min. The supernatant was collected, passed through 0.45 µm filters, mixed with 2.5 ml (packed volume) of lactosyl-Sepharose beads, and rotated at 4ºC for 1 hr. The beads-suspension was transferred into a column and settled down. The column was washed with 30 ml of 50 mM Tris, pH 8.0, 150 mM NaCl, 5 mM EDTA, 0.2 mM PMSF and 1 mM DTT, then washed with 10 ml of PBS with 0.2 mM PMSF and 1 mM DTT. The bound galectin-7 proteins were eluted with 250 mM lactose in PBS with 0.2 mM PMSF and 1 mM DTT into 1-ml fractions. Fractions which contained proteins (measured by Bradford method) were collected and combined. The proteins containing 250 mM lactose were dialyzed against 500 ml of PBS with 5% glycerol three times at 4ºC. The protein concentration was determined by Bradford method and the activity was assessed by RBC agglutination assay. Proteins were stored as small-amount aliquots at -80ºC freezer.

Gal-8 expression and purification: for expression and purification of galectin-8 tagged with glutathione *S*-transferase (GST) (GST-galectin-8), human galectin-8 cDNA was cloned into *Sal*I–*Not*I cut pGEX-4T-3 expression plasmid (Pharmacia Biotech) that provides the sequence of GST in the 5' end, transformed competent cells and plated onto LB agar containing ampicillin (100 µg/ml). The colony that expressed the highest GST-galectin-8 in small-scale expression was used for large scale expression. One hundred µl of bacterial stock was spread on LB agar

containing ampicillin (100 μg/ml) and incubated at 37ºC overnight (no more than 16 hr). Three loopfuls of bacteria were inoculated into 100 ml of LB solution containing ampicillin (100 μg/ml) and were cultured for 2 hours at 37ºC with vigorous orbital shaking. At the end of culture, the 100 ml culture was diluted with 1 L of LB solution containing ampicillin (100 μg/ml) and was incubated at 37ºC with vigorous orbital shaking until the OD600 is around 0.8. IPTG was added to the culture at final concentration of 0.2 mM. After 4 hr of induction at 37ºC, cells were harvest by centrifuging at 5,000 rpm for 10 min at 4ºC, supernatants were discarded and the pellets were washed once with cold PBS. The pellets were resuspended in 20 ml of ice-cold PBS with lysozyme (5 mg/ml) and 2 tablets of complete protease inhibitor cocktail. After incubation on ice for 30 min, the suspension was sonicated at 40% output, 30 sec (pulse module: 4 sec on and 2 sec off) per cycle x 3 cycles with 1 min intervals. Two hundred ul of Triton X-100 was added to the lysates and incubated on ice for 30 min. The lysates were kept on ice all times during the procedure. The cell lysate was centrifuged at 18,000 rpm at 4ºC for 10 min. The supernatant was collected, passed through 0.45 μm filters, mixed with 3 ml (packed volume) of lactosyl-Sepharose beads, and rotated at 4ºC for 1 hr. The beads-suspension was transferred into a column and settled down. The column was washed with 90 ml of PBS with 4 mM β-mercaptoethanol and 0.2 mM PMSF. The bound GST-galectin-8 proteins were eluted with 100 mM lactose in PBS with 4 mM β-mercaptoethanol and 0.2 mM PMSF into 1-ml fractions. Fractions which contained proteins (measured by Bradford method) were collected and combined. The proteins containing 100 mM

lactose were dialyzed against 1 L of PBS with 5% glycerol and 4 mM β-mercaptoethanol three times at 4ºC. The protein concentration was determined by Bradford method and the activity was assessed by RBC agglutination assay. Proteins were stored as small-amount aliquots at -80ºC freezer.

For expression and purification of galectin-8 and Gal-8N tagged with thioredoxin (Trx) (Trx-galectin-8 and Trx-Gal-8N), human galectin-8 and Gal-8N constructs in BL21 (DE3) Star competent cells were plated onto LB agar containing ampicillin (50 μg/ml). The colony that expressed the highest Trx-galectin-8/Gal-8N in small-scale expression was used for large scale expression. One hundred μl of bacterial stock was spread on LB agar containing ampicillin (50 μg/ml) and incubated at 37ºC overnight (no more than 16 hr). Three loopfuls of bacteria were inoculated into 100 ml of LB solution containing ampicillin (50 μg/ml) and were cultured for 2 hours at 37ºC with vigorous orbital shaking. At the end of culture, the 100 ml culture was diluted with 1 L of LB solution containing ampicillin (50 μg/ml) and was incubated at 37ºC with vigorous orbital shaking until the OD600 is around 0.8. IPTG was added to the culture at final concentration of 1 mM. After 4 hr of induction at 37ºC, cells were harvest by centrifuging at 5,000 rpm for 15 min at 4ºC, supernatants were discarded and the pellets were washed once with cold PBS. The pellets were resuspended in 80 ml of ice-cold PBS with 2 mM EDTA and 4 mM β-mercaptoethanol. The resultant suspension was sonicated at 40% output, 1 min (pulse module: 4 sec on and 2 sec off) per cycle and paused for 3 min. This procedure was repeated 9 more times (10 cycles in total). The cell lysate was centrifuged at 12,000 rpm at 4ºC for

30 min. The supernatant was collected, passed through 0.45 μm filters, mixed with 4 ml (packed volume) of lactosyl-Sepharose beads, and rotated at 4ºC for 1 hr to overnight. At the end of incubation, the beads-suspension was centrifuged at 1,000 rpm for 2min, supernatants were removed, beads were resuspended in 10 ml PBS with 2 mM EDTA and 4 mM β-mercaptoethanol and transferred into a column. The column was washed with 50 ml of PBS with with 2 mM EDTA and 4 mM β-mercaptoethanol. The bound galectin-8/Gal-8N proteins were eluted with 150 mM lactose in PBS with with 2 mM EDTA and 4 mM β-mercaptoethanol into 1-ml fractions. Fractions which contained proteins (measured by Bradford method) were collected and combined. The proteins containing 150 mM lactose were dialyzed against 1 L of PBS with 5% glycerol three times at 4ºC. The protein concentration was determined by Bradford method and the activity was assessed by RBC agglutination assay. Proteins were stored as small-amount aliquots at -80ºC freezer.

Tag-free recombinant galectin-8 (35.8 kDa, the predominant isoform of galectin-8, also called galectin-8 isoform b) was used in this study except that GST-galectin-8 was used in affinity precipitation assays. To remove GST tag from GST-galectin-8, the fusion protein was incubated with human thrombin (Sigma, 2 U of thrombin per 1 mg of fusion protein) at 25ºC for 1 hr, followed by incubation with p-Aminobenzamidine-agarose (Sigma) to remove the added thrombin. To remove Trx tag from Trx-galectin-8, the fusion protein was incubated with enterokinase (BioLabs, 6.4 ng per 1 mg of fusion protein) at 4ºC overnight, followed by incubation with trypsin inhibitor agarose to remove the

added enterokinase. Endotoxin was removed by Detoxi-Gel endotoxin removing gel (Thermo Scientific) and endotoxin levels were detected by ToxinSensor chromogenic LAL endotoxin assay kit (Genscript). Endotoxin levels of all recombinant galectins used in this study were <0.1 EU/μg.

2.2 Quantitative RT-PCR.

Total RNA was extracted from normal, infected and chemically burned mouse corneas using the RNeasy Mini Kit (Qiagen, Valencia, CA). At least 4 corneas were pooled and considered one biological replica. Four biological replicas (N=4) were used. The quality and yield of each RNA preparation was determined using the Agilent BioAnalyzer 2100 with RNA Pico Lab-Chips. For normal corneas, expected yield is 0.5 to 1 μg; for inflamed corneas, expected yield is 2 to 5 μg. Quantitative RT-PCR was performed using Mx3000P or Mx4000 thermal cyclers (Stratagene, Santa Clara, CA). cDNA was synthesized from 100 ng total RNA using the High-Capacity cDNA Reverse Transcriptase Kit (Invitrogen). PCR amplification was performed in triplicate using gene-specific primers for β-actin, Gal-1, -3, -7, -8 and -9 (Invitrogen) and a master mix (Taqman® Gene Expression Master Mix; Invitrogen). Assay IDs for β-actin, Gal-1, -2, -3, -4, -7, -8 and -9 are Mm 00607939, Mm00839408, Mm00840285, Mm00802901, Mm01179060, Mm00456135, Mm01332239, and Mm00495295, respectively. For amplification, after an initial denaturation step (95°C for 10 minutes), the reactions were subjected to 40 cycles involving denaturation (95°C for 15 seconds) and annealing plus extension (60°C for 1 minute). A threshold cycle

value (C_t) was calculated from each amplification plot. Quantification data of each gene were normalized to the expression of β-actin. Relative gene expression was calculated with the ΔΔCT method. A value of 1.0 was given to the expression of each gene in the control cornea and the expression values for all other samples were calculated as a change in expression level with respect to the control cornea.

2.3 Immunofluorescence staining.

For immunofluorescence staining, frozen sections of the eyes were fixed with iced acetone (10 min, 25ºC), blocked with Image-iT FX signal enhancer (30 min, 25ºC, Invitrogen), and immunostained using primary antibodies (1:100 dilution in 5% BSA/PBS, overnight; same sources of the antibodies were used as indicated in the Western blot section) and Alexa Fluor® 488-conjugated anti-rat, Alexa Fluor 568®-conjugated anti-rabbit or Alexa Fluor 488®-conjugated anti-goat secondary antibodies (1:300 dilution in 5% BSA/PBS, 1 hr, 25ºC, Invitrogen). Negative controls with no applied primary antibody were also used. Fluorescence images were acquired by Lieca TCS SPE imaging system (Leica).

2.4 Corneal mouse micropocket lymphangiogenesis assay.

The corneal micropocket lymphangiogenesis assay was performed as described previously using implants containing a test agent, hydron, and sucralfate.[199,200] Poly-HEMA polymer (120 mg) was dissolved in 1 ml of absolute ethanol and incubated overnight with vortexing to make 12% stock. Sucralfate (6 mg) was

mixed with test agents in PBS, and the volume was reduced to 10 µl with centrifugal vacuum. The resultant pellets were mixed with 10 µl of 12% poly-HEMA and spread onto a mesh (15x15 squares, 300 µm nitrex nylon). Test agents included full-length galectin-8 (40 – 320 ng/pellet) and VEGF-C (160 ng/pellet). Implants containing poly-HEMA and sucralfate alone served as negative controls. The mice were anesthetized by intraperitoneal injection of a cocktail of ketamine (90 -120 mg/kg) and xylazine (10 mg/kg). The eyes were topically anesthetized with proparacaine and were gently proptosed with forceps. Using a corneal blade and a stereoscope, intrastromal linear keratotomy was performed about 2 mm from the limbus. Using a von Graefe knife (Miltex), a pocket was extended towards the limbus, and the pellet was maneuvered into the pocket. The wound was coated with a veterinary ophthalmic ointment (Akorn) to prevent infection. Mouse corneas were harvested 7 days after pellet implantation, fixed in 4% paraformaldehyde/PBS (1 hour at 4ºC), washed with PBS, and fixed again in iced acetone (15 min at -20ºC). To quantitate the extent of lymphangiogenesis in *Prox1*-EGFP reporter mice, flat mounts of the dissected corneas were evaluated by fluorescence microscopy. Fluorescent images were acquired by EVOS FL cell imaging system (Invitrogen), and vessel areas were calculated using the formula [200]: vessel area = pellet distance × vessel length × clock hours × 0.2 π. To quantitate the extent of lymphangiogenesis in WT and PDPN-deficient mice, corneas were stained with eFluor 570-anti-mouse LYVE-1 (clone ALY7, eBioScience, and 1:75) in 10% goat serum/0.2% Triton X-100/PBS overnight, 4ºC. After several washes with 0.2% Triton X-100/PBS, the corneas

were flattened and mounted with VECTASHIELD mounting medium (Vector Laboratories) and evaluated by fluorescence microscopy. In some experiments, for comparison purposes, corneas were stained with Alexa Fluor® 488-anti-mouse CD31 (clone MEC13.3, 1:100, BioLegend) to visualize blood vessels.

2.5 Mouse model of suture-induced inflammatory corneal lymphangiogenesis.

The mouse model of suture-induced lymphangiogenesis was used as previously described[201,202]. In brief, two 11-0 sutures were placed intrastromally about 2 mm from the limbus at the 12 and 6 o'clock positions in the *Prox1*-EGFP reporter mice. After surgery, a veterinary ophthalmic ointment was applied to prevent infection. Sutures were left in place for 7 days. To assess the effect of galectin inhibitors on suture-induced lymphangiogenesis, 10 µL of vehicle (PBS), TDG (200 mM in PBS), or Gal-8N (15 µg in PBS) were subconjunctivally injected on post-surgery days 0, 2, 4 and 6 using a 32 gauge needle with a 10 µL syringe (Hamilton). On day 7 post-surgery, mouse corneas were harvested and processed for staining with anti-LYVE-1 as described above. The areas of lymphatic vessels covering the whole corneas were calculated.

2.6 Knockdown with siRNA.

ON-TARGET plus human VEGFR-3 and Nrp2 siRNA SMART pool was purchased from Dharmacon/GE Healthcare. Oligonucleotide siRNA duplexes targeting PDPN and AllStars Negative control siRNA were purchased from

Qiagen. Of the four provided siRNA targeting PDPN, Hs_PDPN_1 and Hs_T1A-2_7 siRNA were able to knock down PDPN and were designated as PDPN siRNA1 and siRNA4, respectively. The transfection of siRNA in primary LECs (Lonza) was carried out with the Lipofectamine 2000 reagent (Invitrogen). Briefly, 3 µL of Lipofectamine 2000 in 250 µL of Opti-MEM medium (Invitrogen) and 3 µL of siRNA (20 µM) in 250 µL of Opti-MEM medium were incubated separately for 5 min at 25ºC, and the two mixtures were combined and incubated for an additional 20 min to form Lipofectamine 2000-siRNA complexes. At the end of the incubation period, serum-free Opti-MEM (1.5 ml) was added to each well of a 6-well plate and 500 µL aliquots of Lipofectamine 2000-siRNA complex were added to each well. Final concentration of siRNA was 30 nM. After 3 hr incubation, media were replaced with complete EGM-2MV medium (Lonza). The same procedure was repeated on the next day and knockdown efficiency was assessed by Western blot after 48 hr transfection.

2.7 Lymphatic endothelial cell (LEC) sprouting assay.

LEC spheroids were generated by seeding primary LECs at passage 4 or 5 in each well of 384-well hanging-drop plates (3D Biomatrix) in complete EGM-2 MV medium containing 0.25% methyl cellulose according to the manufacturer's instructions (750 cells/well). (It is critical to use LECs with lower passage numbers, specifically no more than passage 5, because the sprouting response is decreased as passage number increased). After 18 hours, LEC spheroids were collected, resuspended in serum-free EBM-2 basal medium, and mixed with

freshly-prepared collagen solution (PureCol collagen, Advanced BioMatrix, 2.2 mg/ml in M199 medium, pH adjusted to 7.4 with $NaHCO_3$ and NaOH). Aliquots of the LEC spheroid/collagen mixture (250 µl/well of 48-well plate) were incubated in the presence or absence of varying concentrations of various test agents in 50 ul PBS for 24 hr. At the end of the incubation period, spheroids were stained with Calcein AM (Invitrogen, 1 µg/mL, 37ºC, and 30 min). Fluorescent images were acquired using the EVOS FL cell imaging system, pixels were inverted for better visualization and cumulative length of each sprout was calculated. Results were expressed as fold change compared to corresponding controls. Of note, sprout lengths vary from passages to passages. Test agents used included thiodigalactoside (10 to 50 mM, Carbosynth), 3'-sialyl lactose (0.2 to 10 mM, Carbosynth), 6'-sialyl lactose (2 to 10 mM, Carbosynth), LY294002 (20 µM, Abcam), U0126 (20 µM, Abcam), PD0325901 (1 µM, Selleckchem), anti-integrin α9 functional grade antibody (clone Y9A2, 15 µg/ml, Biolegend), anti-integrin αvβ3 functional grade antibody (clone 23C6, 15 µg/ml, eBioscience), anti-integrin α5 (clone NKI-SAM-1, 15 µg/ml, eBioScience), anti-integrin β5 functional grade antibody (clone KN52, 15 µg/ml, eBioScience), mouse IgG isotype control functional grade antibody (15 µg/ml, eBioscience), Obtustatin (a blocking peptide targeting integrin α1β1, 2 µM, R&D Systems), and BIO1211 (a blocking peptide targeting integrin α4β1, 10 µM, R&D Systems).

2.8 Affinity precipitation assay.

Five mg of plant lectins (Vector Labs) and galectins were conjugated to 330 mg of Pierce® NHS-activated agarose dry resin in accordance with the manufacturer's instructions (Thermo Scientific). The agarose gels were stored at 4ºC. AT this temperatire, agarose-conjugated lectins are good for 1 to 2 years. Primary LECs (Lonza) were lysed in Triton lysis buffer (20 mM Tris-HCl, pH 7.4; 150 mM NaCl; 0.5% Triton X-100 with protease inhibitor cocktail). LEC lysates (250 µg in 500 µL lysis buffer supplemented with 10 mM $MgCl_2$) were incubated with 40 µL (50% slurry) of agarose-conjugated lectins (4ºC, overnight). Beads were pelleted by centrifugation at 3000 rpm for 1 min. Non-specific binding proteins were removed by washing the beads with Triton lysis buffer once and PBS twice. Supernatants were discarded; bound proteins were eluted by boiling the beads with 20 µL of 2× Laemmli sample buffer for 7 min, and examined by Western blotting.

2.9 Western blot analysis.

Materials.

- Triton lysis buffer, 2X, Boston BioProducts (Cat. No. BP-117X). Dilute with distilled water.
- Tris-Glycine-SDS running buffer, 10X, Boston BioProducts (Cat. No. BP-150). Dilute with distilled water.
- Transfer buffer, 10X, Boston BioProducts (Cat. No. BP-190). Dilute with distilled water and methanol (final concentration, 10%).

- Trans-Blot SD Semi-dry electrophoretic transfer cell, Bio-Rad (Cat. No. 170-3984). Transfer condition: 16 V, 30 min.
- Amersham® Protran® 0.2 μm nitrocellulose membrane, GE Healthcare (Cat. No. 10600001).
- PerfectWestern® containers, GenHunter (Cat. No. B-101).
- Laemmli (SDS-sample) buffer, reducing, 6X, Boston Bioproducts (Cat. No. BP-111R).
- Blocking buffer: Odyssey's blocking buffer (Li-Cor). Dilute to 0.5X with 0.1% Tween-20/PBS.

Procedures: Primary LECs were lysed with Triton lysis buffer supplemented with protease inhibitor cocktail and Phos-STOP phosphatase inhibitor cocktail (Roche), and subjected to electrophoresis in 4 - 15% SDS-PAGE gels (Bio-Rad). Protein blots of the gels were blocked with 0.5× Odyssey® blocking buffer (OBB, Li-COR). For AKT and ERK signaling, blots were incubated with primary antibodies (rabbit anti-ERK1/2, 1:7,500 dilution in 0.5× OBB, Cell Signaling Technology; mouse anti-phospho-ERK1/2, Thr202/Tyr204, 1:2,000 dilution in 0.5× OBB, Cell Signaling Technology; mouse anti-AKT1/2/3, 1:2,000 dilution in 0.5× OBB, Cell Signaling Technology; rabbit anti-phospho-AKT, Ser473, 1:1,500 dilution in 0.5× OBB, Cell Signaling Technology) in 5 ml of 0.5× OBB overnight at 4ºC. After washing with 0.5% Tween-20/PBS three times, the blots were incubated with appropriate secondary antibodies (donkey anti-rabbit IRDye 680LT and anti-mouse IRDye 800CW, Li-Cor) diluted in 5 ml of 0.5× OBB for 45

min at 25ºC. The blots were scanned by an Odyssey® Infrared Imaging System using Image Studio v2.0 software (Li-COR). For integrin signaling, blots were incubated with primary antibodies (rabbit anti-phospho-integrin β1, Tyr783, 1:750 dilution in 0.5× OBB, Abcam; rabbit anti-phospho-integrin β1, Thr788/789, 1:750 dilution in 0.5× OBB, Invitrogen; goat anti-integrin β1, N-20, 1:1,000, Santa Cruz Biotechnology; mouse anti-FAK, clone 77, 1:2,000 dilution in 0.5× OBB, BD Bioscience; anti-phospho-FAK, Tyr397, 1:2,000 dilution in 0.5× OBB, Invitrogen) in 5 ml of 0.5× OBB overnight at 4ºC. After washing with 0.5% Tween-20/PBS three times, the blots were incubated with appropriate secondary antibodies for 45 min at 25ºC. The blots were scanned by an Odyssey® Infrared Imaging System using Image Studio v2.0 software (Li-COR).

After scanning, the blots were stripped with NewBlot Nitrocellulose stripping buffer (25ºC, 10 min, Li-Cor) and were reprobed with primary antibodies (rabbit anti-VEGFR-3, clone C-20, 1:500 dilution in 0.5× OBB, Santa Cruz Biotechnology; rat anti-human PDPN, 1:2,000 dilution in 0.5× OBB, BioLegend; mouse anti-GAPDH, clone 6C5, 1:10,000 dilution in 0.5× OBB, Santa Cruz Biotechnology; mouse anti-β-actin, clone AC-15, 1:10,000 dilution in 0.5× OBB, Santa Cruz Biotechnology) in 5 ml 0.5× OBB overnight at 4ºC. The blots were developed using appropriate secondary antibodies (goat anti-rabbit IRDye 800CW; anti-rat IRDye 800CW; anti-mouse IRDye 680LT, 1:10,000 dilution in 5 ml of 0.5× OBB, Li-Cor) for 45 min at 25ºC. Signals were detected by Odyssey® Infrared Imaging System.

2.10 LEC chemotaxis assay.

Transwell (6.5 mm) with 8 μm-pore polycarbonate membrane inserts (Corning) were used in the migration assay. Both sides of the insert membranes were coated with fibronectin from human plasma (10 μg/ml, Sigma, F0895) (37ºC, overnight). LECs were serum-starved in serum-free EBM-2 medium overnight, detached with StemPro® Accutase® cell dissociation reagent, and resuspended in 0.5% FBS/EBM-2 medium (3×10^5 cells/ml). Aliquots of LEC suspension (200 μL of 3×10^5 cells/ml) were added to the upper chamber. The bottom chamber was filled with 600 μL of 1% FBS/EBM-2 in the presence or absence of VEGF-C (100 ng/ml) or galectin-8, and the plates were incubated at 37ºC for 2 hours. Inserts were fixed in absolute methanol (6 min, 25ºC) and stained with Giemsa stain (40 min, 25ºC, Sigma) per manufacturer's instructions. Membranes were wiped free of cells on the upper surface and mounted with Permount mounting medium (Fisher) on glass slides. The number of migrating cells in each condition was counted in 4 random fields at 10× magnification, averaged, and normalized to control condition to generate percent-change in migration activity.

2.11 LEC haptotaxis assay.

Transwell (6.5 mm) with 8 μm-pore polycarbonate membrane inserts (Corning) were used in the migration assay. The lower-side of the insert membranes were coated with 400 μL of fibronectin (10 μg/ml, Sigma) or galectin-8 (0.5 μM) (37ºC, overnight), and then the inserts were blocked with 0.1% BSA in PBS, 37ºC, 3 hr.

LECs were serum-starved in serum-free EBM-2 medium overnight, detached with StemPro® Accutase® cell dissociation reagent, and resuspended in serum-free EBM-2 medium (2×10^5 cells/ml). Aliquots of LEC suspension (200 µL of 2×10^5 cells/ml) were added to the upper chamber. The bottom chamber was filled with 600 µL of serum-free EBM-2 and the plates were incubated at 37ºC for 2 hours. Inserts were fixed in absolute methanol (6 min, 25ºC) and stained with Giemsa stain (40 min, 25ºC, Sigma) as described in "LEC chemotaxis assay". In some experiments, the cells were incubated in the presence of isotype control Ab (10 µg/ml, eBioScience) or the anti-PDPN functional blocking Ab (10 µg/ml, eBioScience). No LECs attached to BSA-coated membranes, and therefore this group was not included in the graphs.

2.12 Immunoprecipitation assay.

To determine the association among PDPN, galectin-8 and integrins, co-immunoprecipitation kit from Pierce was used (Cat. No. 26149). Briefly, mouse isotype antibody (15 µg, Santa Cruz Biotechnology) and anti-PDPN (15 µg, clone E-1, Santa Cruz Biotechnology) were immobilized onto AminoLink Plus coupling resin (Pierce) provided by the kit by sodium cyanoborohydride according to manufacturer's instructions. Primary LECs were serum-starved overnight and treated with galectin-8 (0.2 µM) for 15 min at 37ºC. After treatment, cells were lysed with IP lysis/wash buffer (25 mM Tris, 150 mM NaCl, 1 mM EDTA, 1% NP-40, 5% glycerol; pH 7.4) supplemented with protease inhibitor cocktails (Roche). After centrifugation (10 min, 13,000 rpm), supernatants (500 µg protein lysates)

were pre-cleared by incubation for 1 hr with Pierce control agarose resin provided by the kit at 4ºC. The clarified samples were incubated with the Ab-conjugated agarose resins overnight at 4ºC. Immunoprecipitates were washed three times with IP lysis/wash buffer provided by the kit and once with conditioning buffer provided by the kit (Pierce). The bound proteins were eluted with 50 µl of low pH elution buffer provided by the kit, neutralized with 3 µl of Tris-HCl (pH 9.0), and analyzed alongside with inputs by Western blotting using anti-integrin α1 (1:1,000 dilution in 0.5x OBB, Abcam), anti-integrin α5 (clone H-104, 1:1,000 dilution in 0.5x OBB, Santa Cruz Biotechnology), anti-integrin β1 (clone N-20, 1:1,000 dilution in 0.5x OBB, Santa Cruz Biotechnology), anti-PDPN, anti-galectin-8 (clone NBP1-66520, 1:1,000 dilution in 0.5x OBB, Novus Biologicals) and anti-GAPDH as describe above.

2.13 Glycosidase treatment.

To determine whether treatment with neuraminidase inhibits VEGFR-3 and PDPN interaction with galectin-8, primary LECs (3× 10^5 cells) were lifted with StemPro® Accutase® cell dissociation reagent, resuspended in 100 µL of PBS with 200 units of α2-3 neuraminidase (BioLabs), or 100 µL of G7 reaction buffer containing 2,000 units of peptide-N-glycosidase F (BioLabs) and 3 U of DNase I (Fisher). The reaction mixtures were incubated at 37ºC for 1 hr. Cell lysates were then subjected to affinity precipitation using galectin-8-conjugated agarose beads and bound proteins were analyzed by Western blot analysis using anti-VEGFR-3, anti-PDPN, anti-integrin α5, and anti-integrin β1.

2.14 Mice.

Lymphatic-specific *Prox1*-EGFP reporter mice (FVB background)[133] were purchased from Mutant Mouse Regional Resource Centers, FVB/NCrl mice were purchased from Charles River Laboratories, and C57BL/6 mice were purchased from Jackson Laboratory. Mice with inducible deletion of PDPN (*Pdpn$^{f/f}$;CagCre*) and wild-type littermates (*Pdpn$^{f/w}$;CagCre*) in mixed background (C57BL/6 and 129/Sv) were generated as previously described[203] (**Fig. 1**). PDPN deletion was accomplished by administering tamoxifen orally (20 μg each day) from P1 to P6. After weaning, the mice were orally administered 1 mg tamoxifen weekly. The *Lgals8* KO mouse strain used for this study was created from embryonic stem cell clone (14305A-F8), obtained from the KOMP Repository (www.komp.org) and generated by Regeneron Pharmaceuticals, Inc[204]. Details of the primer sequences and predicted PCR products are available at the Velocigene website (www.velocigene.com/komp/detail/14305). The *Lgals8* KO mice have no obvious defects in lymphatic vessel development examined by gross morphological analysis. The galectin-8 null status of the KO mice is confirmed by Western blotting (**Fig. 2**).

2.15 X-gal staining.

As the Lgals8 deletion was achieved by *LacZ* (bacterial β-galactosidase, β-gal) reporter gene replacement of Chromosome 13 from 12,440,786 (deletion start) to 12,459,212 (deletion end), expression of *LacZ* (β-gal) reflects the activity of the

promoter of galectin-8. To detect β-gal activity, we used an X-gal (substrate for β-gal) staining kit according to the manufacturer's instructions (Invivogen). Briefly, whole-mount tissues or frozen sections were fixed with 0.5% glutaraldehyde/PBS for 10 min, washed with PBS 3 times, and incubated the tissues or frozen sections in PBS-based staining solution (6 mM potassium ferricyanide, 6 mM potassium ferrocyanide, 2 mM $MgCl_2$, 0.02% Igepal, 0.01% sodium deoxycholate, 1 mg/ml X-Gal solution) for hours at room temperature. After extensive washes with PBS, the frozen sections were mounted with ProLong Gold anti-fade mounting medium (Invitrogen) and evaluated by the EVOS XL core imaging system.

Figure 1

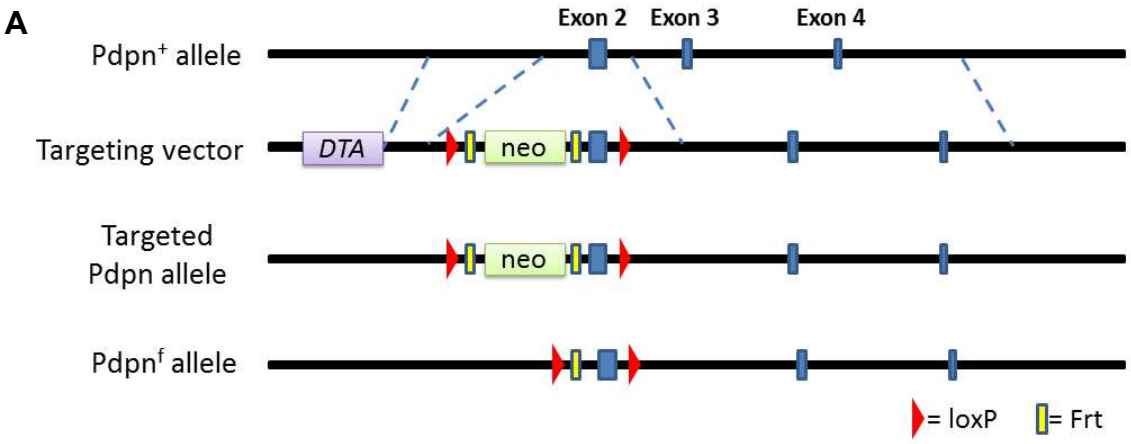
A
Exon 2
Exon 3
Exon 4
Pdpn+ allele
Targeting vector
DTA
neo
Targeted
Pdpn allele
neo
Pdpnf allele
= loxP
= Frt


B
Pdpnf/f
CagCre-ERT2
Pdpnf/f;CagCre

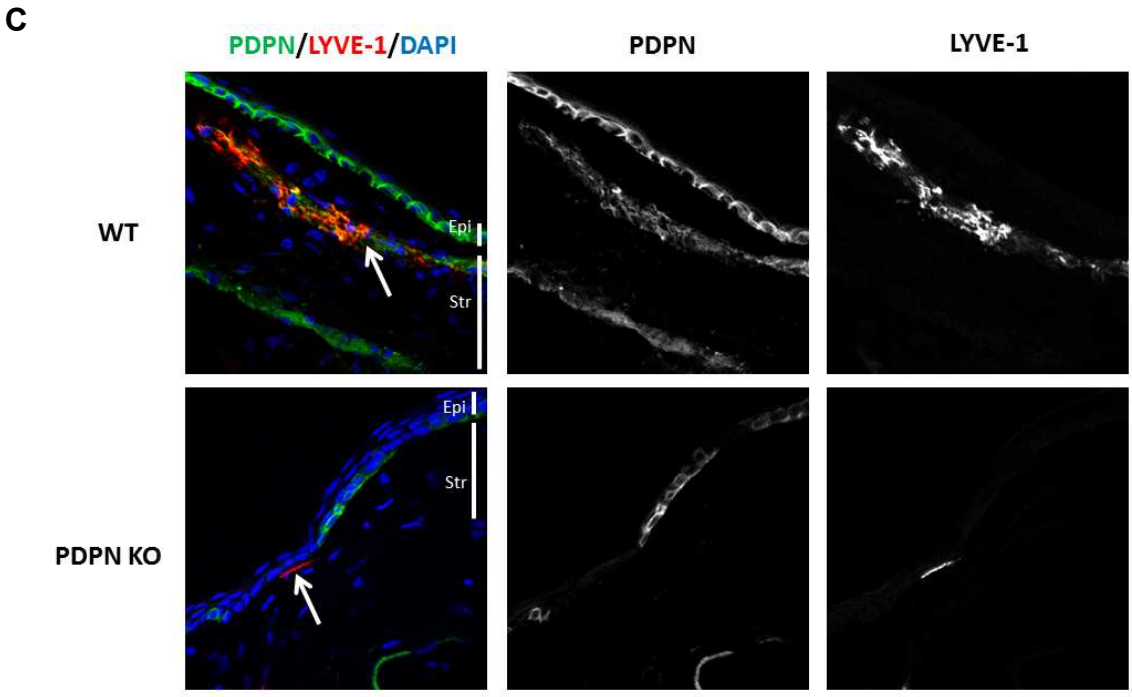
C
PDPN/LYVE-1/DAPI
PDPN
LYVE-1
WT
PDPN KO
Epi
Str
Epi
Str

Figure 1 (cont.)

D

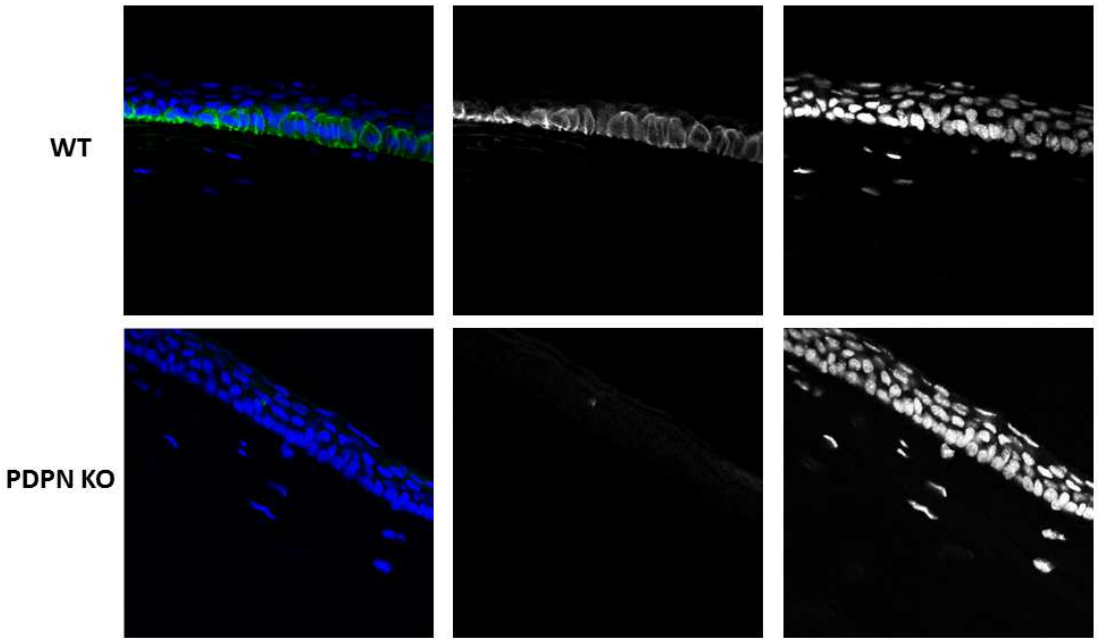

Figure 1. Generation of *Pdpn* floxed and globally inducible *Pdpn*-deficient mice, and confirmation of *Pdpn* null status in corneas. (A) Gene targeting strategy for generating mice with a Pdpn allele flanked by loxP sites (*Pdpn*^{f}). Exon 2 of *Pdpn* was flanked by loxP sites. (B) Breeding strategy to develop tamoxifen tamoxifen-inducible global PDPN-deficient mice, *Pdpn*$^{f/f}$*;CagCre* mice, by crossing *Pdpn*$^{f/f}$ mice with tamoxifen-inducible Cre-recominase transgenic mice (CAG-Cre-ER^{T2} Tg) under control of a ubiquitous fusion promoter, CMV-early enhancer element/chicken β-actin. (C and D) frozen sections were fixed with iced acetone for 10 min at room temperature, washed with 1% Tween-20/PBS (PBST) twice, blocked with Image-iT signal enhancer (Invitrogen) for 30 min at room temperature, washed with PBST once, stained with Alexa Fluor 488-conjugated anti-PDPN (1:100, BioLegend) and eFlour 570-conjugated anti-LYVE-1 (1:50, eBioScience) antibodies for 1.5 hr at RT, washed with PBST three times and washed with PBS once. Slides were mounted with ProLong Gold antifade reagent with DAPI and fluorescent images were captured by Leica SPE confocal microscopy. PDPN expression in lymphatic vessels in limbus area was not detectable after tamoxifen treatment. In addition, in the PDPN KO mice, staining pattern of PDPN was patched in basal epithelium around limbus area (C), but was homogenously undetectable in central corneal epithelium (D). Arrow: lymphatic vessel. Epi: epithelium; Str: stroma.

Figure 2

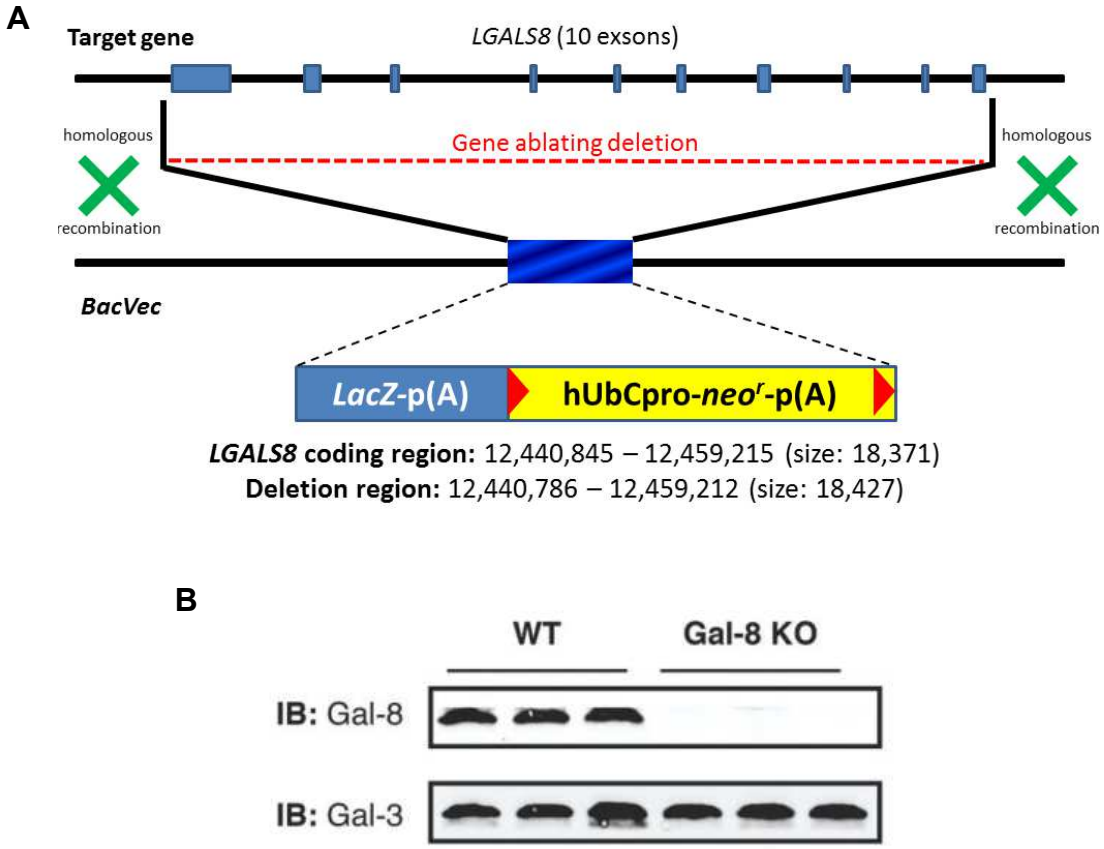

Figure 2. Galectin-8 knockout construct and confirmation of galectin-8 null status of the knockout mice. (A) *Lgals8* deletion was achieved by bacterial LacZ replacement of Chromosome 13 12,440,786 (deletion start) to 12,459,212 (deletion end). The whole coding region was deleted. Mice were genotype confirmed via PCR by the KOMP Repository. LacZ: β-galactosidase coding sequence from the *E. coli lacZ* gene; *neo*^{r}: coding sequence for neomycin; hUbCpro: promoter from the human ubiquitin C gene; p(A): polyadenylation signal; BacVec: large BAC-based targeting vector; red triangle: loxP site. (B) Equal amounts of liver tissue lysates (500 µg) from the WT and galectin-8 KO mice were incubated with lactosyl Sepharose beads at 4^0C overnight. Unbound proteins were removed, the bound proteins were eluted with 20 µL of 2× Laemmli sample buffer, and subjected to Western blotting by anti-galectin-8 and anti-galectin-3.

Results

3.1 Galectin expression pattern in control and inflamed corneas.

Pseudomonas aeruginosa infection in mouse corneas. To determine the galectin expression levels in normal and *P. aeruginosa*-infected corneas, tissue lysates of whole corneas collected on day 2 and day 8 post-infection (pi) (30μg) were subjected to electrophoresis. Protein blots were probed with specific antibodies for β-actin and galectins-1, -3, -7, -8, and -9. Fold-change values relative to β-actin expression of various galectins on day 2 and day 8 pi are shown in **Fig. 3**. Expression level of galectins-1, -3 and -7 were significantly decreased compared to normal mouse corneas on day 2 (% reduction: galectins-1 and -3: 70%; galectin-7: 35%) and day 8 pi (% reduction: galectin-1: 37%; galectin-3: 55%; galectin-7: 32%). In contrast, expression of galectins-8 and -9 was upregulated compared to normal mouse corneas on day 2 (% increase: galectin-8: 21%; galectin-9: 78%) and day 8 pi (% increase: galectin-8: 270%; galectin-9: 420%). Prior to use, each antibody was tested for specificity against recombinant human galectins-1, -3, -7 and -8 by Western blot analysis. Antibodies against galectins-1, -3, -7 and -8 did not cross-react with any other human galectins tested. The anti-mouse galectin-9 Ab does not cross-react to human galectin-9,[205-207] so the specificity of the Ab was not tested.

To investigate galectin expression pattern at the tissue level, frozen sections of normal and infected corneas were immunostained with anti-galectin antibodies. In normal corneas, galectin-1 immunoreactivity was mainly detected in corneal stroma, immunoreactivity of galectin-3 was detected mainly in corneal

epithelium (**Fig. 4**), and immunoreactivity of galectins-7, -8 and -9 was detected in both epithelium and stroma (**Fig. 4**). In *P. aeruginosa*-infected corneas, immunoreactivity of galectins-3, -7, -8 and -9 was detected in stroma as well as epithelium, whereas galectin-1 immunoreactivity was detected mainly in corneal stroma (**Fig. 4**). No staining was detected in control tissue sections.

To further analyze the galectin expression in different layers of corneas, corneal epithelium and stroma were separated by incubation in 20 mM EDTA for 20 min. Protein lysates (30 μg) from corneal epithelium and stroma collected on day 8 pi were subjected to electrophoresis (**Fig. 5A**). Protein blots were probed with specific antibodies for β-actin and galectins-1, -3, -7, -8, and -9. On day 8 pi, galectin-3 expression was markedly downregulated (% reduction: 58%), whereas galectins-1, -7, -8 and -9 were upregulated in epithelium of infected corneas compared to that of control corneas (fold increase: galectin-1: 10 fold; galectin-7: 2.6 fold; galectin-8: 1.6 fold; galectin-9: 2.6 fold) (**Fig. 5Bi**). In contrast, all five galectins were upregulated in the stroma of the infected corneas (fold increase: galectin-1: 1.8 fold; galectin-3: 1.3 fold; galectin-7: 2.9 fold; galectin-8: 3.0 fold; galectin-9: 6.4 fold) (**Fig. 5Bii**). Of note, although, in the immunofluorescence staining, galectin-1 was not detected in epithelium on day 8 pi (**Fig. 4**), Western blot analysis revealed that the lectin is upregulated in the epithelium of day 8 pi corneas. We reason that, in the IHC study, the robust immunoreactivity of galectin-1 in corneal stroma outshines the immunoreactivity of galectin-1 in corneal epithelium.

As determined by qRT-PCR, mRNA expression levels of galectins mRNA were ranked as galectin-3 > galectin-7 > galectin-8 > galectin-1 > galectin-9 in normal corneas; galectin-3 > galectin-7 > galectin-1 > galectin-8 > galectin-9 on day 2 pi corneas; and galectin-3 > galectin-1 > galectin-7 > galectin-8 > galectin-9 in day 8 pi corneas. Fold changes relative to β-actin expression of various galectins on day 2 and day 8 pi is shown in **Fig. 6**. Statistically significant differences were observed in relative gene expression levels of various galectins between normal and infected corneas on day 2 and day 8 pi. Galectin-1 mRNA expression levels increased 10-fold by day 2 and day 8 pi while galectin-3 and galectin-8 showed a 50% decrease by day 2 pi and a 75% decrease by day 8 in the infected corneas compared to the control cornea. Galectin-7 mRNA expression increased by 2-fold on day 2 pi but restored to normal levels by day 8 pi. Galectin-9 mRNA expression increased at both time points by 2.5- and 1.5-fold, respectively. Thus, consistent with changes in protein expression, galectin-3 mRNA was downregulated and galectin-9 mRNA expression was upregulated in infected corneas (**Fig. 3** and **6**). However, changes in protein expression level of galectins-1, -7, and -8 did not reflect changes in corresponding mRNA expression level. For example, compared to normal corneas, infected corneas exhibited: (i) increased galectin-1 mRNA but reduced galectin-1 protein expression on both day 2 and 8 pi, (ii) decreased galectin-7 protein expression, but increased galectin-7 mRNA expression on day 2 pi, and (iii) increased galectin-8 protein expression but reduced galectin-8 mRNA on day 8 pi. These

results were reproducible in four independent preparations of corneal protein extracts and mRNA.

Silver nitrate (AgNO3) cautery in mouse corneas. To determine the galectin expression levels in chemically injured corneas, tissue lysates of whole corneas collected on day 7 post injury (30µg) were subjected to electrophoresis. Analysis of the lysates of whole corneas revealed that compared to normal corneas, in chemically injured corneas, galectin-1 expression did not change, galectin-3 expression was significantly reduced (% reduction: 60%) and the expression of galectins-7, -8 and -9 was significantly increased (fold increase: galectin-7: 8.2 fold; galectin-8: 11 fold; galectin-9: 5 fold) (**Fig. 7**). Thus in both infected and cauterized corneas, galectin-3 expression was downregulated, whereas galectins-8 and -9 were upregulated (**Fig. 3** and **7**). Changes in the expression level of galectins-1 and -7 were distinct in infected and cauterized corneas. Expression of these two galectins were downregulated in infected corneas but was either upregulated (galectin-7) or did not change (galectin-1) in cauterized corneas.

Similar to infected corneas, robust immunoreactivity of all five galectins was detected in corneal stroma of the cauterized eyes (**Fig. 8**). Four different cauterized eyes were used and the immunofluorescence staining of all galectins tested in this study showed consistent results.

To further analyze the galectin expression in different layers of corneas, corneal epithelium and stroma of normal and cauterized (day 7) corneas were

separated, lysed with lysis buffer, and subjected to Western blotting (**Fig. 9A**). Compared to control corneas, in epithelium of cauterized corneas, galectin-1 expression was upregulated (% increase: galectin-1: 223%), whereas galectin-3 expression was markedly downregulated (% reduction: 96%), and there was no change in galectins-7, -8 and -9 expression (**Fig. 9Bi**). In the stroma of cauterized corneas, expression of these five galectins was upregulated (fold increase: galectin-1: 1.9 fold; galectin-3: 3.0 fold; galectin-7: 5.1 fold; galectin-8: 2.4 fold; galectin-9: 1.4 fold) (**Fig. 9Bii**).

As determined by qRT-PCR using RNA preparations of whole corneas, mRNA expression levels of galectins were ranked as galectin-3 > galectin-7 > galectin-8 > galectin-1 > galectin-9 in normal corneas and galectin-1 > galectin-7 > galectin-3 > galectin-8 > galectin-9 in cauterized corneas. Messenger RNA expression levels of galectins-1, -3, -7, -8 and -9 were all increased on day 7 post-cauterization compared to normal mouse cornea (**Fig. 10**; fold increase: galectin-1: 41 fold; galectin-3: 1.85 fold; galectin-7: 34 fold; galectin-8: 1.82 fold; galectin-9: 16 fold). Thus, consistent with changes detected by Western blot analysis, galectins-7, -8, and -9 mRNA expression was upregulated in cauterized corneas. However, changes in the protein expression of galectins-1 and -3 did not reflect changes in corresponding mRNA expression level. Compared to normal corneas, cauterized corneas expressed decreased galectin-3 protein, but increased galectin-3 mRNA. While galectin-1 protein expression level was similar in both normal and cauterized corneas, galectin-1 mRNA expression was higher in cauterized corneas. The extent of change in the expression level of mRNA

transcripts and the respective proteins may not be identical for a variety of reasons, such as variation in the RNA and protein turnover rates and stability as well as variations in the translational ratio of mRNA per protein among different cell types of the infiltrated infected and cauterized corneas.[208-213]

Mouse corneal allografts. To determine the galectin expression levels in corneal allografts, tissue lysates of whole corneas of accepted and rejected corneal allografts were collected on postoperative week 4, and analyzed separately. As a control, corneal discs marked with a 2 mm trephine and excised from normal C57BL/6 mice were mixed at a 1:1 ratio with corneas from normal BALB/c mice without the central corneal regions. Fold-change values relative to β-actin expression of various galectins are shown in **Fig. 11A**. Expression levels of all five galectins in both rejected and accepted corneal allografts were significantly increased compared to controls. There were distinct differences in the expression levels of galectins-8 and -9 between accepted and rejected grafts, as galectin-8 expression level in rejected corneal allografts was markedly higher (26.8-fold) than in accepted (9.0-fold) corneal allografts (**Fig. 11B**). Conversely, galectin-9 expression level in rejected corneal allografts was substantially lower (2.5-fold) compared to the accepted (11.5-fold) corneal allografts (**Fig. 11B**). Expression levels of galectins-1, -3 and -7 exhibited no significant differences between rejected and accepted corneal allografts (**Fig. 11B**).

To investigate galectin expression pattern at the tissue level, frozen sections from normal corneas and corneas with accepted and rejected allografts

on postoperative week 4 (N=3 each) were immunostained with anti-galectin antibodies. In normal corneas, galectin-1 was mainly expressed in corneal stroma; galectin-3 was mainly expressed in corneal epithelium, and galectins-7, -8 and -9 were expressed in both corneal stroma and epithelium (**Fig. 12**). Galectin-9 immunoreactivity in the normal corneal stroma was visible but at a much reduced intensity compared to that in the normal epithelium. In both rejected and accepted allografts, immunoreactivity of all five lectins was stronger compared to control. In addition, consistent with the results of the Western blot analysis, compared to the accepted grafts, there was increased galectin-8 immunoreactivity and decreased galectin-9 immunoreactivity in the rejected grafts. In addition, galectin-3 immunoreactivity in donor stroma was stronger in rejected grafts, whereas galectin-9 immunoreactivity in recipient stroma was stronger in accepted grafts (**Fig. 12**).

Galectin-8 expression in inflamed human corneas. In corneas of patients with graft failure and bacterial keratitis, numerous inflammatory cells were detected in the stroma as highlighted by periodic acid Schiff (PAS) staining (**Fig. 13**). Normal corneas expressed little galectin-8 (**Fig. 13**). In contrast, robust galectin-8 immunoreactivity was detected in corneas of patients with graft failure and bacterial keratitis (**Fig. 13**). No immunoreactivity was detected in the control human corneas which were treated the same way as the experimental group except that the step involving incubation with the primary antibody was omitted.

Cellular sources of galectin-8 in mouse corneas. To determine the expression pattern of galectin-8 in normal and inflamed mouse corneas, two different murine models of corneal inflammation were used. In mouse corneas treated with either thermal cautery or $AgNO_3$ cautery, intense galectin-8 immunoreactivity was detected in the stromal matrix (colocalization of type I collagen), whereas in untreated control corneas, galectin-8 expression was minimal (**Fig. 14**). In some areas, particularly in the anterior stroma region, galectin-8 and type I collagen immunoreactivity colocalized (**Fig. 14**). In addition, strong galectin-8 immunoreactivity was detected in lymphatic vessels ($CD31^{dim}LYVE\text{-}1^{+}$), whereas weak immunoreactivity of galectin-8 was observed in blood vessels ($CD31^{+}LYVE\text{-}1^{-}$) (**Fig. 14**). Consistent with our previous results,[214] trabecular meshwork also exhibited strong galectin-8 immunoreactivity (**Fig. 14**).

As for cellular source of galectin-8 in inflamed mouse corneas, galectin-8 immunoreactivity was detected in neutrophils ($Ly6G^{+}CD11b^{+}$), macrophages as well as a subset of dendritic cells ($F4/80^{+}CD11b^{+}$) and $CD4^{+}$ T cells ($CD4^{+}CD45^{+}$) (**Fig. 15**). Interestingly, some $F4/80^{+}$ cells in the posterior corneal stroma were negative for galectin-8 immunoreactivity (**Fig. 15**), suggesting that either a subset of $F4/80^{+}$ cells express galectin-8, or the cells need to be activated to express galectin-8. While it is reasonable to suggest that cells stained positively may be the possible source of the lectin, we note that paracrine actions of galectins have been reported. In this respect, galectins secreted by one cell type may bind to the glycan receptors on the adjacent cells. Therefore, the cells that exhibit

immunoreactivity with galectin-8 may not necessarily be the cells that produce the lectin.

As galectin-8 knockout was achieved by replacing *lgals8* with a bacterial reporter gene *LacZ*, which encodes bacterial β-galactosidase (β-gal), *LacZ* expression is under the control of the galectin-8 promoter and can be used to determine the tissue distribution and cellular sources of galectin-8. I first employed histochemical staining to localize *LacZ* expression in the galectin-8 KO mice. The substrate, 5-bromo-4-chloro-3-indolyl-β-D-galactoside (X-gal), is hydrolyzed by β-gal to generate galactose and soluble indoxyl molecules, which in turn are oxidized to insoluble indigo. The deep blue color generated by the hydrolysis of X-gal by β-gal was localized in corneal epithelium layer of untreated galectin-8 KO mice (**Fig. 16B**), indicating corneal epithelium is the major source of galectin-8 in control (untreated) corneas. In cauterized mouse corneas of galectin-8 KO mice, reporter protein β-gal activity was detected in both epithelium and stroma (**Fig. 16C**), indicating both corneal epithelial cells and stromal cells contribute to the upregulation of galectin-8 in injured mouse corneas. No X-gal precipitate was detected in the WT mouse corneas which were treated the same way as the KO mouse corneas (**Fig. 16A**).

To further determine the cellular sources of galectin-8, mouse corneas of galectin-8 KO mice were immunostained with anti-bacterial β-gal and other antibodies against immune cell markers. ($\beta\text{-gal}^+$ cells represent galectin-8-expressing cells). Similar to the immunofluorescence results in **Fig. 15**, some but not all immune cells expressed galectin-8, as some leukocytic ($CD45^+$) cells and

myeloid ($CD11b^+$) cells were negative for the reporter protein β-gal (**Fig. 17**). Of note, in the corneal epithelial layer, robust immunoreactivity of reporter protein β-gal was detected (**Fig. 17**), whereas weaker immunoreactivity of galectin-8 was observed using the anti-galectin-8 Ab from Novus Biologicals (**Fig. 15**). Such discrepancy may be explained by the epitope recognized by the anti-galectin-8 antibody (Novus Biologicals), which was raised against a synthesized peptide corresponding to amino acid 61-110 of the protein. The epitope is within the carbohydrate-binding groove of galectin-8 N-CRD, so it may be masked in the corneal epithelial layer. Accordingly, I used another anti-galectin-8 Ab (clone H-80, Santa Cruz Biotech) that recognizes the linker region of galectin-8 to perform the immunofluorescence staining. Consistent with the immunoreactivity of β-gal, robust galectin-8 immunoreactivity was observed in corneal epithelium (**Fig. 18**). In addition, strong galectin-8 immunoreactivity was shown in inflamed mouse stroma (**Fig. 18**) as observed in immunostaining using the anti-galectin-8 Ab from Novus Biologicals.

Figure 3.

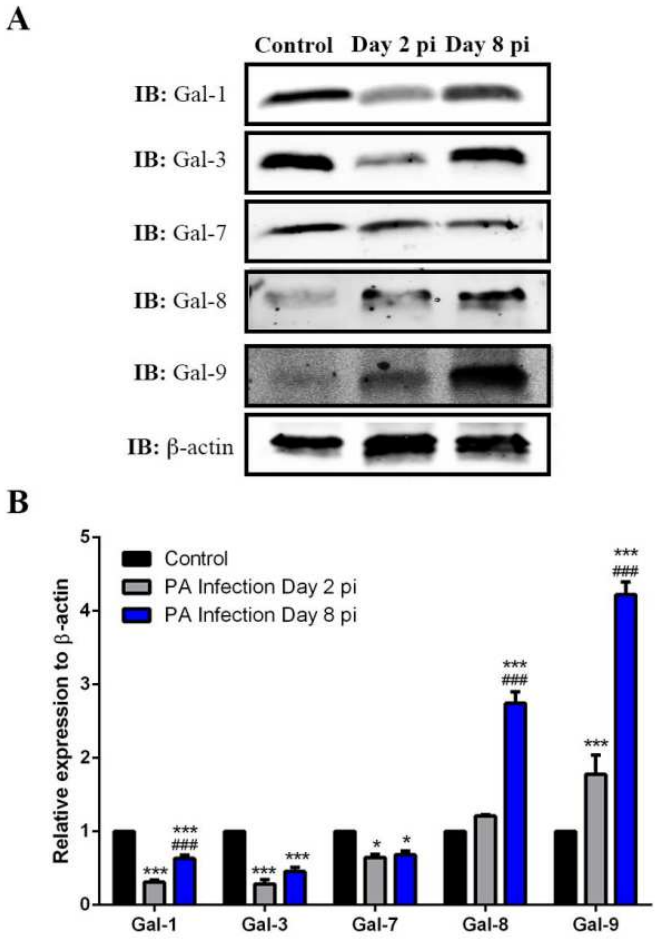

Figure 3. Analysis of galectin expression of normal and P. aeruginosa-infected corneas by Western blotting. Lysates of whole corneas containing 30 µg of protein were subjected to electrophoresis in 4% to 15% SDS-PAGE gels. Protein blots of the gels were probed using antibodies as descried in Methods. (A) Representative immunoblots. (B) Relative band intensity was quantified by ImageStudio. Expression value of each galectin was normalized to β-actin, a value of 1.0 was given to the expression of each galectin in the normal cornea and the expression values of galectins in the infected corneas were calculated as fold changes with respect to the control cornea. Three to four corneas were pooled and considered one biological replica. N = 4. Data are plotted as mean ± SEM and analyzed using one-way ANOVA. *P < 0.05, **P < 0.01, ***P < 0.001 versus control. ### P < 0.001 versus day 2 pi.

Figure 4.

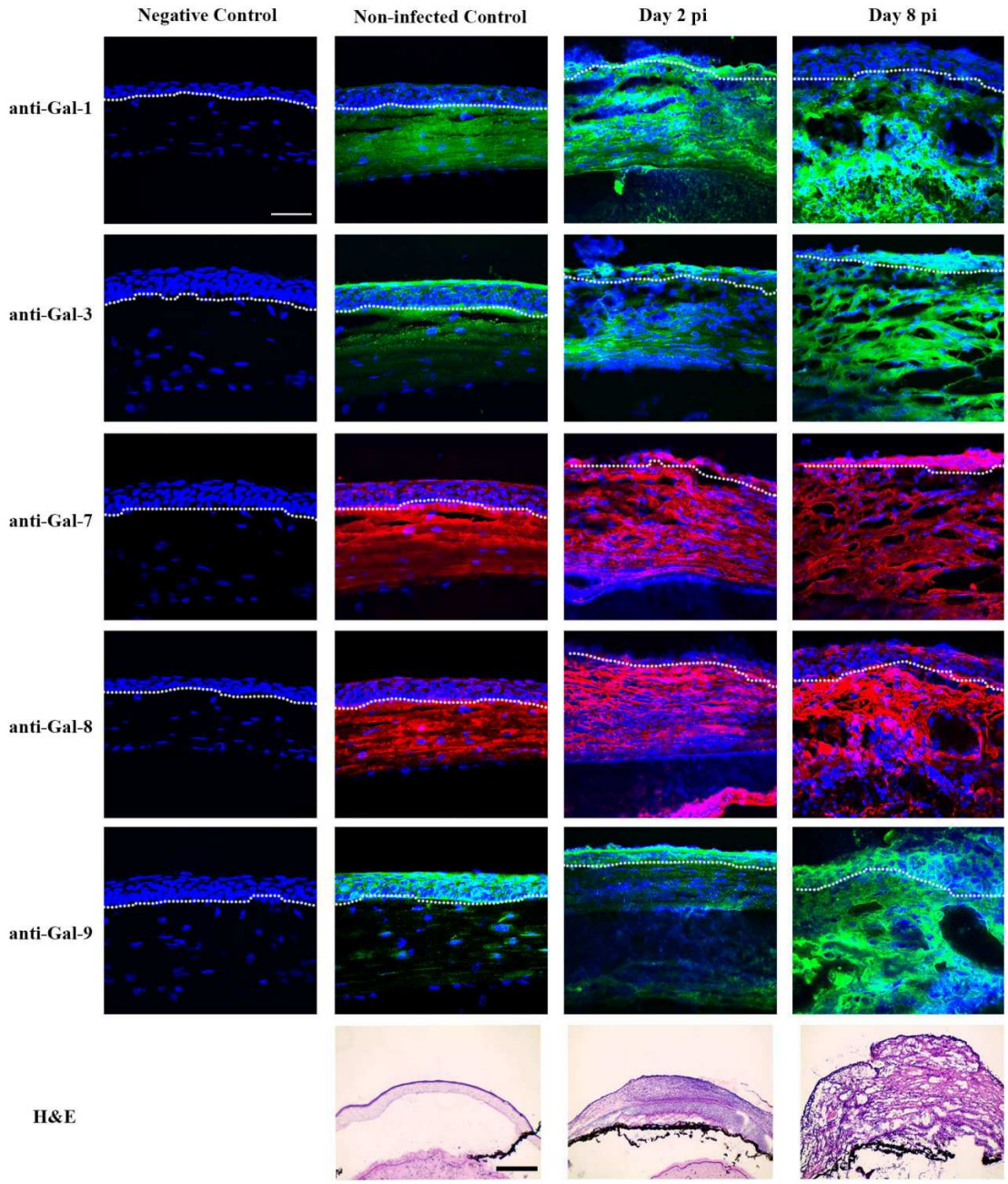

Figure 4. Immunofluorescence localization of galectins in normal and P. aeruginosa-infected mouse corneas. Frozen tissue sections of normal and infected eyes were immunostained using antibodies against Gal-1, -3, -7, -8, and -9, and Alexa fluor 488-conjugated anti-goat (for Gal-1, green), Alexa fluor 488-conjugated anti-rat (for Gal-3 and -9, green) and Alexa fluor 568-conjugated anti-rabbit (for Gal-7 and Gal-8, red), followed by counterstaining with DAPI (blue). No immunoreactivity was detected in corneas, which were treated the same way as

the experimental group except that the step involving incubation with the primary antibody was omitted (negative control). Tissue sections of the corneas stained with hematoxylin and eosin (H&E) are shown in the bottom panel. N ‡ 4 for each galectin. White dash lines outline the border between corneal epithelium and stroma. Note that in normal corneas, Gal-1 is expressed mainly in corneal stroma, Gal-3 is expressed mainly in corneal epithelium, and Gal-7, -8, and -9 are present in both epithelium and stroma, and in P. aeruginosa–infected corneas, immunoreactivity of Gal-3, -7, -8 and -9 is detected in both corneal epithelium and stroma, whereas Gal-1 is localized mainly in corneal stroma. Scale bar in immunofluorescence images: 50 lm. Scale bar in H&E staining images: 100 μm.

Figure 5.

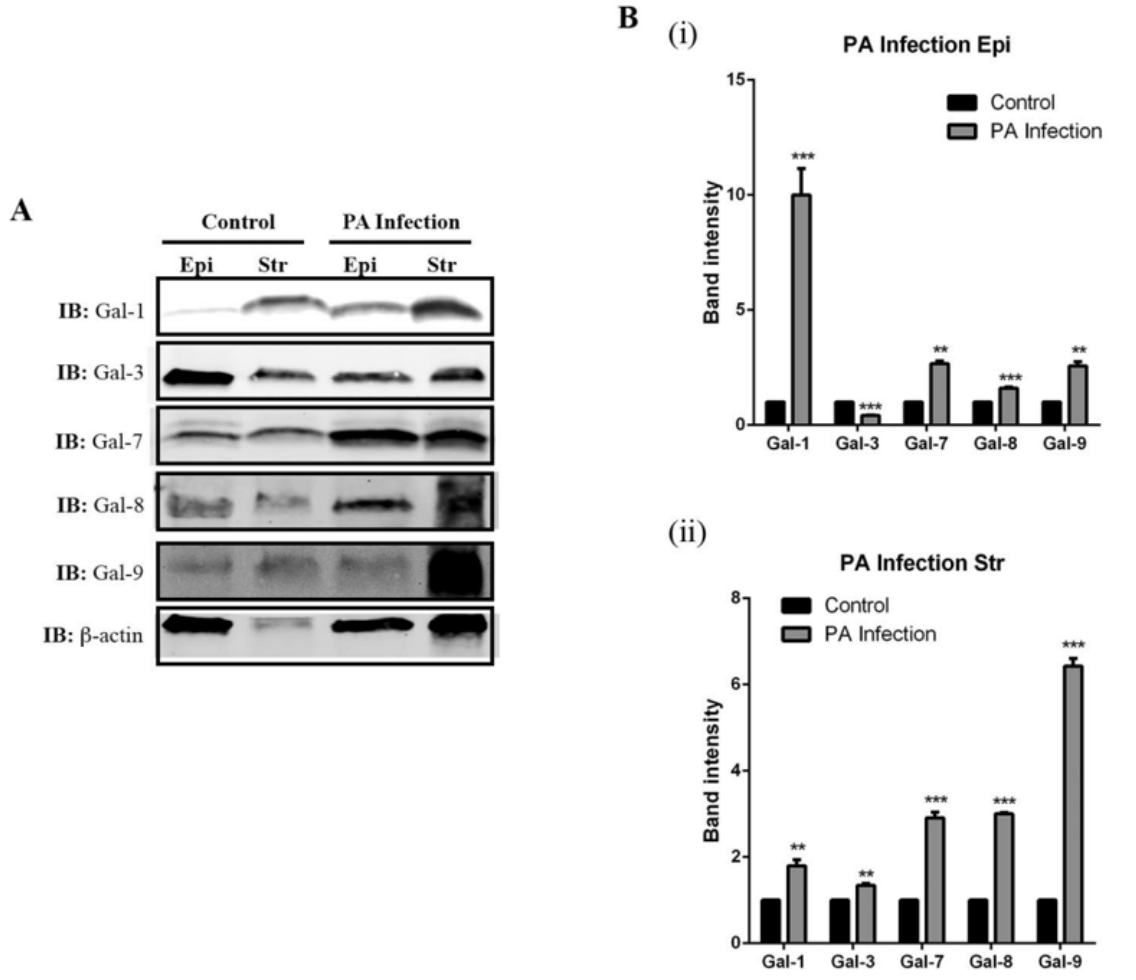

Figure 5. Galectin expression in corneal epithelium and stroma in normal and P. aeruginosa-infected eyes on day 8 pi. Corneal epithelial and stromal sheets were separated by incubation in 20 mM EDTA for 20 minutes. Aliquots of the lysates containing 30 lg of protein were subjected to electrophoresis in 4% to 15% SDS-PAGE gels. Protein blots of the gels were probed using antibodies as descried in Methods. (A) Representative immunoblots. (B) Band intensity was quantified by ImageStudio. Although equal amounts of lysates were used, the intensity of β-actin in normal cornel stroma is less than other conditions. Therefore, the galectin expression is not normalized to β-actin. Instead, a value of 1.0 was given to the expression of each galectin in the normal cornea and the expression values of galectins in the infected corneas were calculated as fold changes with respect to the control cornea. Three to four corneas were pooled and considered one biological replica. N = 3. Data are plotted as mean ± SEM and analyzed using Student's t-test. **P < 0.01, ***P < 0.001 versus control.

Figure 6.

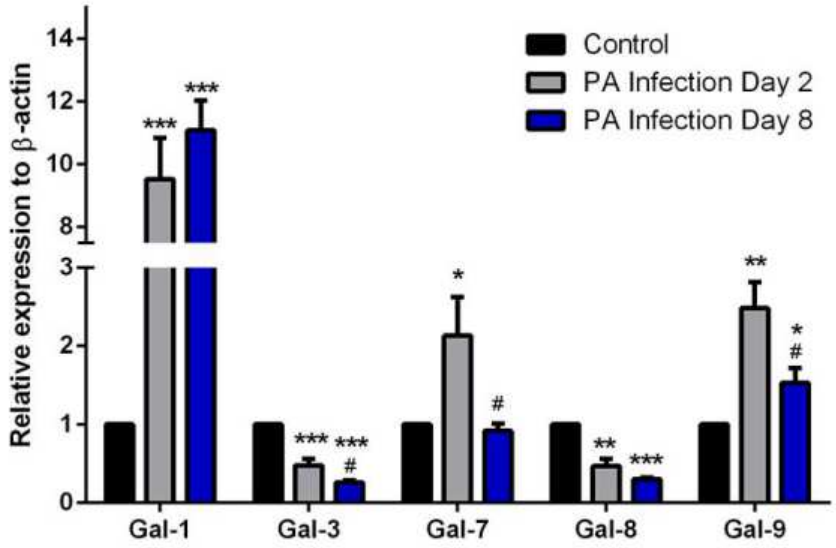

Figure 6. Analysis of mRNA expression levels of galectins in normal and P. aeruginosa-infected corneas by qRT-PCR. Complementary DNA was synthesized from 100 ng each of total RNA preparations of normal and infected corneas using the High-Capacity cDNA Reverse Transcriptase Kit, and PCR amplification was performed in triplicate using gene-specific primers for β-actin, galectins-1, -3, -7, -8, and -9 and a Taqman master mix according to the manufacturer's instructions. A threshold cycle value (Ct) was calculated from each amplification plot. Quantification data of each gene were normalized to the expression of β-actin, a value of 1.0 was given to the expression of each gene in the control cornea and the expression values for galectins in infected corneas were calculated as a change in expression level with respect to the control cornea. At least four corneas were pooled and considered one biological replica. N = 4 for all galectins. Data are plotted as mean ± SEM and analyzed using one-way ANOVA. *P < 0.05, **P < 0.01, ***P < 0.001 versus control. $^{\#}$P < 0.05 versus day 2 pi.

Figure 7.

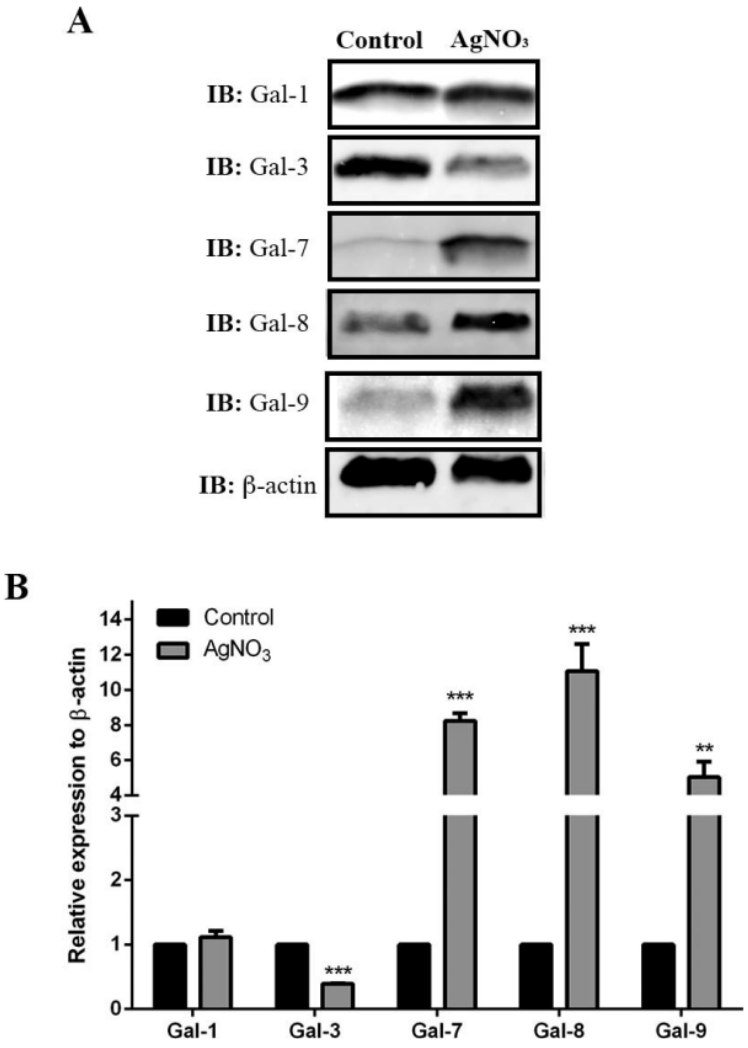

Figure 7. Analysis of galectin expression of normal and cauterized mouse corneas by Western blot. (A) Lysates of whole corneas were used to assess galectins-1, -3, -7, -8, and, -9 protein expression on day 7 post cauterization by Western blot analysis as described in Methods. (A) Representative immunoblots. (B) Relative band intensity was quantified by ImageStudio. Expression value of each galectin was normalized to β-actin, a value of 1.0 was given to the expression of each galectin in the normal cornea and the expression values of galectins in the infected corneas were calculated as fold changes with respect to the control cornea. Three to four corneas were pooled and considered one biological replica. N = 3. Data are plotted as mean ± SEM of four independent experiments. *P < 0.05, **P < 0.01, ***P < 0.001 versus control.

Figure 8.

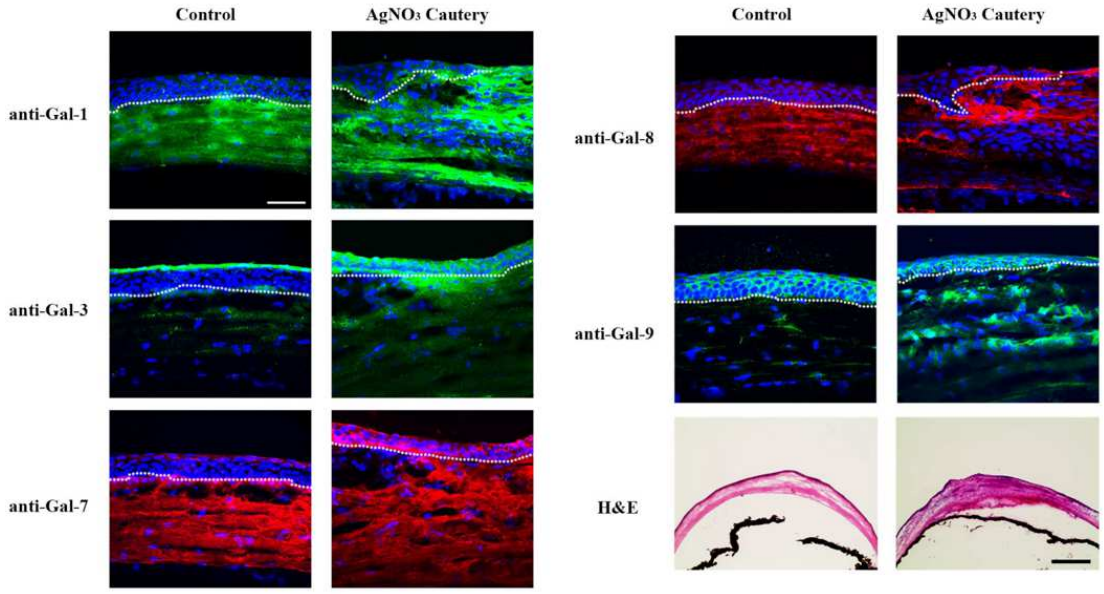

Figure 8. Immunofluorescence localization of galectins in normal and cauterized mouse corneas. Immunofluorescence localization of galectins in normal and cauterized mouse corneas. Frozen sections of normal and cauterized corneas (day 7) were stained with antibodies against galectins-1, -3, -7, -8, and -9 as described in Figure 3 legend. Mouse corneas stained with H&E are shown in the bottom panel. Note that in cauterized corneas, galectin-1 is detected mainly in the stroma, whereas galectins-3, -7, -8, and -9 are detected in both corneal epithelium and stroma. N = 4 for each galectin. Bar in immunofluorescence images: 50 μm. Bar in H&E staining images: 100 μm.

Figure 9.

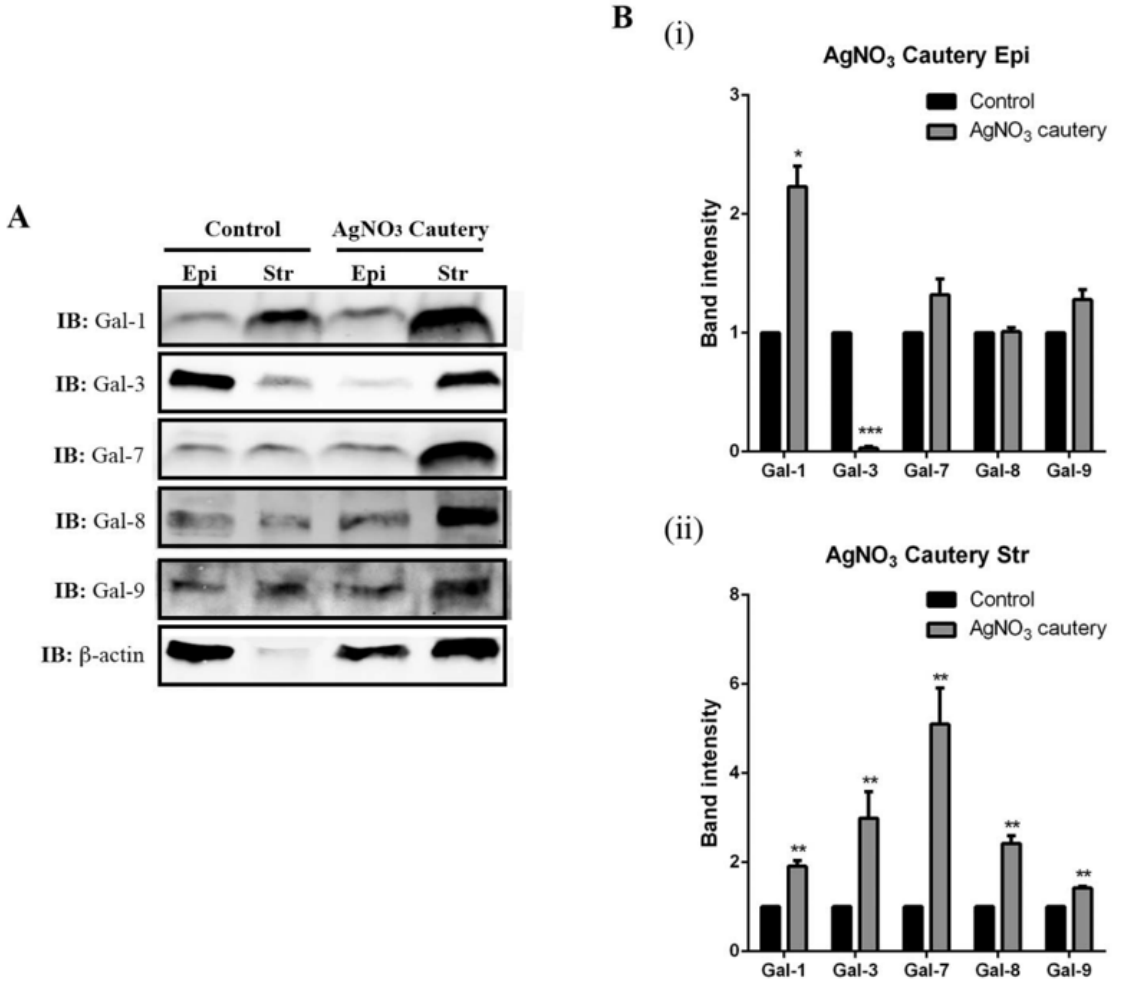

Figure 9. Galectin expression in corneal epithelium and stroma in normal and cauterized mouse eyes on day 7 post injury. Corneal epithelial and stromal sheets were separated by incubation in 20 mM EDTA for 20 minutes. Aliquots of the lysates containing 30 µg of protein were subjected to electrophoresis in 4% to 15% SDS-PAGE gels. Protein blots of the gels were probed using antibodies as descried in Methods. (A) Representative immunoblots. (B) Band intensity was quantified by ImageStudio. A value of 1.0 was given to the expression of each galectin in the normal cornea and the expression values of galectins in the cauterized corneas were calculated as fold changes with respect to the control cornea. Three to four corneas were pooled and considered one biological replica. N = 3. Data are plotted as Mean ± SEM and analyzed using Student's t-test. *P < 0.05, **P < 0.01, ***P < 0.001 versus control.

Figure 10.

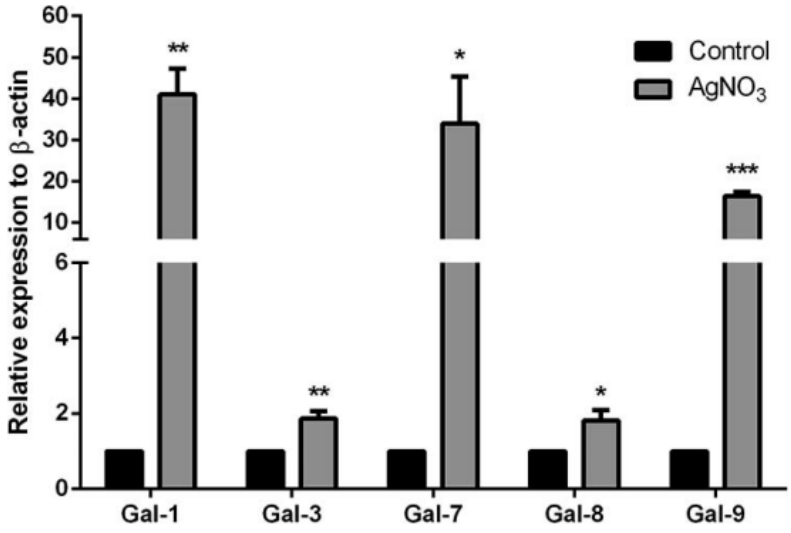

Figure 10. Analysis of mRNA expression levels of galectins in normal and cauterized mouse corneas by qRT-PCR. Messenger RNA expression levels were analyzed for galectins-1, -3, -7, -8, and -9 by RT-qPCR on day 7 post cauterization as described in Figure 5 legend. At least four corneas were pooled and considered one biological replica. N = 4 for all galectins. Quantification data of each gene were normalized to the expression of β-actin. A value of 1.0 was given to the expression of each gene in the control cornea and the expression values for all other samples were calculated as a change in expression level with respect to the control cornea. Data are plotted as mean ± SEM and analyzed using Student's t-test. *P < 0.05, **P < 0.01, ***P < 0.001 versus control.

Figure 11.

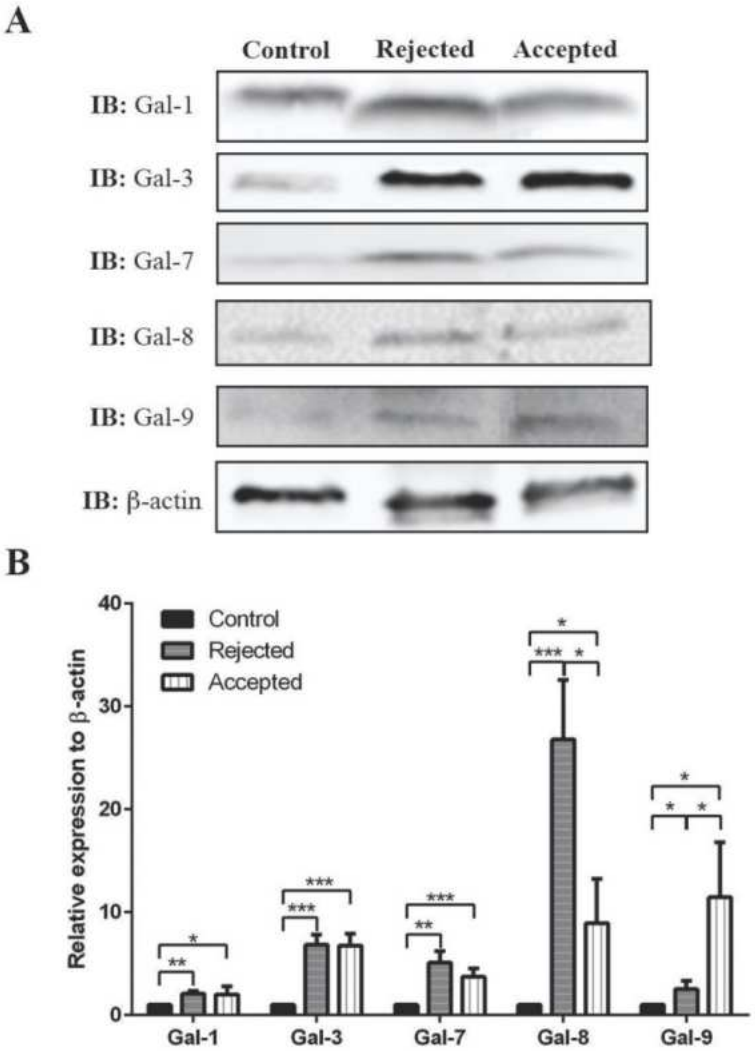

Figure 11. Analysis of galectin expression of normal mouse corneas and mouse corneas with rejected and accepted allografts by Western blot. Lysates of whole corneas containing 30 μg of protein were subjected to electrophoresis in 4% to 15% SDS-PAGE gels. Protein blots of the gels were probed using anti-galectin antibodies as described in Materials and Methods. A, Representative immunoblots. B, Relative band intensity was quantified by Image Studio. Expression value of each galectin was normalized to β-actin. A value of 1.0 was given to the expression of each galectin in the normal cornea, and the expression values of galectins in the rejected and accepted allografts were calculated as fold changes with respect to the cornea treated as control. Four or more corneas were pooled and considered 1 biological replica; N = 4. Data are plotted as mean ± SEM and analyzed using Student t test. *P < 0.05, **P < 0.01, ***P < 0.001.

Figure 12.

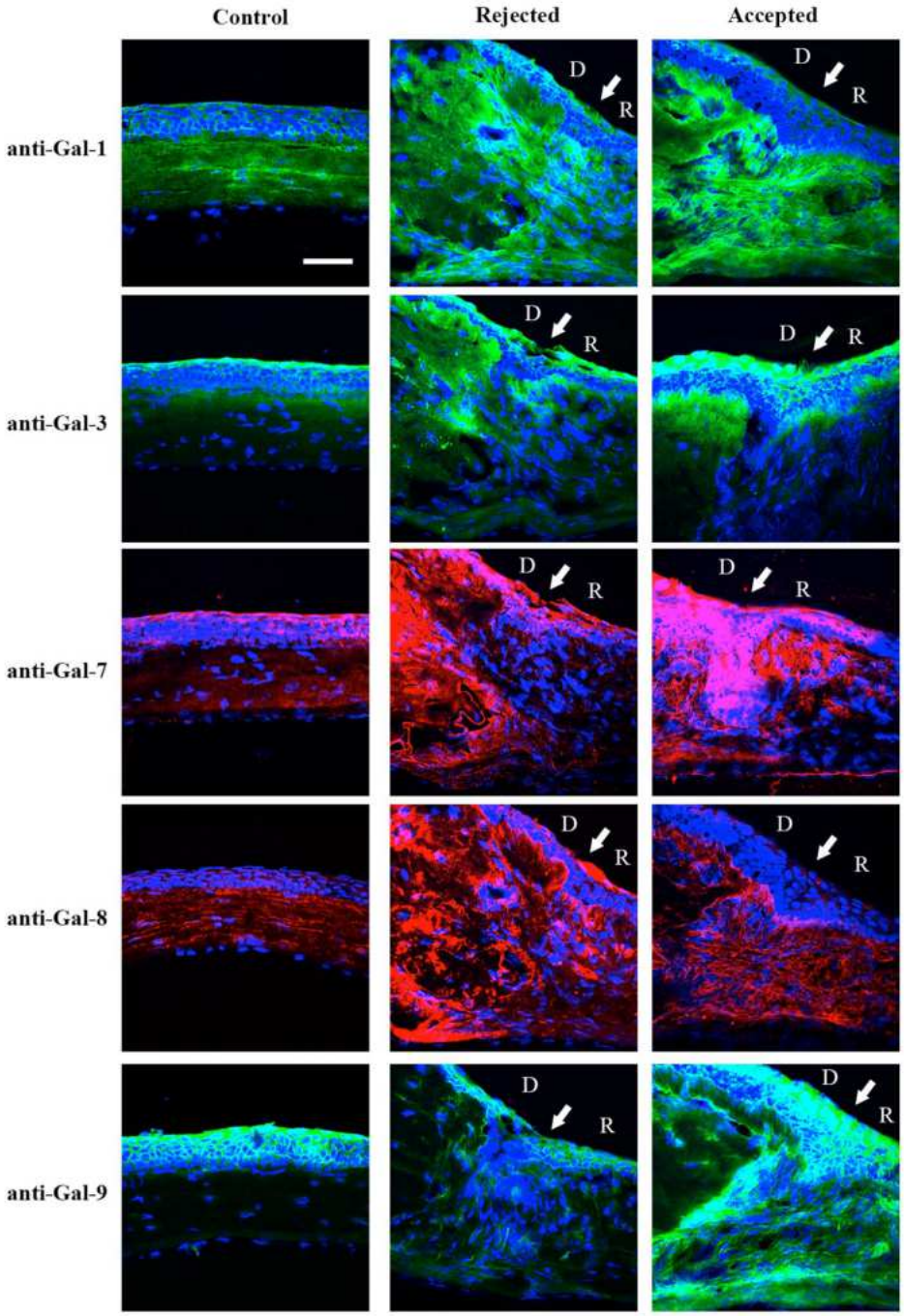

Figure 12. Immunofluorescence localization of galectins in normal mouse corneas and mouse corneas with rejected and accepted allografts. Frozen tissue sections were immunostained using antibodies against galectins-1, 3, 7, 8, and 9, and Alexa fluor 488–conjugated anti-goat (for galectin-1, green), Alexa fluor 488–conjugated anti-rat (for galectins-3 and 9, green) and Alexa fluor 568–

conjugated anti-rabbit (for galectins-7 and 8, red), followed by counterstaining with DAPI (blue). White arrows indicate the interface between the donor (D) and recipient (R). Immunostaining processing and exposure time of images in rejected and accepted allografts were the same. Note that in normal corneas, galectin-1 is expressed mainly in the corneal stroma, galectin-3 is expressed mainly in the corneal epithelium, and galectins-7, 8 and 9 are present in both epithelium and stroma. In both the rejected and accepted allografts, immune-reactivity of the 5 lectins is detected in both corneal epithelium and stroma. No immunoreactivity was detected in the corneas treated as controls that were treated the same way as the experimental group except that isotype control IgG was used as primary antibody or the step involving incubation with the primary antibody was omitted; N = 3 for each galectin. Bar = 50 μm.

Figure 13.

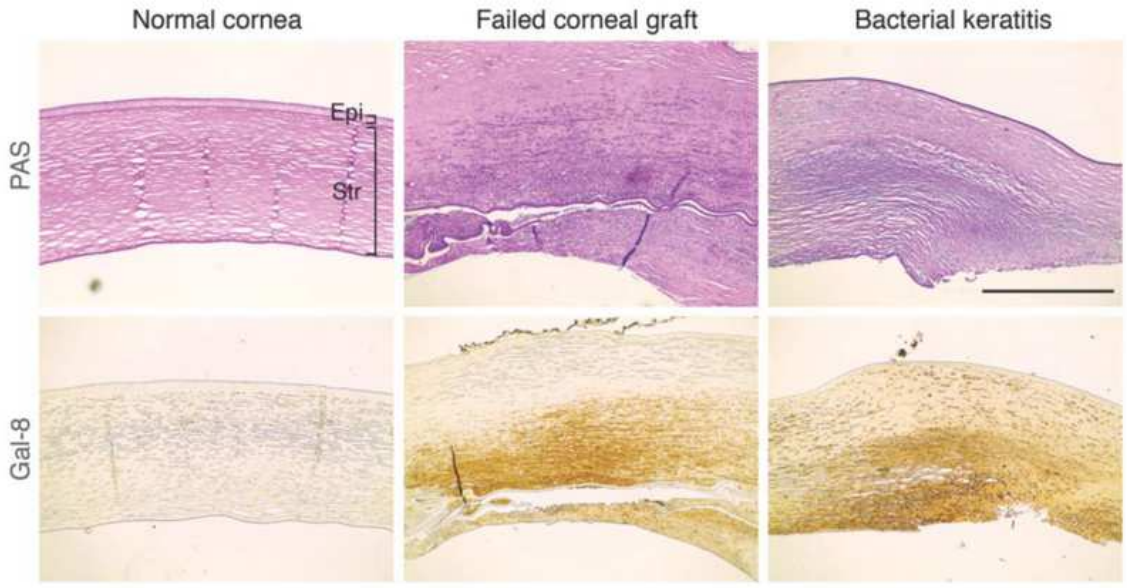

Figure 13. Immunohistochemical localization of galectin-8 in normal and inflamed human corneas. Normal human corneas and corneal buttons removed at keratoplasty from patients with corneal graft failure and bacterial keratitis were analyzed for galectin-8 immunoreactivity in paraffin sections. Brown color indicates positive immunostaining. Periodic acid-Schiff stained corneas from the corresponding cases are shown in the upper panel. Compared with the normal corneas, markedly greater galectin-8 immunoreactivity was detected in the corneal stroma of patients with graft failure and bacterial keratitis. In this study, 4 normal corneas and corneal buttons from 6 patients with graft failure, 4 patients with bacterial keratitis and 2 patients with Acanthamoeba keratitis were examined with reproducible results. Epi: epithelium; LV: lymphatic vessel; SC: endothelium of Schlemm's canal; Str: stroma; TM: trabecular meshwork. Bar: 400 μm.

Figure 14.

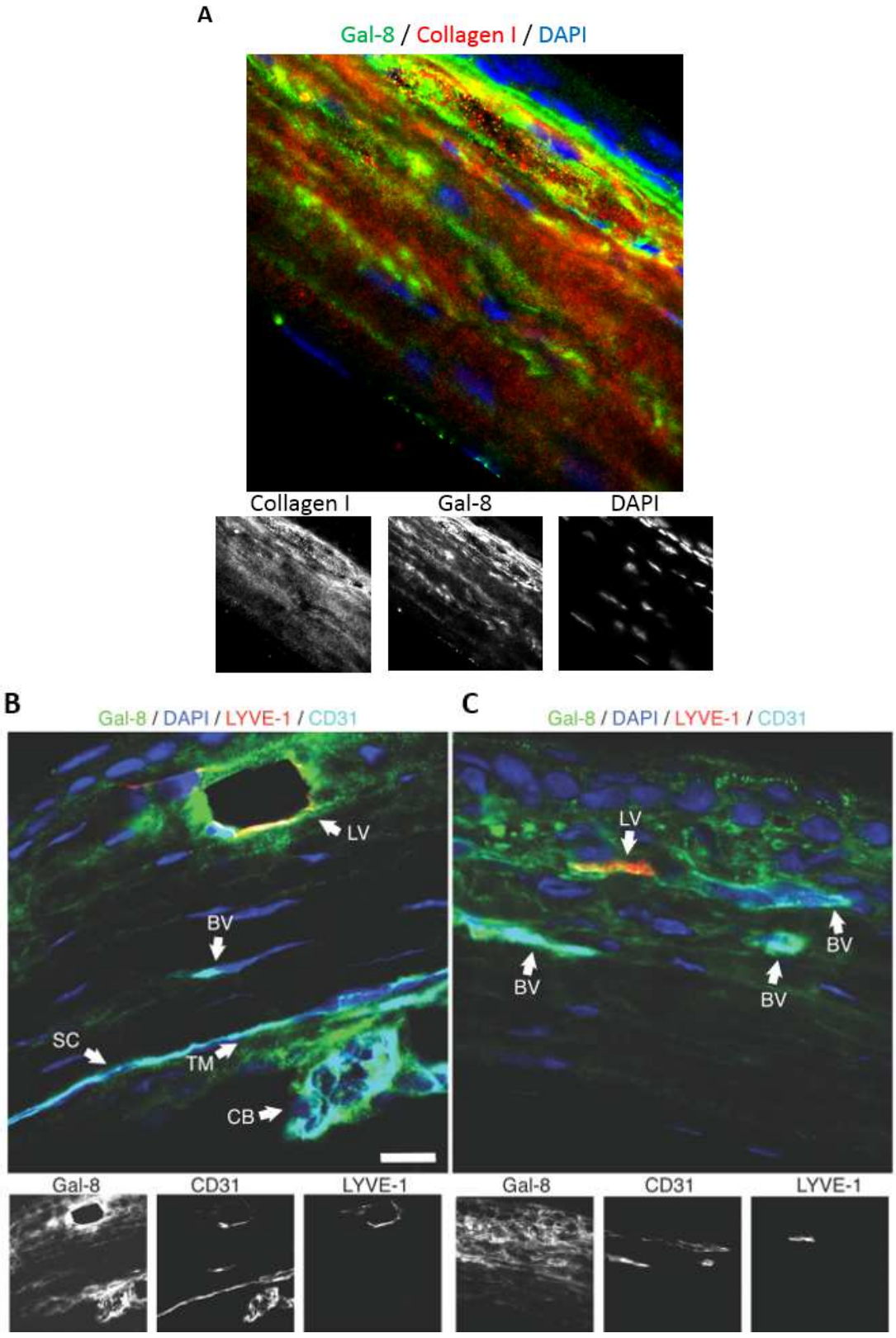
A
Gal-8 / Collagen I / DAPI
Collagen I
Gal-8
DAPI
B
Gal-8 / DAPI / LYVE-1 / CD31
LV
BV
SC
TM
CB
C
Gal-8 / DAPI / LYVE-1 / CD31
LV
BV
BV
BV
Gal-8
CD31
LYVE-1
Gal-8
CD31
LYVE-1

Figure 14. Immunofluorescence localization of galecin-8 in extracellular matrix and blood/lymphatic vessels in mouse corneas. (**A**) Mouse corneas subjected to alkaline burn were allowed to heal *in vivo* for 2 weeks and were then analyzed for galectin-8 (green) and type I collagen (red) immunoreactivity. Immunoreactivity of galectin-8 colocalizes with collagen I, especially in the anterior corneas. (**B**) Frozen sections of normal mouse corneas were analyzed for galectin-8 (green), CD31 (cyan) and LYVE-1 (red) immunoreactivity. Immunoreactivity of galectin-8 are detected in lymphatic vessels, endothelium of Schlemm's canal, and trabecular meshwork. (**C**) Frozen sections of mouse rejected allografts were analyzed for galectin-8 (green), CD31 (cyan) and LYVE-1 (red) immunoreactivity. Immunoreactivity of galectin-8 is detected in both lymphatic vessels and blood vessels in the inflamed mouse cornea. Bar: 10 μm. BV: blood vessel, CB: ciliary body, Epi: epithelium; LV: lymphatic vessel; SC: endothelium of Schlemm's canal; Str: stroma; TM: trabecular meshwork.

Figure 15.

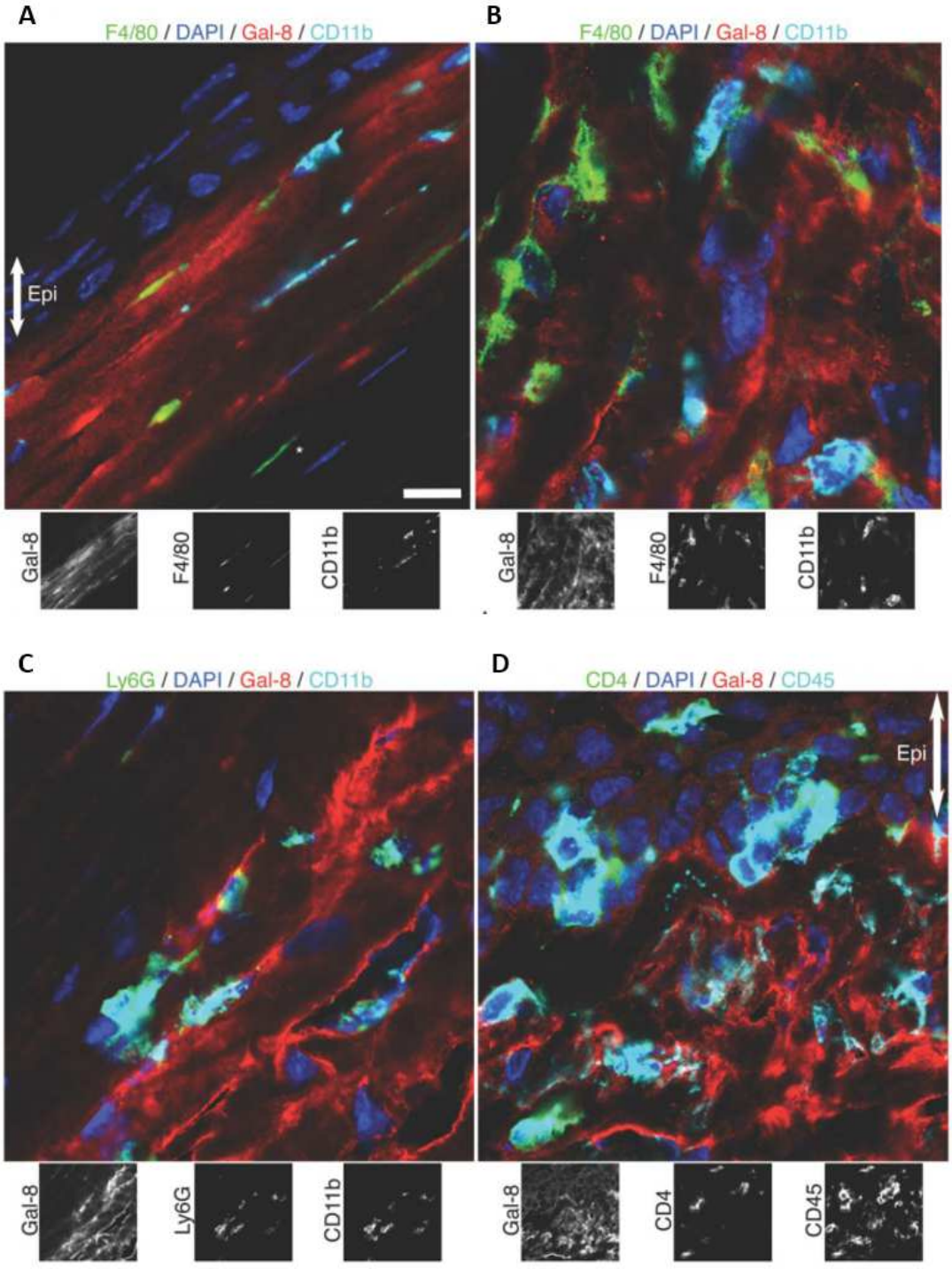
A
F4/80 / DAPI / Gal-8 / CD11b
Epi
Gal-8
F4/80
CD11b
B
F4/80 / DAPI / Gal-8 / CD11b
Gal-8
F4/80
CD11b
C
Ly6G / DAPI / Gal-8 / CD11b
Gal-8
Ly6G
CD11b
D
CD4 / DAPI / Gal-8 / CD45
Epi
Gal-8
CD4
CD45

Figure 15. Immunofluorescence localization of galecin-8 in infiltrated immune cells in inflamed mouse corneas. (A−D) Frozen sections of thermal cauterized mouse corneas on postoperative day 1 (a) and rejected mouse corneal allografts on postoperative week 4 (B−D) were fixed in 4% paraformaldehyde/PBS, permeabilized with 0.3% Triton X-100/PBS, stained with anti-galectin-8 and biotinylated anti-Ly6G, followed by incubation with Alexa Fluor 488-labeled F4/80 (green), Alexa Fluor 488-labeled CD4 (green), Alexa Fluor 647-labeled CD11b (cyan), Alexa Flour 647-labeld CD45 (cyan), Alexa Fluor 488-labeled streptavidin (green) and Alexa Fluor 568-labeled anti-rabbit IgG (red). Nuclei were counterstained with DAPI (blue). Macrophages and a subset of dendritic cells were stained positively with anti-F4/80 and anti-CD11b, and most of the $F4/80^{+}$ cells were $CD11b^{dim}$ (A, B); neutrophils were stained positively with anti-Ly6G and anti-CD11b (C); $CD4^{+}$ T cells were stained positively with anti-CD4 and anti-CD45 (D). The white asterisk indicates a $F4/80^{+}$ but galectin-8^{-} cell (A). Bar: 10 μm. Epi: epithelium.

Figure 16.

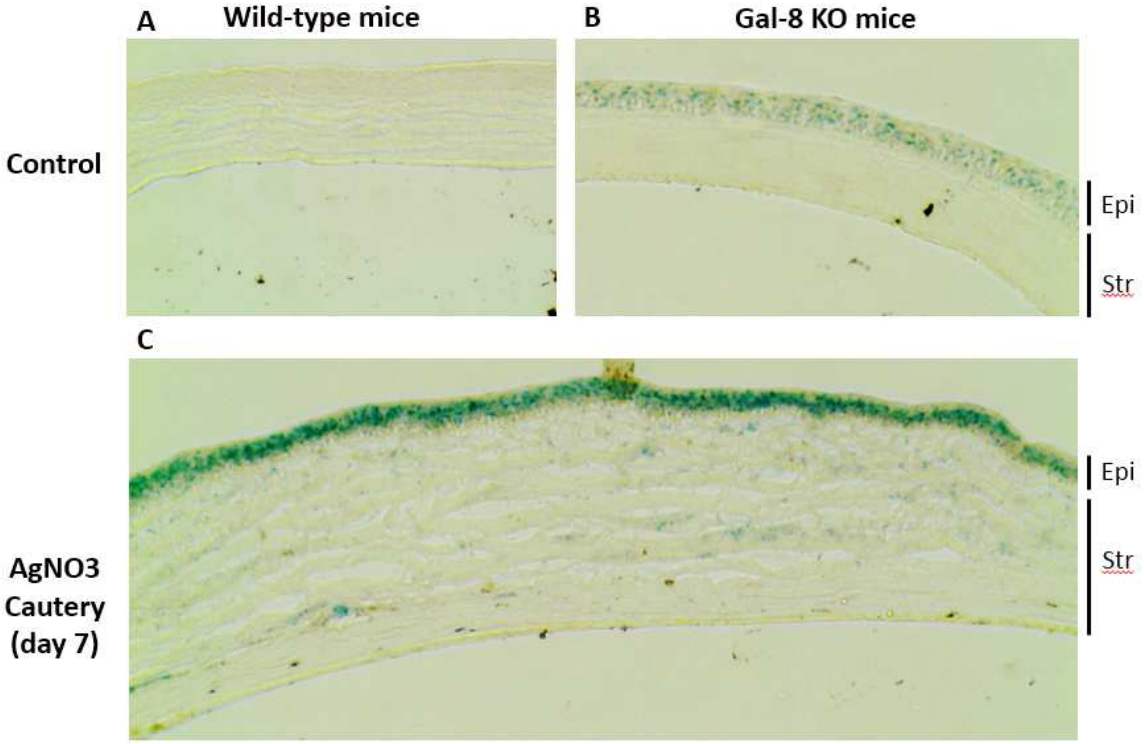

Figure 16. X-gal staining in control and cauterized mouse corneas of galectin-8 KO mice. Frozen sections of normal mouse corneas of WT (**A**), untreated mouse corneas of galectin-8 KO mice (**B**), and AgNO3-cauterized mouse corneas of galectin-8 KO mice (**C**) were fixed with glutaraldehyde, washed with PBS, and stained for β-gal activity using X-gal as described in the Method. Note that deep blue color (X-gal precipitate) is observed in corneal epithelium of untreated and cauterized corneas of galectin-8 KO mice, whereas X-gal precipitate is only observed in corneal stroma of cauterized corneas. Epi: epithelium; Str: stroma.

Figure 17.

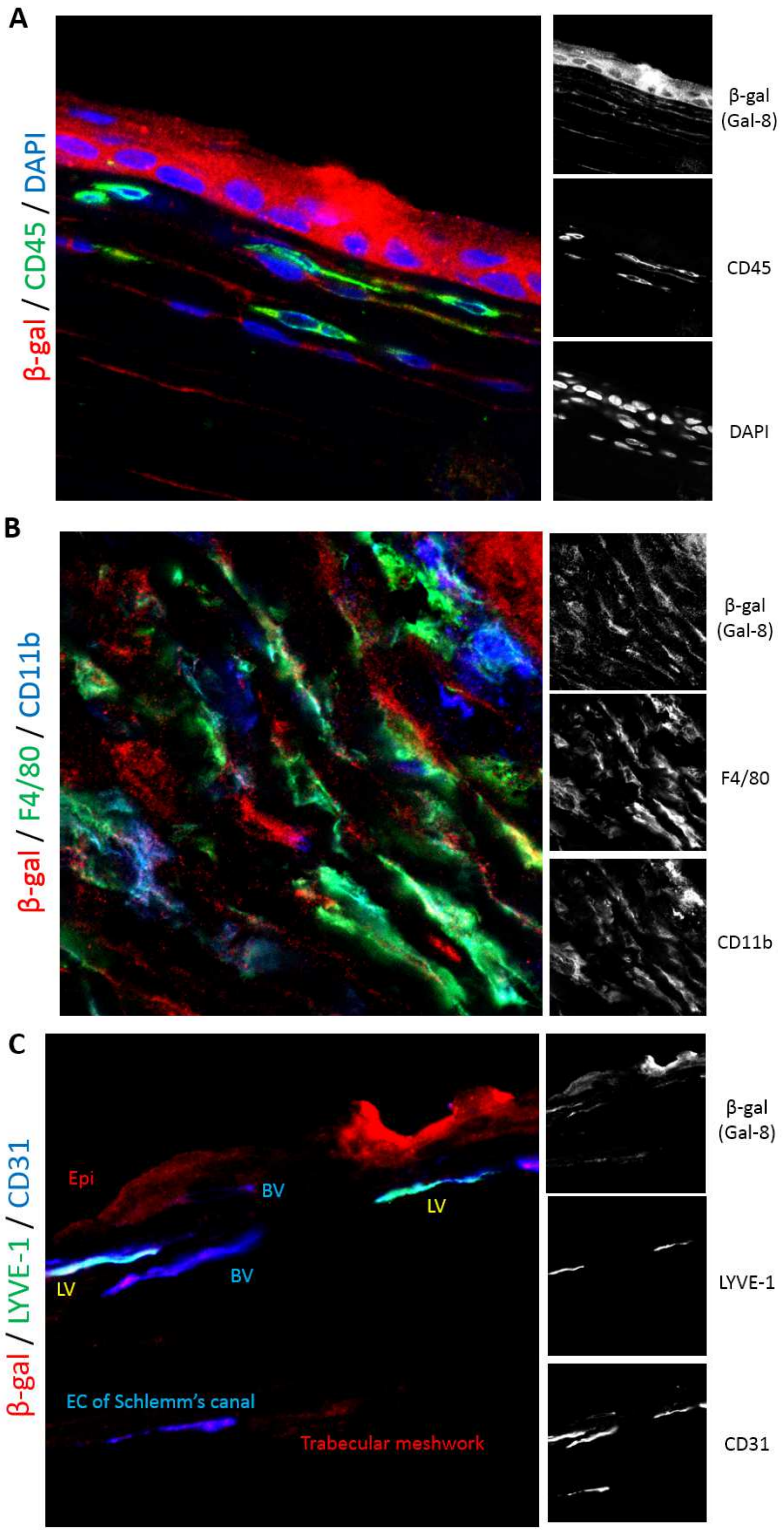
A
β-gal / CD45 / DAPI
β-gal (Gal-8)
CD45
DAPI
B
β-gal / F4/80 / CD11b
β-gal (Gal-8)
F4/80
CD11b
C
β-gal / LYVE-1 / CD31
Epi
BV
LV
LV
BV
EC of Schlemm's canal
Trabecular meshwork
β-gal (Gal-8)
LYVE-1
CD31

Figure 17. Immunofluorescence localization of bacterial β-galactosidase in cauterized mouse corneas of galectin-8 KO mice. (A−C) Frozen sections of $AgNO_3$-cauterized corneas of galectin-8 KO mice on postoperative day 7 were fixed in 4% paraformaldehyde/PBS, permeabilized with 0.3% Triton X-100/PBS, stained with anti-β-gal (red), anti-CD45 (green), anti-F4/80 (green), anti-CD11b (blue), anti-CD31 (blue) and anti-LYVE-1 (green). Nuclei were counterstained with DAPI (blue) in A. Note that immunoreactivity of β-gal (representing galectin-8^+ cells) are detected in epithelial layers (A to C), $CD45^+$ cells (A), $F4/80^+CD11b^+$ cells, blood vessels (C), lymphatic vessels (C), endothelium of Schlemm's canal (C) and trabecular meshwork (C). However, some $CD45^+$ cells (A) and some $F4/80^+CD11b^+$ cells (B) are β-gal^-. Epi: epithelium; BV: blood vessels; LV: lymphatic vessels.

Figure 18.

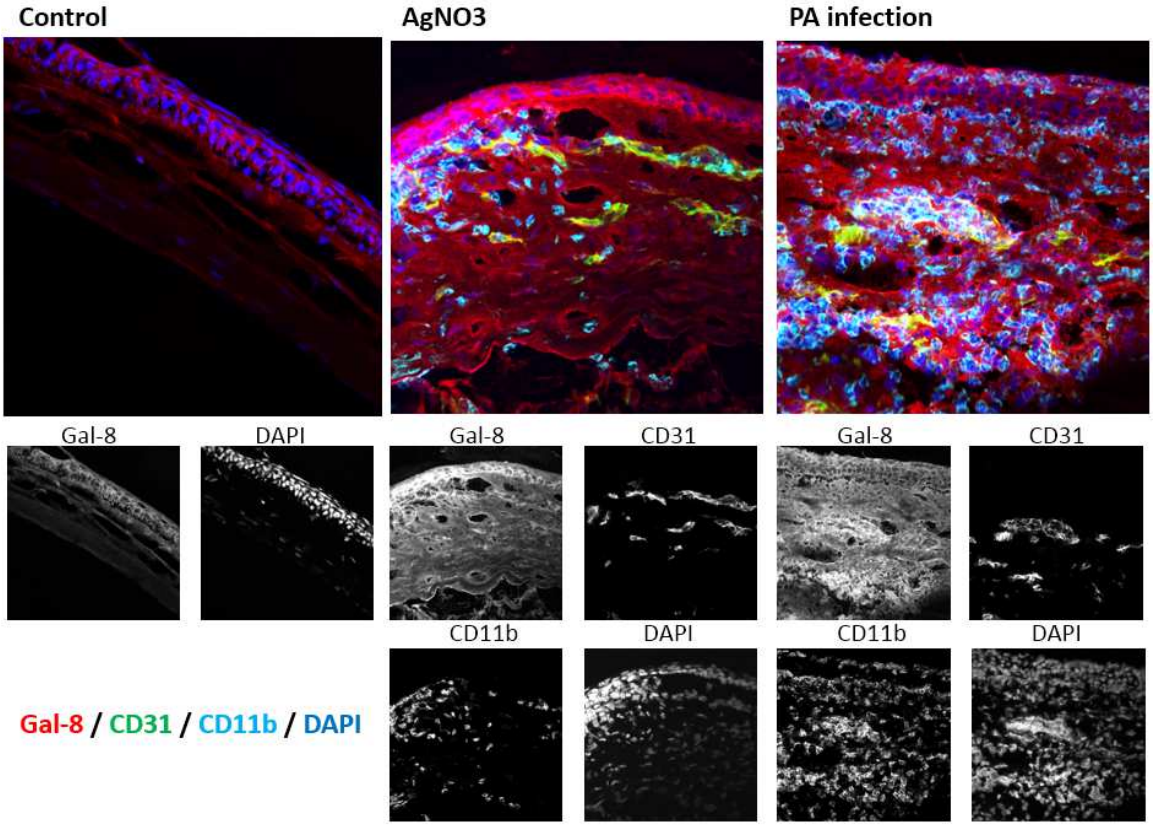

Figure 18. Immunolocalization of galectin-8 using anti-galectin-8 (clone H-80) antibody. Frozen sections of untreated control, $AgNO_3$-cauterized (day 7) and P. aeruginosa-infected (day 8) mouse corneas were fixed with acetone, blocked with Image-iT FX signal enhancer, and stained with anti-galectin-8 (clone H-80, red), anti-CD31 (green) and anti-CD11b (cyan), followed by counterstaining with DAPI (blue). Immunostaining processing and exposure time of the images were the same. Note that immunoreactivity of galectin-8 localizes in both epithelium and stroma, and is much stronger in $AgNO_3$-cauterized and infected mouse corneas compared to untreated control corneas.

3.2 Galectin-8 promotes lymphangiogenesis in a carbohydrate-dependent manner.

Normally avascular cornea has been extensively used as the in vivo model to investigate the molecular mechanism of hemangiogenesis and to examine the efficacy of the inhibitors and activators of hemangiogenesis.[199,200] In recent years, cornea has also proven to be an invaluable in vivo model for defining general mechanisms of lymphangiogenesis. To determine whether galectin-8 promotes lymphangiogenesis, I used the mouse corneal micropocket assay. The vessel area, representing the extent of lymphangiogenesis, was calculated one week after galectin-8 pellets were implanted in the mouse corneas. In the concentration range tested (40–320 ng), the extent of lymphangiogenesis increased in a dose-dependent manner (**Fig. 19**).

To better characterize the role of galectin-8 in the regulation of lymphangiogenesis, an in vitro three-dimensional sprouting assay using LEC spheroids was used. Galectin-8, but not galectins-1, -3 or -7, promoted LEC sprouting (**Fig. 20A**). The stimulatory effect of galectin-8 on LEC sprouting was concentration-dependent (**Fig. 20B**). Next, I tested whether the stimulatory effect of galectin-8 on LEC sprouting was carbohydrate-dependent. First, galectin-8-induced LEC sprouting was almost completely inhibited by thiodigalactoside (TDG, 20 mM), a pan inhibitor of galectins, whereas sucrose (20 mM), a non-inhibiting disaccharide for galectins, had no effect (**Fig. 20C**). Similar to other galectin-mediated cellular response[215], a sigmoidal dose response with a delay preceding the rise in response (ultrasensitive response) with a Hill coefficient (nH)

greater than 1 was observed in my study (**Fig. 20D**). The nH of galectin-8-induced LEC sprouting was 3.7, indicating a positively cooperative effect of galectin-8-induced LEC sprouting (**Fig. 20D**). Secondly, unlike wild type galectin-8, a galectin-8 mutant, Gal-8Q47A, which has lost its ability to bind α2,3-sialylated glycans[32,183], did not promote lymphangiogenesis (**Fig. 21A**). Thirdly, 3'-sialyllactose (3'-SL, 10 mM), which binds N-CRD but not C-CRD of galectin-8[32], inhibited galectin-8-induced LEC sprouting by 90%, whereas 6'-SL, which does not bind galectin-8, had no effect (**Fig. 21B**). The half maximal inhibitory concentration (IC_{50}) of 3'-SL for galectin-8 was 1.25 mM; the inhibitory constant (Ki) of 3'-SL was 1.67 mM; nH was more than 1, indicating a positively cooperative inhibition (**Fig. 22**). These data establish that the stimulatory effect of galectin-8 on lymphangiogenesis is carbohydrate-dependent and that N-CRD of galectin-8 plays a critical role in the process of galectin-8-induced lymphangiogenesis.

Next, I tested whether N-CRD can serve as a dominant negative inhibitor of galectin-8. Most galectins form either dimers or oligomers on ligand encounter. Isolated CRDs, which retain their carbohydrate binding ability but are unable to dimerize or oligomerize and cross-link cell surface receptors, may compete with the carbohydrate-binding ability of the endogenous galectins and, hence, act as a dominant-negative inhibitor[155,216,217]. Published studies have shown that isolated CRDs of galectin-8 retain the carbohydrate binding activity but manifest impaired biological activity[32,218], suggesting that the biological function of the lectin is dependent on cooperative interactions of the two CRDs. As described before, N-

CRD of galectin-8 (Gal-8N) is unique among galectins in exhibiting a very high affinity for α2,3-sialyl glycans. To determine whether the prolymphangiogenic property of galectin-8 is dependent on the cooperative action of both CRDs, I tested whether N-CRD is able to promote lymphangiogenesis. Unlike full-length galectin-8, Gal-8N failed to induce LEC sprouting (**Fig. 23A**). Moreover, Gal-8N effectively inhibited galectin-8-induced lymphangiogenesis in a dose-dependent manner (**Fig. 23B**). IC_{50} of Gal-8N was 1.98 μM; Ki was 0.81 μM; nH was more than 1, indicating a positively cooperative inhibition (**Fig. 24**). These results suggest that Gal-8N serves as a dominant negative inhibitor of galectin-8 and that α2,3-sialyl glycans recognized by Gal-8N as well as cooperative action of both CRDs are required for galectin-8-induced lymphangiogenesis.

AKT and ERK1/2 are essential to lymphangiogenesis.[219,220] I, therefore, tested the activation of AKT and ERK1/2 pathways by galectin-8. In addition, I tested the effect of inhibitors of PI3K and MEK, the upstream signaling molecules of AKT and ERK1/2 pathways, on Gal-8-induced LEC sprouting. To test the effect of Gal-8 on AKT and ERK1/2 activation, primary LECs were serum starved and incubated either with 0.5 μM Gal-8 for 0 to 60 minutes or with 0 to 0.5 μM Gal-8 for 30 minutes. At the end of the incubation period, the whole cell lysates were electrophoresed and the protein blots of the gels were probed with phospho-specific antibodies directed against S473 of AKT and T202/Y204 of ERK. Gal-8 induced phosphorylation of AKT and ERK1/2 in time- and dose-dependent manner (**Fig. 25A**), suggesting that Gal-8 interacts with cell surface proteins to activate AKT and ERK1/2 in LECs. To determine the role of these

pathways on Gal-8-induced lymphangiogenesis, LEC spheroids were stimulated with Gal-8 (0.75 μM) in the presence or absence of PI3K inhibitor (LY294002, 20 μM) and two different MEK inhibitors (U0126, 20 μM; PD0325901, 1 μM). After overnight treatment with Gal-8, accumulated sprout lengths were quantified. All three inhibitors markedly inhibited Gal-8-induced LEC sprouting (**Fig. 25B**), indicating that PI3K-AKT and MEK-ERK signaling axes play a crucial role in Gal-8-induced LEC sprouting. As expected, VEGF-C-induced sprouting was also inhibited by PI3K and MEK inhibitors (**Fig. 25C**, positive control).

Figure 19.

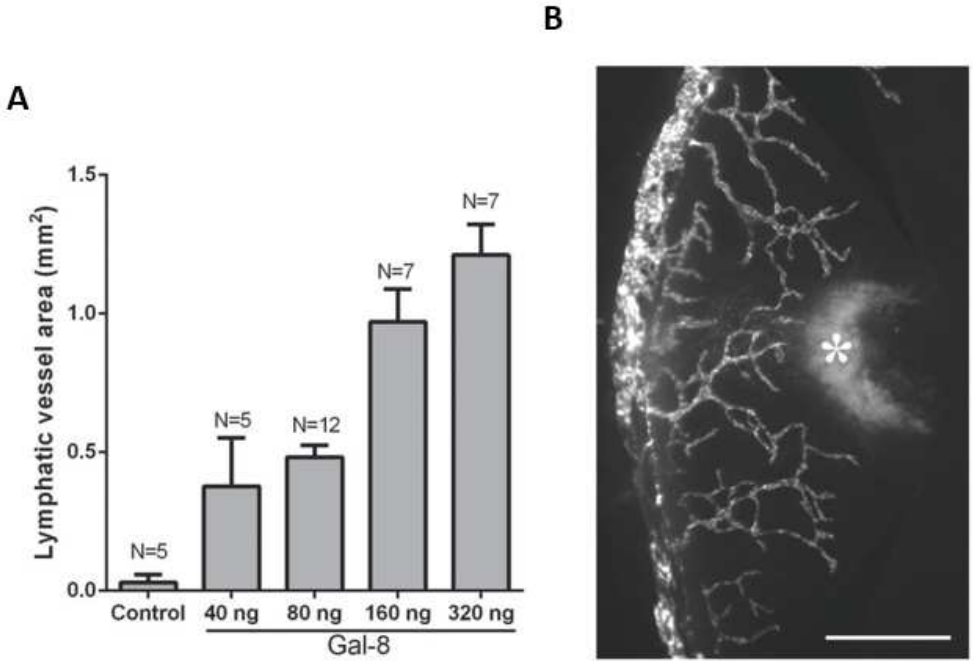

Figure 19. Galectin-8 promotes lymphangiogenesis in vivo in a micropocket assay. Sustained-release polymer pellets containing various doses of galectin-8 were implanted in the corneas of *Prox1*-EGFP reporter mice. One week after surgery, the vessel area was calculated. Data are expressed as mean ± SEM (A). A representative fluorescence image of a cornea implanted with galectin-8 pellet (160 ng/pellet) is shown in panel B. White asterisk indicates pellet. Bar = 400 μm.

Figure 20.

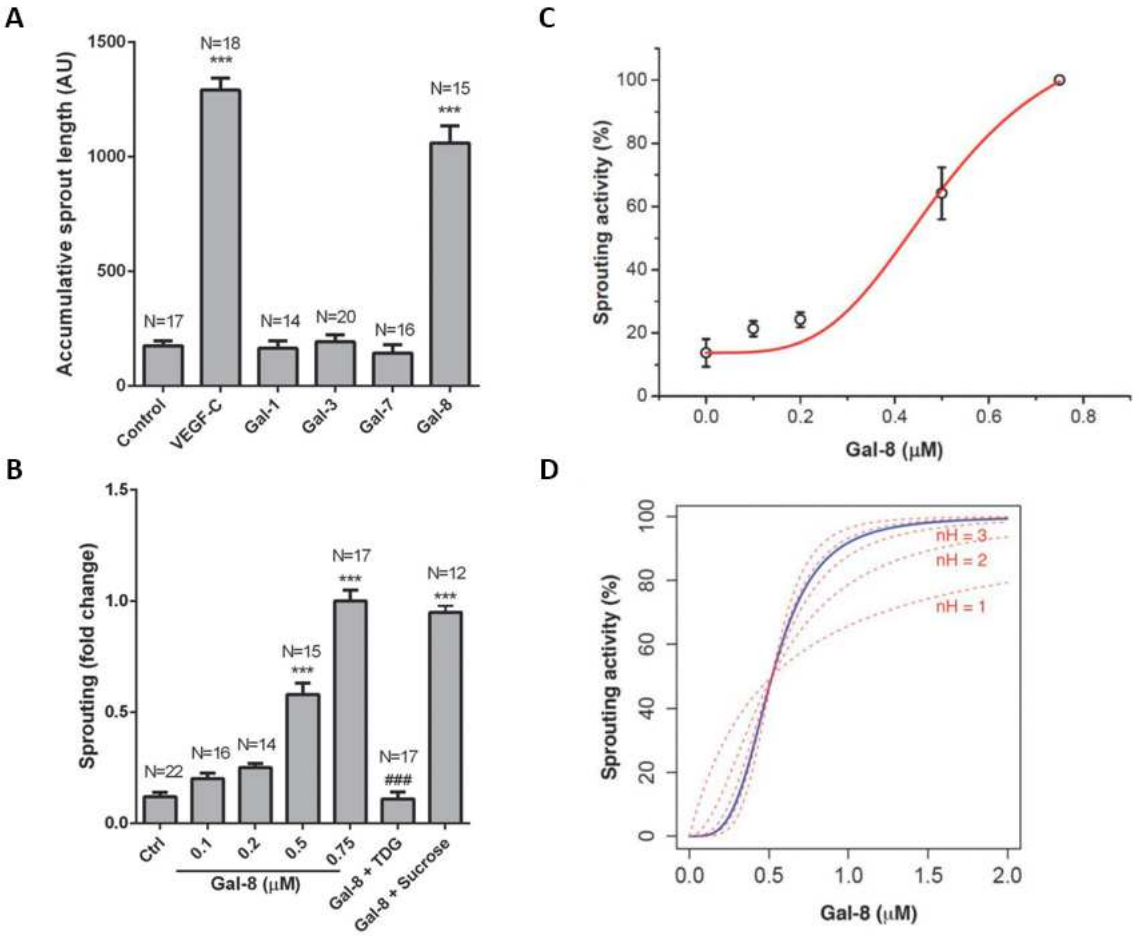

Figure 20. Galectin-8 promotes lymphangiogenesis in vitro in a dose-dependent manner. LEC spheroids were incubated with media containing various test agents. After 24 hours, the cumulative length of the sprouts was quantified. (**A**) Galectin-8, but not galectin-1, -3 or -7, promotes LEC sprouting. Concentrations of VEGF-C and galectins are 50 ng/ml and 0.75 μM, respectively. (**B**) Galectin-8 promotes lymphangiogenesis in a dose- and carbohydrate-dependent manner. Galectin-8-induced LEC sprouting is abolished by TDG (an inhibiting carbohydrate), but not sucrose (a non-competing carbohydrate). TDG and sucrose: 20 mM. A value of 1.0 was assigned to the sprout length of galectin-8 (0.75 μM)-treated cells. Data are expressed as mean ± SEM and analyzed with one-way ANOVA. ***P<0.001 vs control. ###P<0.001 vs Gal-8 (0.75 μM). TDG: thiodigalactoside. (C and D) Galectin-8 stimulates LEC sprouting in a positively cooperative manner. (**C**) Dose-response of galectin-8-mediated LEC sprouting. Open circles indicate actual data points. LEC sprouting activity of galectin-8 at 0.75 μM is 100%. EC_{50} of galectin-8-mediated LEC sprouting is 0.52 μM and Hill's coefficient (nH) is 3.7. (**D**) Theoretical curves of different nH (red broken lines, nH=1 to 5) were simulated and the blue line indicates galectin-8-mediated LEC sprouting based on experimental results. The results are plotted in Origin 9.1 (C) and R programing language (D).

Figure 21.

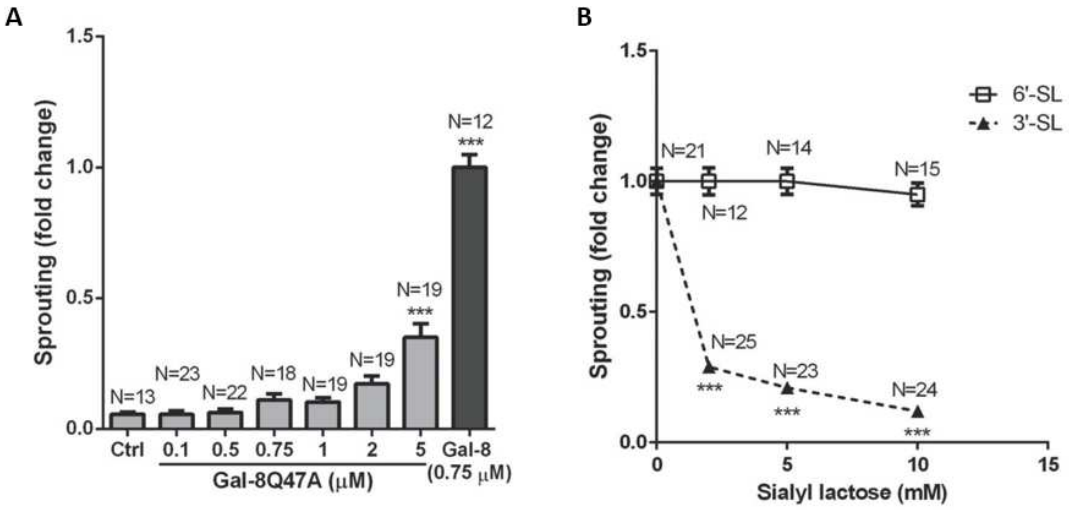

Figure 21. Galectin-8 promotes lymphangiogenesis in vitro by recognition of sialylated glycans. LEC spheroids were incubated with media containing various test agents. After 24 hours, the cumulative length of the sprouts was quantified. (A) A galectin-8 mutant, Gal-8Q47A, which has lost its ability to bind to α2,3-sialylated glycans, does not promote LEC sprouting at lower concentrations. The prolymphangiogenic effect of Gal-8Q47A is only observed at 5 μM. (B) 3'-SL, but not 6'-SL, inhibits galectin-8-induced LEC sprouting. A value of 1.0 was assigned to the sprout length of galectin-8 (0.75 μM)-treated cells. Data are expressed as mean ± SEM and analyzed with one-way ANOVA (A) and Student's t test (B). ***P<0.001 vs control. SL: sialyl lactose.

Figure 22.

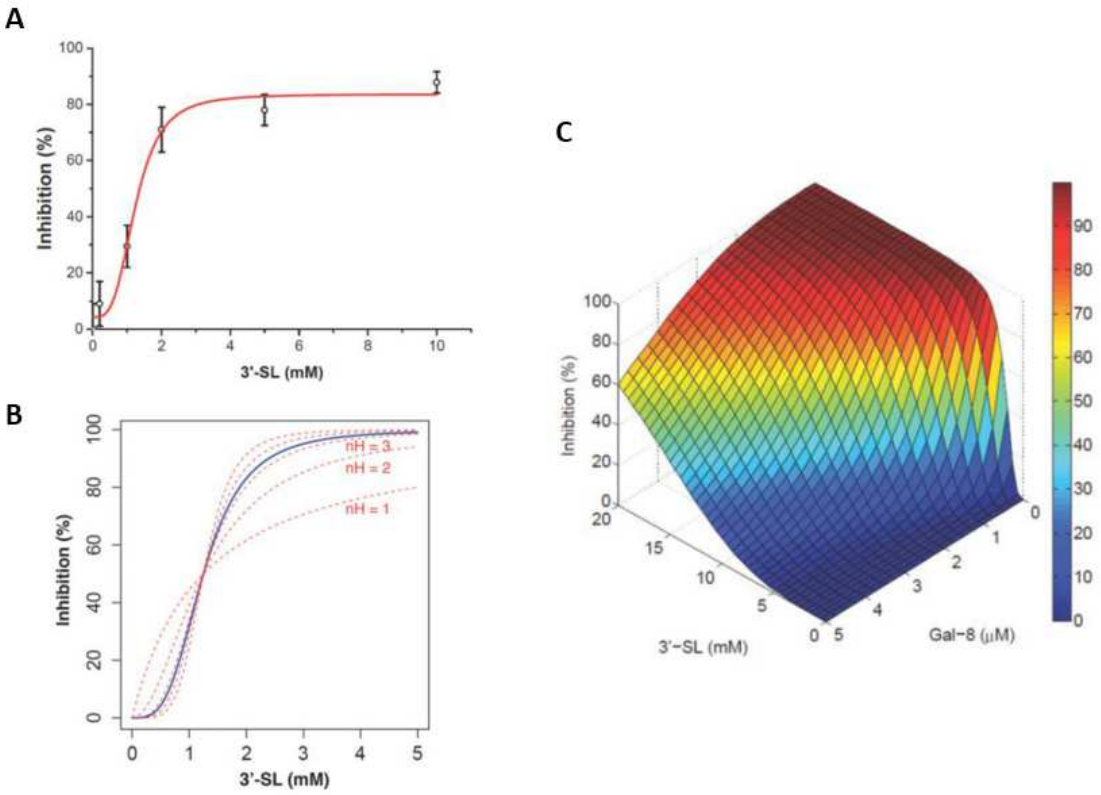

Figure 22. Kinetic characteristics of inhibitory effect of 3'-SL on galectin-8-mediated LEC sprouting. (**A** and **B**) Inhibitory effect of 3'-SL on galectin-8-mediated LEC sprouting at 0.75 μM. (A) Open circles indicate the actual data points. IC_{50} of the inhibitory effect of 3'-SL is 1.25 mM. nH of 3'-SL is 3.38. Ki of 3'-SL is 1.67 mM. ($Ki = \frac{IC50}{1+[A]/EC50}$). (B) Theoretical curves of different nH (red broken lines, nH=1 to 5) were simulated and the blue lines indicate the inhibitory curves of 3'-SL based on the experimental results. (**C**) Inhibitory effect of 3'-SL on galectin-8-mediated LEC sprouting at varying concentrations is simulated. The results are plotted in Origin 9.1 (A), R programing language (B) and MATLAB2013 (C).

Figure 23.

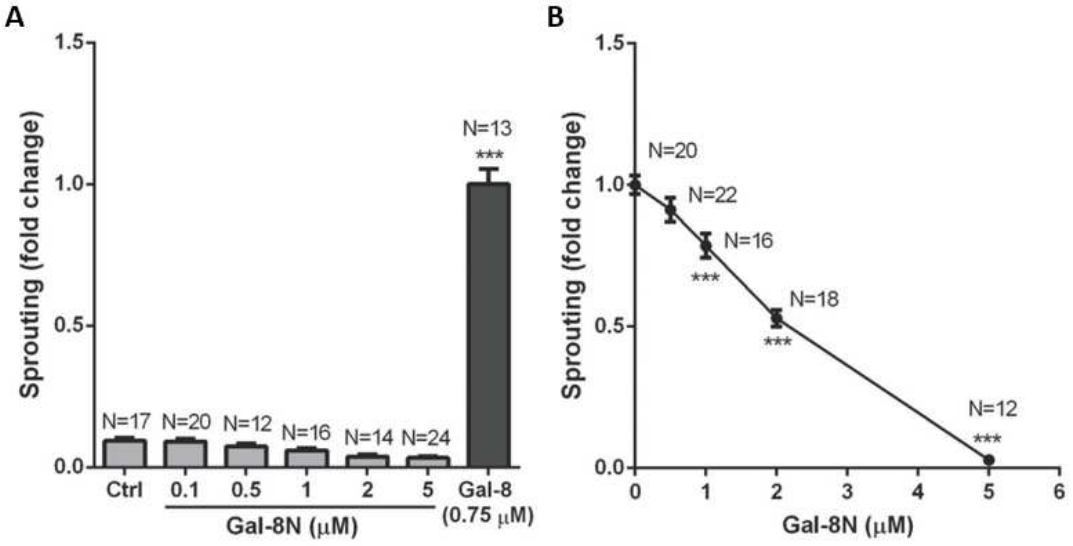

Figure 23. Gal-8N inhibits galectin-8-mediated LEC sprouting. LEC spheroids were incubated with media containing various test agents. After 24 hours, the cumulative length of the sprouts was quantified. (**A**) Gal-8N does not promote LEC sprouting. (**B**) Gal-8N inhibits galectin-8-induced sprouting in a dose-dependent manner. A value of 1.0 was assigned to the sprout length of galectin-8 (0.75 μM)-treated cells. Data are expressed as mean ± SEM and analyzed with one-way ANOVA (A) and Student's t test (B). ***P<0.001 vs control.

Figure 24.

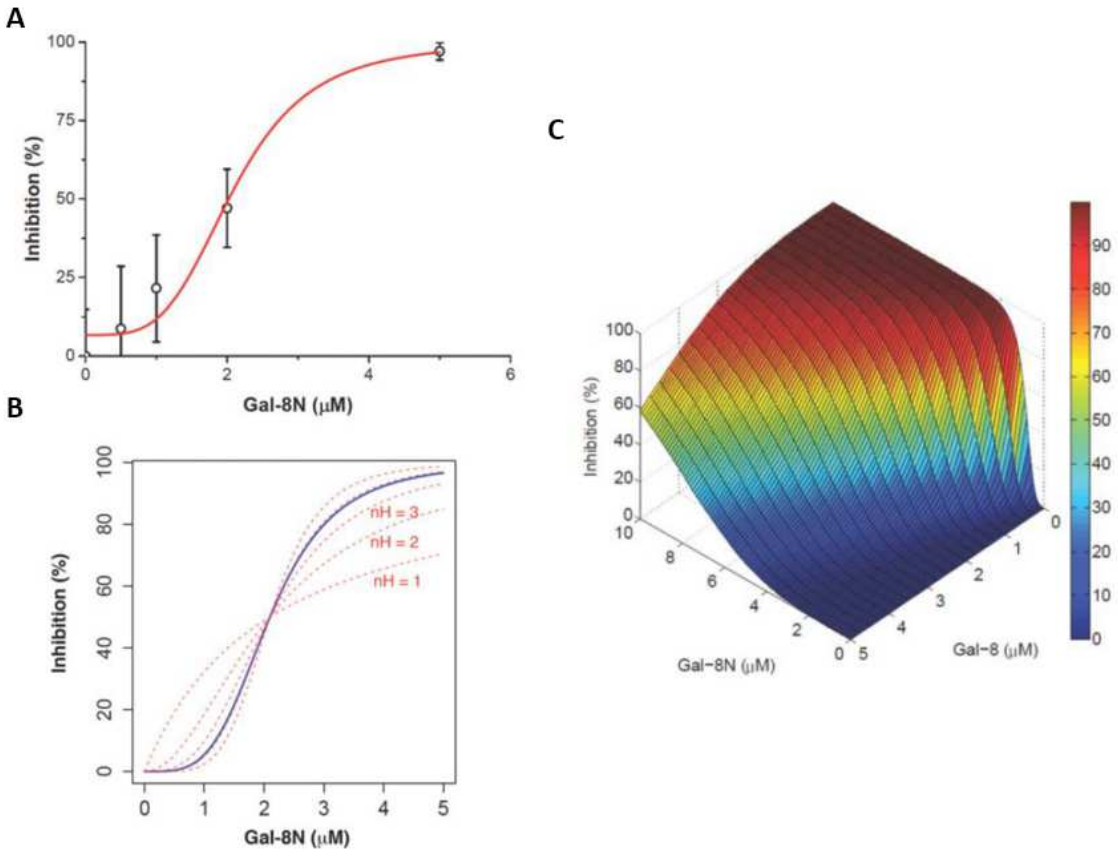

Figure 24. Kinetic characteristics of inhibitory effect of Gal-8N on galectin-8-mediated LEC sprouting. (**A** and **B**) Inhibitory effect of Gal-8N on galectin-8-mediated LEC sprouting at 0.75 μM. Open circles indicate the actual data points. IC_{50} of the inhibitory effect of Gal-8N is 1.98 μM. nH of Gal-8N is 3.85. Ki of Gal-8N is 0.86 μM. ($Ki = \frac{IC50}{1+[A]/EC50}$). (B) Theoretical curves of different nH (red broken lines, nH=1 to 5) were simulated and the blue lines indicate the inhibitory curves of Gal-8N based on the experimental results. (C) Inhibitory effect of Gal-8N on galectin-8-mediated LEC sprouting at varying concentrations is simulated. The results are plotted in Origin 9.1 (A), R programing language (B) and MATLAB2013 (C).

Figure 25.

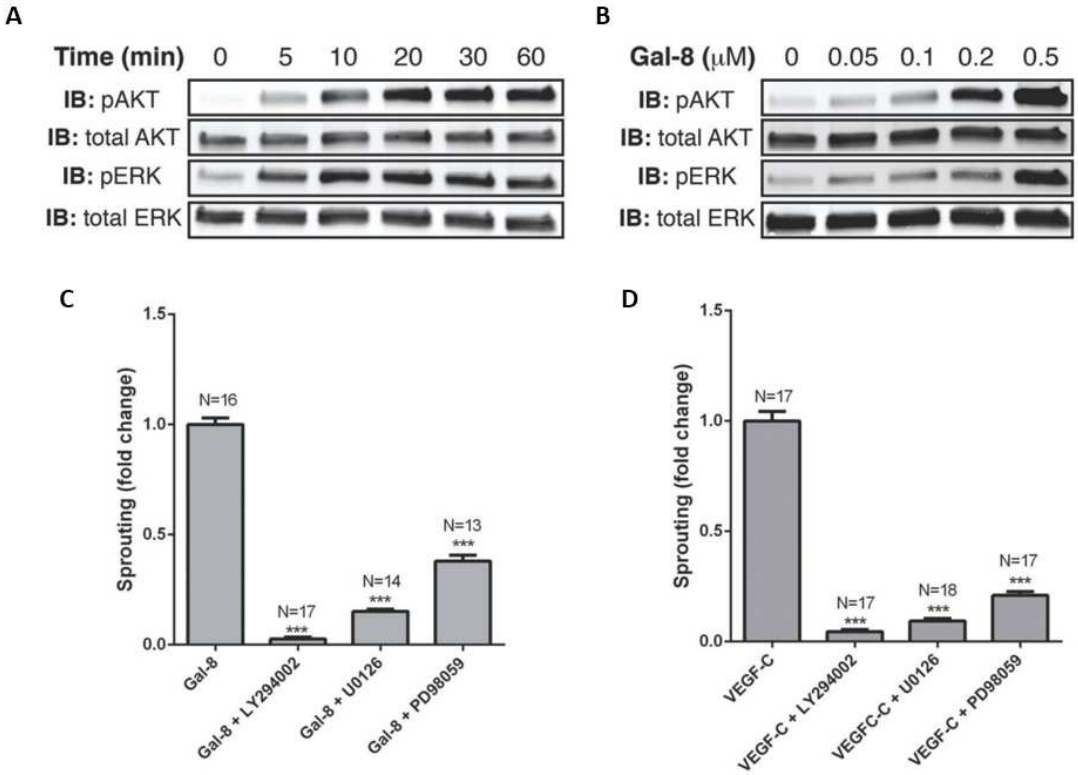

Figure 25. Galectin-8 promotes lymphangiogenesis through AKT and ERK signaling pathways. (**A** and **B**) Galectin-8 treatment activates AKT and ERK pathways. Primary LECs were treated with galectin-8 prior to lysis. Samples were separated by SDS-PAGE and analyzed by Western blot with phospho-specific antibodies directed against S473 of AKT and T202/Y204 of ERK. (A) LECs were incubated with galectin-8 (0.5 μM) for 0 – 60 minutes prior to lysis. (B) LECs were incubated with varying concentrations of Gal-8 for 30 minutes prior to lysis. (**C** and **D**) Inhibitors of PI3K and MEK inhibit galectin-8-induced LEC sprouting. (C) LEC spheroids were stimulated with galectin-8 (0.75 μM) in the presence or absence of PI3K inhibitor (LY294002, 20 μM) and two different MEK inhibitors (U0126, 20 μM; PD0325901, 1 μM). (D) LEC spheroids were stimulated with VEGF-C (50 ng/ml) in the presence or absence of the PI3K inhibitor and MEK inhibitors. Accumulated sprout lengths were quantified. A value of 1.0 was assigned to the sprout length of galectin-8 treated cells. Data are expressed as mean ± SEM and analyzed with one-way ANOVA. ***P<0.001 vs control.

3.3 Galectin-8 modulates VEGF-C-induced lymphangiogenesis

To gain mechanistic insight on galectin-8-mediated lymphangiogenesis, first I tested whether the lectin influences the function of a well-known lymphangiogenic molecule, VEGF-C. Here, I tested the effect of exogenous galectin-8 on VEGF-C-induced LEC sprouting. Galectin-8, but not galectin-1, -3 and -7, markedly enhanced VEGF-C-induced LEC sprouting (**Fig. 26A**). Synergistic effect of galectin-8 on VEGF-C-induced LEC sprouting was dose-dependent. At 0.75 μM of galectin-8, VEGF-C-induced LEC sprouting was 5 times higher than that seen by VEGF-C alone or galectin-8 alone (**Fig. 26B**), indicating that galectin-8 has a synergistic effect on VEGF-C-induced LEC sprouting. To determine whether galectin-8 also enhances VEGF-C-induced lymphangiogenesis in vivo, two separate pellets (VEGF-C and galectin-8) were implanted in close proximity to one another, in the corneas of *Prox1*-EGFP reporter mice. In the in vivo micropocket assays also, galectin-8 augmented VEGF-C-induced lymphangiogenesis (**Fig. 27**).

Next, I tested whether VEGF-C-induced lymphangiogenesis is dependent on galectin-8. In this study, LEC spheroids were stimulated with VEGF-C in the presence or absence of three different galectin inhibitors. VEGF-C-induced LEC sprouting was inhibited by TDG (a pan inhibitor of galectins, **Fig. 28A**), 3'-sialyl lactose (the high affinity ligand of the N-CRD of galectin-8, **Fig. 28B**), and by Gal-8N (the dominant negative inhibitor of galectin-8, **Fig. 28C**). These data establish the critical role of galectin-8-dependent carbohydrate–mediated recognition in VEGF-C-induced lymphangiogenesis.

Figure 26.

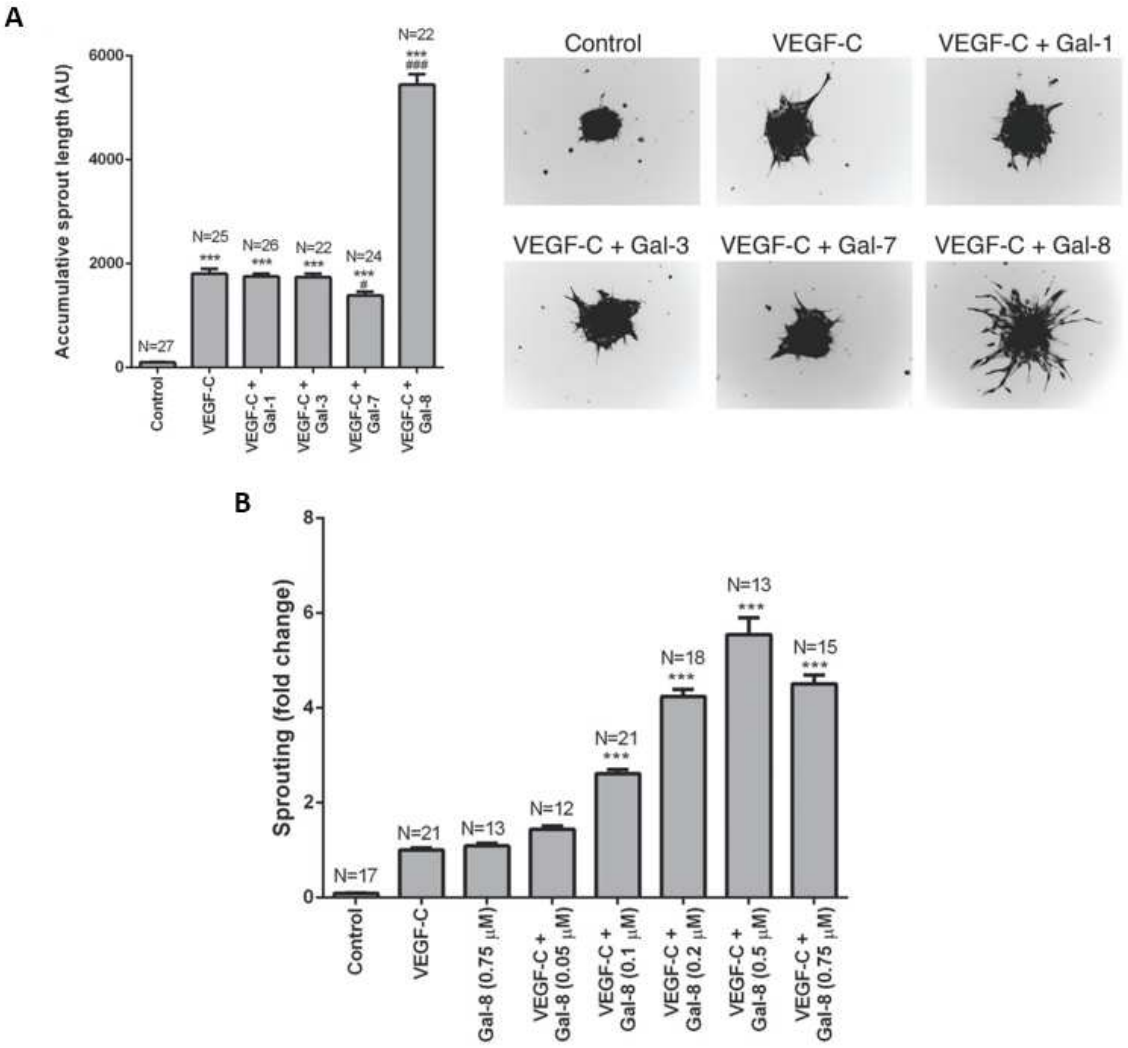

Figure 26. Galectin-8 potentiates VEGF-C-induced lymphangiogenesis in vitro. (**A**) Galectin-8, but not galectin-1, -3 or -7, has a synergistic effect on VEGF-C-induced LEC sprouting. The LEC spheroids were treated with VEGF-C (50 ng/ml) in the presence or absence of galectin-1, -3, -7 or -8. Accumulated sprout lengths were quantified by ImageJ. Representative fluorescent images are shown in the right panel. (**B**) Synergistic effect of galectin-8 on VEGF-C-induced LEC sprouting is dose-dependent. The LEC spheroids were treated with VEGF-C (50 ng/ml) in the presence or absence of varying concentrations of galectin-8. A value of 1.0 was assigned to the sprout length of VEGF-C treated cells. The values for all other groups are expressed as a change in the sprout length with respect to VEGF-C-treated LEC spheroids. Data are expressed as mean ± SEM and analyzed with one-way ANOVA. ***P<0.001 vs control (A) or VEGF-C (B); $^{\#}$P<0.05 vs VEGF-C (A); $^{\#\#\#}$P<0.001 vs VEGF-C (A).

Figure 27.

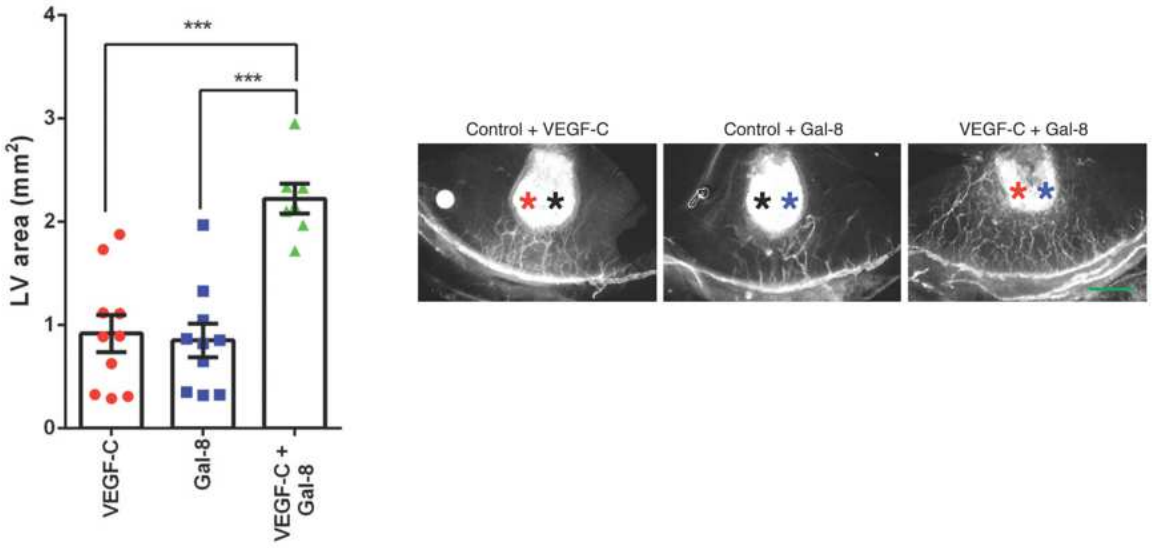

Figure 27. Galectin-8 potentiates VEGF-C-induced lymphangiogenesis in vivo. Two separate pellets, one containing VEGF-C and the other galectin-8, were implanted in the corneas of *Prox1*-EGFP reporter mice. One week after surgery, the vessel area in the left panel was calculated as described in the text. Representative fluorescent images are shown in the right panel. Black asterisk: control pellet; red asterisk: VEGF-C pellet; blue asterisk: galectin-8 pellet. Data are plotted as mean ± SEM and analyzed using one-way ANOVA. ****P*< 0.001.

Figure 28.

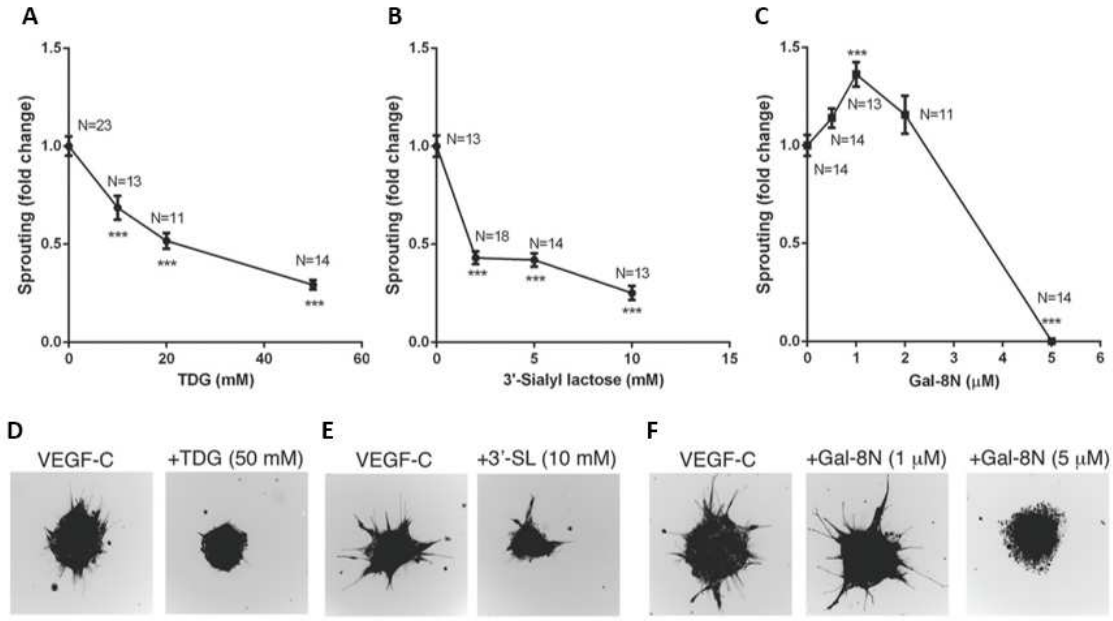

Figure 28. Galectin-8 inhibitors attenuates VEGF-C-induced LEC sprouting. LEC spheroids were stimulated with VEGF-C (50 ng/ml) in the presence or absence of varying concentrations of TDG (A), 3'-SL (B) or Gal-8N (C). After 24 hr, accumulated sprout lengths were quantified. A value of 1.0 was assigned to the sprout length of VEGF-C treated LEC spheroids. The values for inhibitor treated groups are expressed as a change in the sprout length with respect to VEGF-C (50 ng/ml) treated LEC spheroids. Representative images of sprouts from corresponding experiments are shown in the lower panels (D, E, F). Data are plotted as mean ± SEM and analyzed using Student's t test. **P*<0.05, ***P*<0.01, ****P*<0.001 vs VEGF-C. 3'-SL, 3'-sialyllactose.

3.4 Galectin-8 deficiency ameliorates inflammatory lymphangiogenesis.

To test the role of galectin-8 in postnatal lymphangiogenesis in vivo, we performed mouse corneal micropocket assays and induced inflammatory lymphangiogenesis in wild type (WT) and galectin-8 knockout (KO) mice. For micropocket assays, pellets containing 160 ng of VEGF-C were implanted into mouse corneas and, one week after surgery, the vessel area representing the extent of lymphangiogenesis was calculated. In WT mice, VEGF-C induced robust growth of lymphatic vessels (**Fig. 29**). The extent of vessel formation mediated by VEGF-C was significantly reduced in galectin-8 KO mice as compared with WT mice (**Fig. 29**). Similarly, the extent of inflammatory lymphangiogenesis induced by suture placement (**Fig. 30**) and $AgNO_3$ cautery (**Fig. 31**) in the cornea was reduced in galectin-8 KO mice as compared with WT mice.

Figure 29.

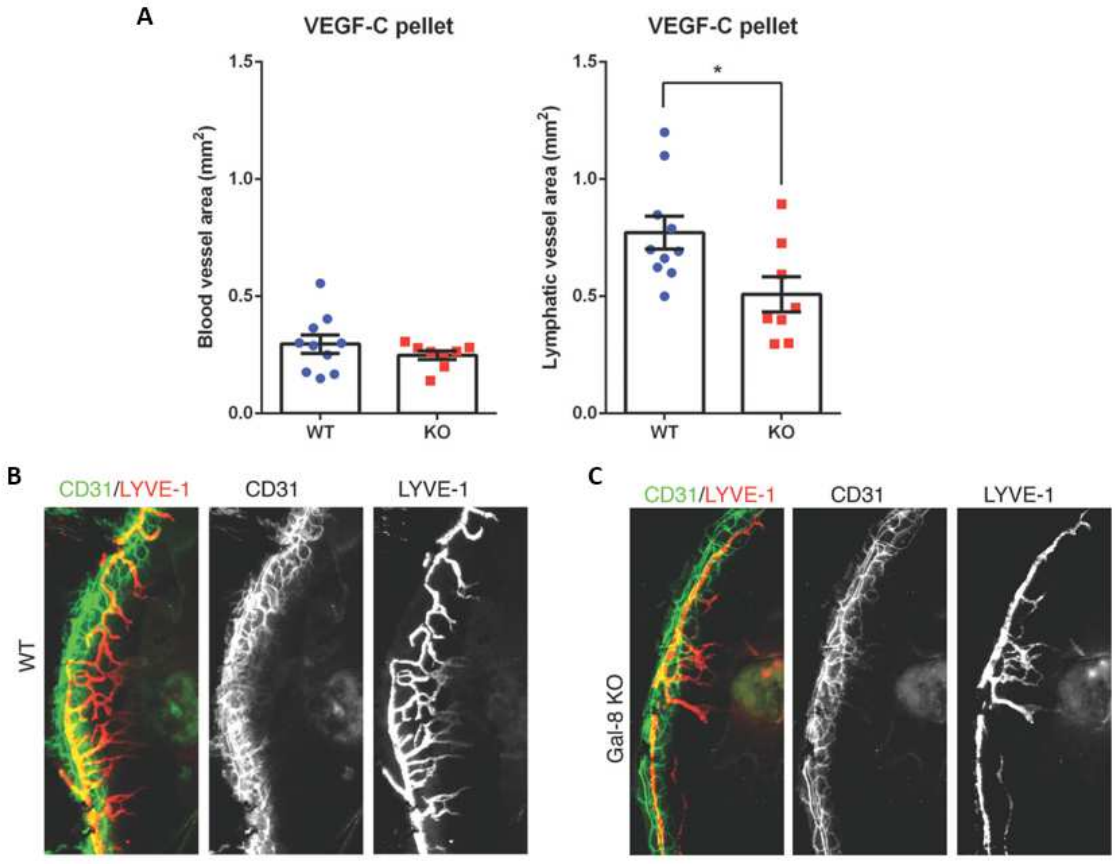

Figure 29. Galectin-8 deficiency attenuates VEGF-C-induced lymphangiogenesis in vivo. VEGF-C-induced hemangiogenesis and lymphangiogenesis. VEGF-C pellets (160 ng) were implanted into wild type (WT, N=10) (B) and galectin-8 KO (N=10) (C) mice. After 7 day post implantation, the corneal flat mounts were stained with anti-CD31 and anti-LYVE-1 to visualize blood and lymphatic vessels, respectively. Blood vessel and lymphatic vessel areas were quantified (A). Representative fluorescence images from each group are shown in the bottom panels (B, C). Data are plotted as mean ± SEM and analyzed using Student's t test. **P*<0.05 vs WT.

Figure 30.

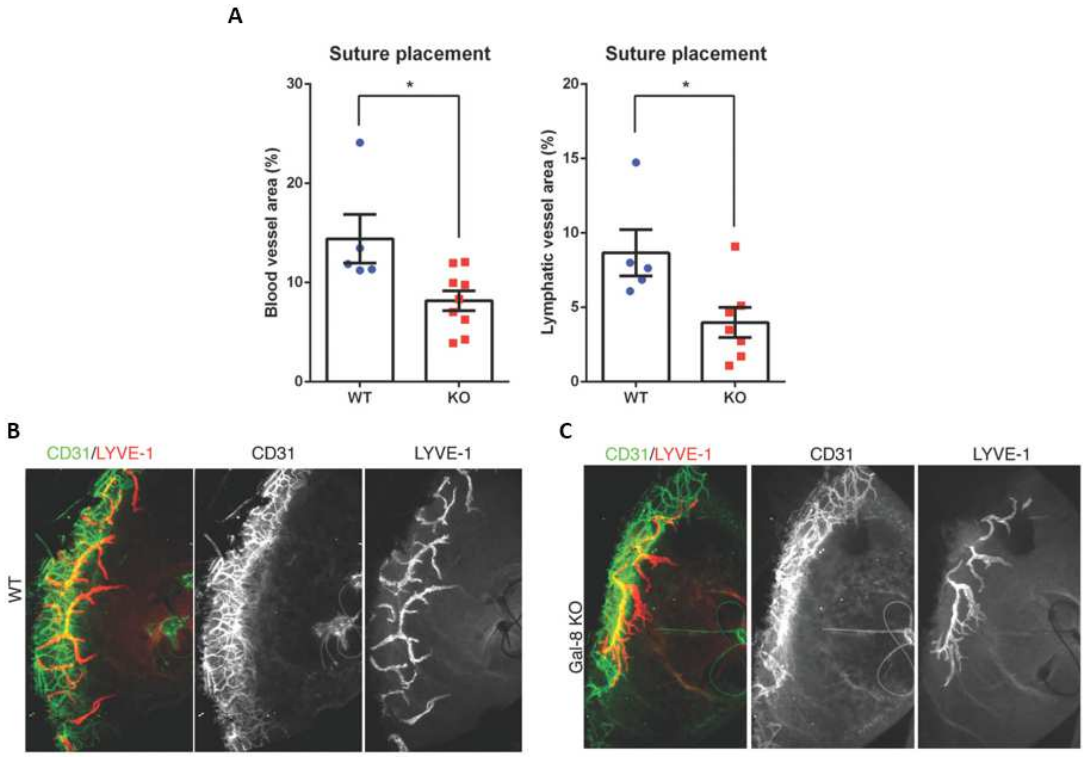

Figure 30. Galectin-8 deficiency attenuates suture-induced lymphangiogenesis in vivo. Sutures were placed 2 mm above the limbal vessel in the corneas of WT (N=5) (B) and galectin-8 KO (N=10) (C) mice. After 7 day post surgery, the corneal flat mounts were stained with anti-CD31 and anti-LYVE-1 to visualize blood and lymphatic vessels, respectively. Blood vessel and lymphatic vessel areas were quantified (A). Representative fluorescence images from each group are shown in the bottom panels (B, C). Data are plotted as mean ± SEM and analyzed using Student's t test. **P*<0.05 vs WT.

Figure 31.

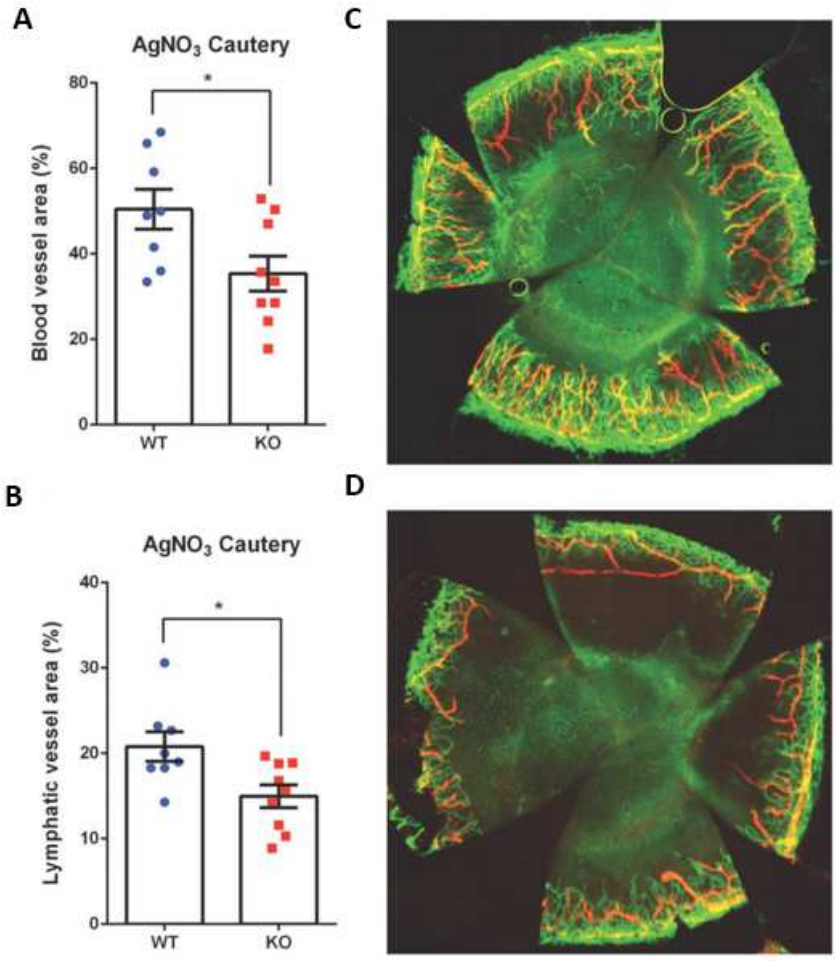

Figure 31. Galectin-8 deficiency attenuates cautery-induced lymphangiogenesis in vivo. Silver nitrate cautery was introduced in the center of the corneas of the galectin-$8^{+/+}$ and galectin-$8^{-/-}$ mice. At the end of the treatment period (day 7), blood and lymphatic vessel areas were quantified (A, B). Representative images of WT (C) and galectin-8 KO (D) are shown. Anti-CD31: green; anti-LYVE-1: red. Data are plotted as mean ± SEM and analyzed using Student's t test. *P<0.05.

3.5 VEGF-C binding receptors play little role on galectin-8-induced lymphangiogenesis.

It has been reported that the galectin-glycan lattices increase receptor residency time by inhibiting endocytosis of glycoprotein receptors from the cell surface, and this in turn, increases the magnitude or duration of signaling from the cell surface.[221,222] Therefore, in an effort to characterize the mechanism by which galectin-8 modulates VEGF-C-induced lymphangiogenesis, I first conducted a study to determine whether the lectin modulates VEGFR-3, the predominant VEGF-C receptor. This study revealed that VEGFR-3, but not VEGF-C, is a galectin-8 binding protein (**Fig. 32**), that galectin-8 clusters VEGFR-3 on cell surface (**Fig. 33**), and that galectin-8 retains VEGFR-3 on cell surface (**Fig. 34**). However, surprisingly, knockdown of VEGFR-3 had little effect on galectin-8-induced LEC sprouting (**Fig. 35**), suggesting that molecules besides VEGFR-3 are involved in galectin-8-induced lymphangiogenesis. Therefore, I sought to determine whether galectin-8-mediated lymphangiogenesis involves other receptors for VEGF-C. In this respect, it is known that VEGFR-2, which also binds VEGF-C, is not involved in VEGF-C-induced sprouting.[223,224] My siRNA knockdown and/or antibody blocking studies revealed that several other known receptors of VEGF-C including neuropilin-2 and integrin α9β1[225-228] are not possible targets of galectin-8 (**Fig. 36** and **Fig. 43**).

Figure 32.

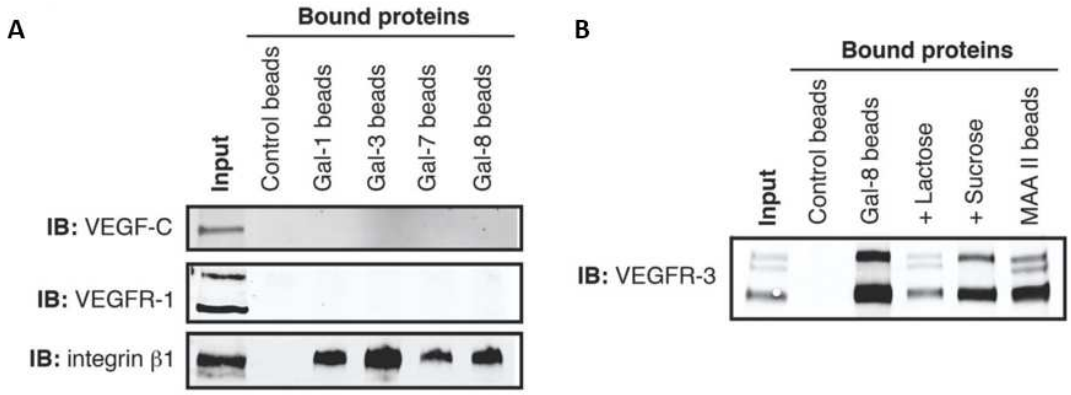

Figure 32. Galectin-8 binds to VEGFR-3 but not VEGF-C or VEGFR-1. (**A**) None of the four galectins tested bind VEGF-C or VEGFR-1. Primary LECs were incubated with agarose beads (control), and galectin-conjugated agarose beads at 4ºC overnight. Unbound proteins were removed and the bound proteins were eluted with 20 µL of 2× Laemmli sample buffer and examined along with input by Western blotting. The results are representative of two independent experiments. (**B**) VEGFR-3 is a galectin-8 binding protein. LEC lysates were incubated with galectin-8-conjugated agarose beads in the presence or absence of 100 mM of lactose (an inhibiting sugar) or sucrose (a non-inhibiting sugar). Bound proteins were examined along with total cell lysates (input) by Western blot using anti-VEGFR-3 antibody. LEC lysates incubated with unconjugated beads served as a negative control. To determine whether VEGFR-3 contains α2,3-sialylated glycans, preferred ligands of galectin-8, binding of VEGFR-3 to a plant lectin, MAA II, which binds selectively to α2,3-linked sialic acids was examined. MAA II, *Maakia Amurensis* agglutinin II. The results are representative of three independent experiments.

Figure 33.

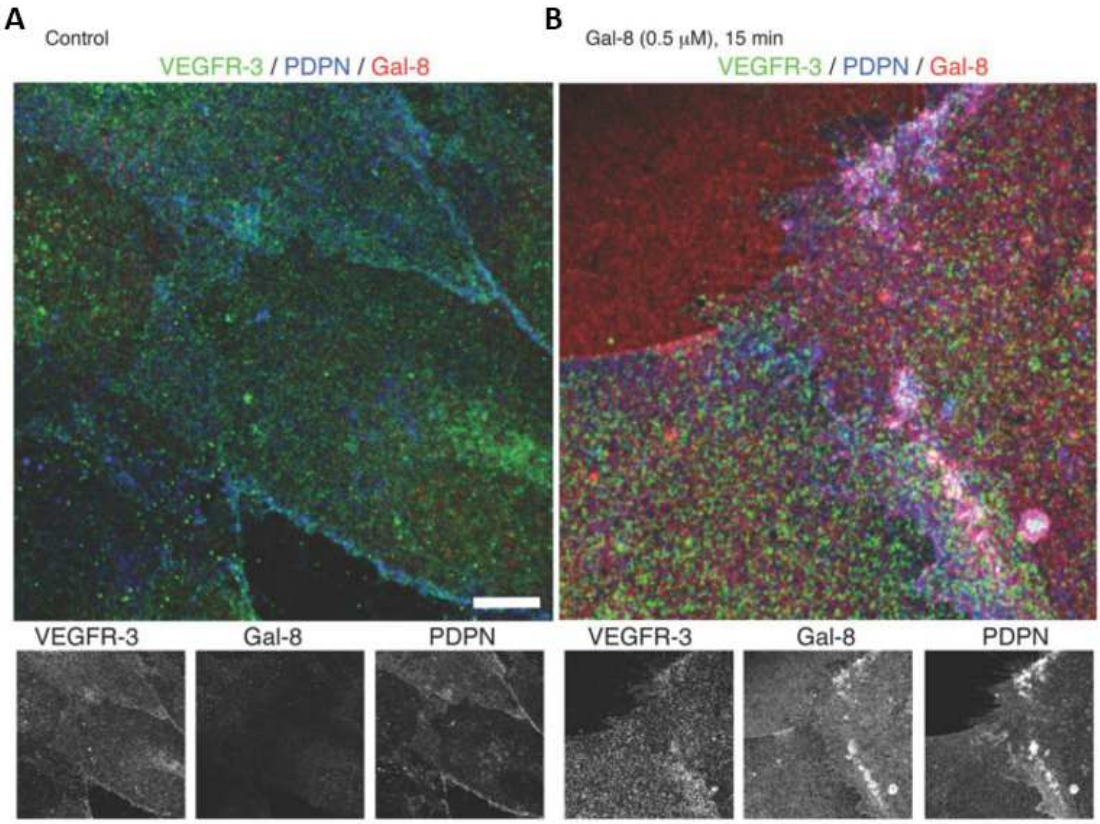

Figure 33. Galectin-8 clusters VEGFR-3 on cell surface. LECs were treated with or without galectin-8 for 15 min, fixed without permeabilization, stained with antibodies to anti-VEGFR-3 (green), PDPN (blue) and galectin-8 (red), and examined by confocal microscopy. Merged images are shown in the top panel. (**A**) In control LECs, no obvious colocalization of VEGFR-3, galectin-8 and PDPN. (**B**) Exogenous galectin-8 sequesters VEGFR-3 and PDPN. PDPN and VEGFR-3 distribution reorganized and colocalized (white spots in the merged image) at cell borders after galectin-8 treatment. Scale bar: 7.5 μm.

Figure 34.

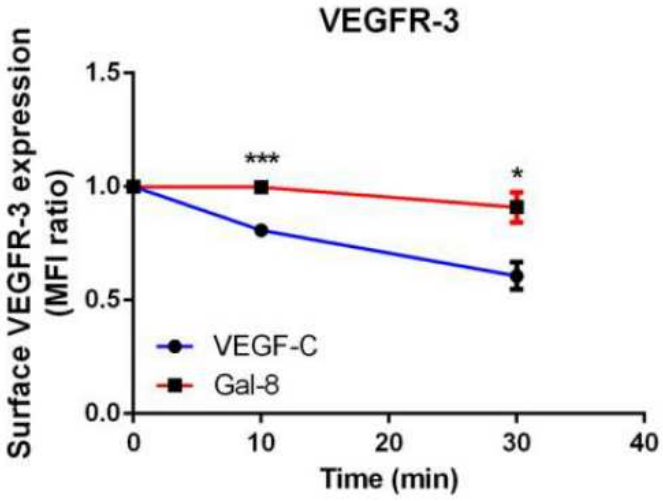

Figure 34. Galectin-8 retains VEGFR-3 on cell surface. Gal-8 increases cell-surface residency VEGFR-3. Primary LECs were treated with VEGF-C (50 ng/ml) or galectin-8 (0.2 μM) for 10 and 30 min. Cells were fixed and stained with anti-VEGFR-3 antibody. Cell surface expression of VEGFR-3 was analyzed with flow cytometry and quantified with FlowJo. Data are plotted as Mean ± SEM from three independent experiments and analyzed with Student's t test. *P<0.05, ***P<0.001 vs VEGF-C treatment. MFI: mean fluorescence intensity.

Figure 35.

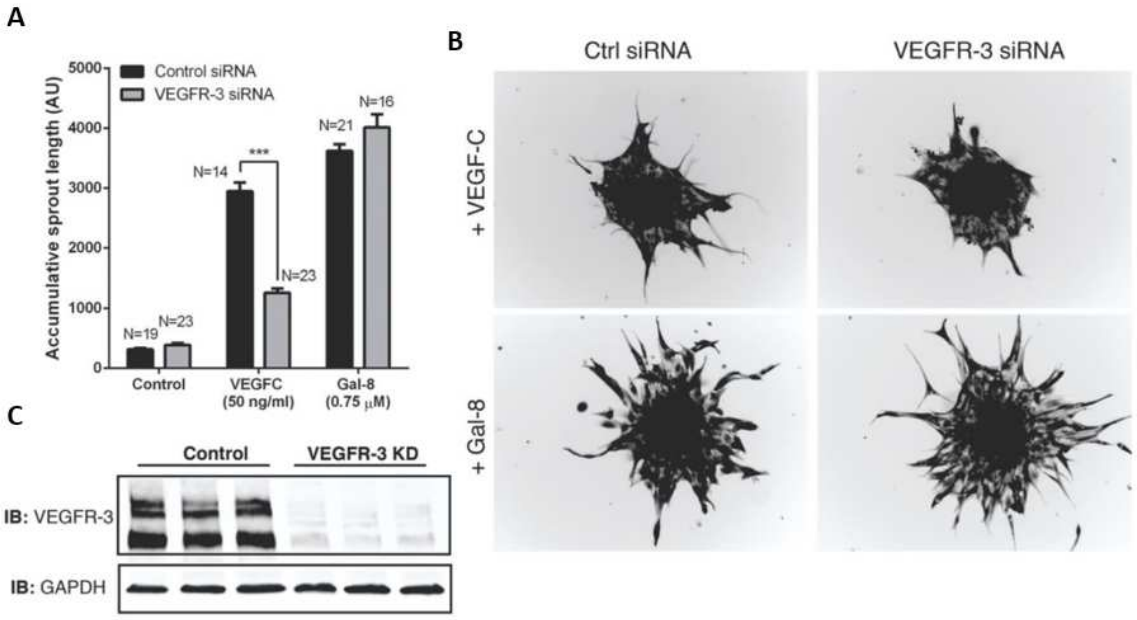

Figure 35. VEGFR-3 is dispensable for galectin-8-mediated lymphangiogenesis in vitro. (**A** and **B**) LEC spheroids prepared using primary LECs transfected with control and VEGFR-3 siRNA were treated with galectin-8 (0.75 μM) or VEGF-C (50 ng/ml). After 24 hr, accumulated sprout lengths were quantified (A). Representative images are shown in the right panel (B). Data are plotted as mean ± SEM and analyzed using Student's t test. (**C**) Assessment of VEGFR-3 knockdown efficiency. Cell lysates from control and VEGFR-3 knockdown cells were subjected to SDS-PAGE followed by immunoblotting with anti-VEGFR-3 and anti-GAPDH. Three independent samples were used in the control and VEGFR-3 knockdown.

Figure 36.

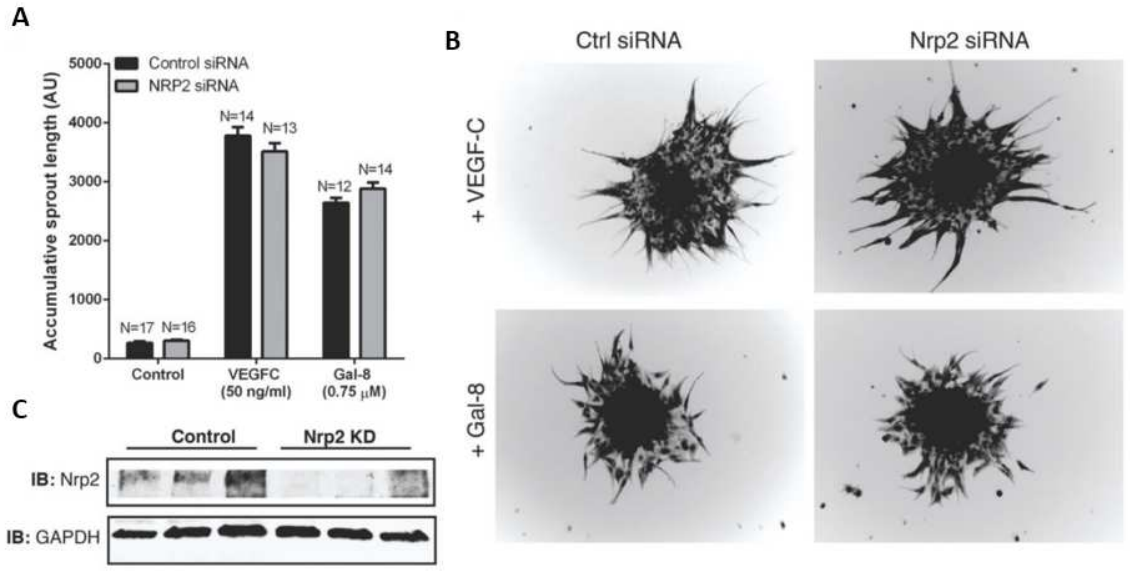

Figure 36. Neuropilin-2 (Nrp2) is dispensable for galectin-8-mediated lymphangiogenesis in vitro. (**A** and **B**) LEC spheroids prepared using primary LECs transfected with control and Nrp2 siRNA were treated with galectin-8 (0.75 μM) or VEGF-C (50 ng/ml). After 24 hr, accumulated sprout lengths were quantified (A). Representative images are shown in the right panel (B). Data are plotted as mean ± SEM and analyzed using Student's t test. (**C**) Assessment of Nrp2 knockdown efficiency. Cell lysates from control and Nrp2 knockdown cells were subjected to SDS-PAGE followed by immunoblotting with anti-Nrp2 and anti-GAPDH. Three independent samples were used in the control and Nrp2 knockdown.

3.6 Galectin-8 and VEGF-C-induced lymphangiogenesis is dependent on podoplanin.

Next I performed studies to determine whether galectin-8-induced lymphangiogenesis is dependent on PDPN. PDPN, which is expressed by LECs but not blood ECs, is thought to play a role in the process of lymphangiogenesis.[116,117] However, the role of Gal-8 in the modulation of PDPN has thus far not been fully investigated and virtually nothing is known about the role of PDPN in VEGF-C-induced lymphangiogenesis. Here, I performed studies to determine whether: (i) PDPN binds galectin-8 in a carbohydrate-dependent manner, (ii) PDPN knockdown inhibits galectin-8- and/or VEGFC-induced LEC sprouting and activation of AKT and ERK pathways, and (iii) galectin-8- or VEGF-C-induced lymphangiogenesis is attenuated in mice with inducible deletion of PDPN (*Pdpn$^{f/f}$;CagCre*). As determined by the affinity precipitation assay, PDPN interacted with galectin-8, but not galectin-1, -3 or -7, and the binding of PDPN to galectin-8 was carbohydrate-dependent (**Fig. 37A**). Additionally, pulldown experiments with agarose beads conjugated with the plant lectin MAAII (specificity: α2,3-sialylated glycans) revealed that PDPN contains α2,3-sialylated glycans (**Fig. 37B**). Removal of α2,3-sialylated glycans by treatment with α2-3 neuraminidase abrogated the interaction of PDPN and galectin-8, suggesting that galectin-8 binds α2,3-sialylated glycans on the *O*-glycans of PDPN (**Fig. 38**). To determine whether PDPN plays a role in Gal-8- and/or VEGF-C-induced lymphangiogenesis, spheroids prepared using primary LECs transfected with control or pooled PDPN siRNA were treated with galectin-8 or VEGF-C. The

expression of PDPN was reduced by 82% in the siRNA transfected LECs (**Fig. 39A**). PDPN knockdown not only markedly inhibited galectin-8-induced LEC sprouting, but also substantially reduced VEGF-C-induced LEC sprouting (**Fig. 39B**). Additionally, PDPN knockdown in LECs substantially reduced galectin-8- and VEGF-C-induced activation of AKT but not ERK (**Fig. 40**), suggesting that PDPN modulates galectin-8- and VEGF-C-induced lymphangiogenesis largely by activation of AKT pathway.

To determine whether PDPN plays a role in galectin-8- and/or VEGF-C-induced lymphangiogenesis in vivo, I used mice with tamoxifen-inducible global deletion of PDPN (*Pdpn$^{f/f}$;CagCre*)[203] to perform the corneal micropocket assays. As expected, VEGF-C pellets markedly induced both hemangiogenesis and lymphangiogenesis in WT mice. The extent of VEGF-C-induced hemangiogenesis was similar in both WT and PDPN-deficient mice (**Fig. 41**). In contrast, VEGF-C-induced lymphangiogenesis was significantly reduced in the PDPN-deficient mice (**Fig. 41**). Likewise, galectin-8-induced lymphangiogenesis, but not hemangiogenesis, was reduced in PDPN-deficient mice (**Fig. 42**). Together, the data suggest that PDPN is a key player, not only in galectin-8-induced lymphangiogenesis but also in VEGF-C-induced lymphangiogenesis.

Figure 37.

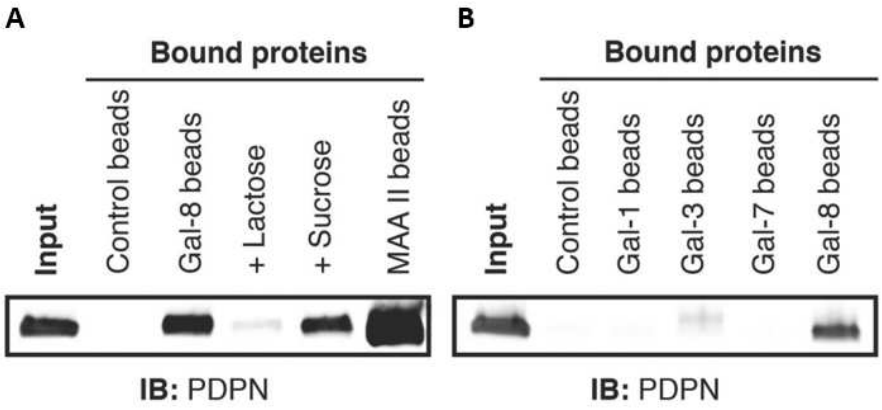

Figure 37. Galectin-8 binds to PDPN in LECs. PDPN binds to galectin-8, but not to galectin-1, -3 or -7. (**A**) LEC lysates were incubated with galectin-8-Agarose beads in the presence or absence of lactose or sucrose (100 mM), and with MAAII-conjugated agarose beads. (**B**) LEC lysates were incubated with galectin-conjugated to agarose beads. Bound proteins were examined along with total cell lysates (input) by Western blot using anti-PDPN.

Figure 38.

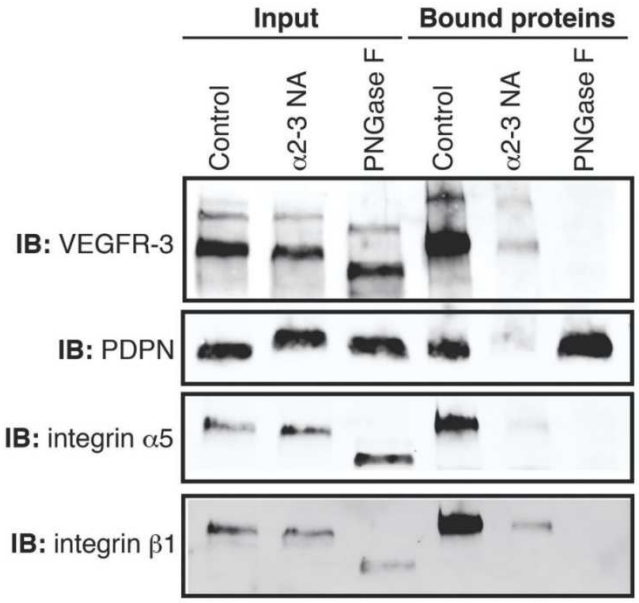

Figure 38. Galectin-8 interacts with the α2,3-sialyl glycans of VEGFR-3, PDPN and integrins. Primary LECs were incubated with buffer only (control), α2-3 neuraminidase (α2-3NA) that removes α2,3-sialyl glycans, or peptide-N-glycosidase F (PNGase F) that removes complex glycans from N-linked glycoproteins at 37ºC for 1 hr. After the incubation, reaction was stopped by adding 400 µl Triton lysis buffer and the reaction mixture was incubated with galectin-8 agarose beads at 4ºC overnight. Unbound proteins were removed and the bound proteins were eluted with 20 µL of 2× Laemmli sample buffer and examined along with input by Western blotting. Note that without complex N-glycan, VEGFR-3 and integrins do not interact with galectin-8; PDPN without α2,3 sialyl glycans does not interact with galectin-8. The results are representative of three independent experiments.

Figure 39.

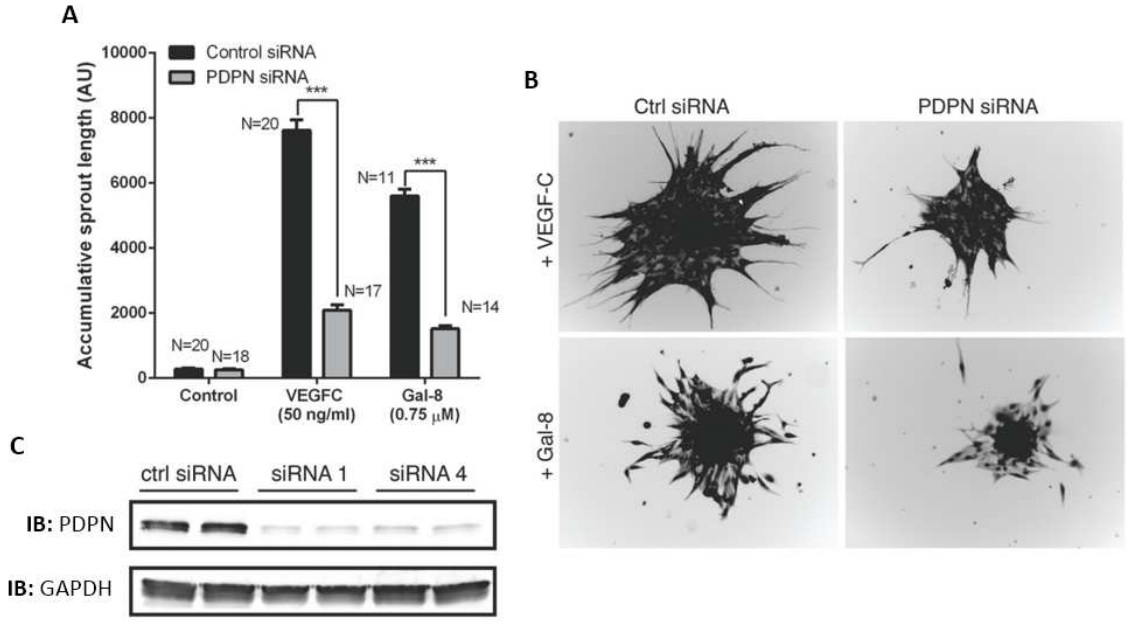

Figure 39. PDPN is required for galectin-8-mediated LEC sprouting. (**A** and **B**) PDPN knockdown inhibits VEGF-C- as well as galectin-8-induced LEC sprouting. Spheroids prepared using primary LECs transfected with control or pooled PDPN siRNA were treated with galectin-8 (0.75 μM) or VEGF-C (50 ng/ml). After 24 hr, accumulated sprout lengths were quantified (A). Representative images of the sprouts are shown in the right panel (B). Data are plotted as mean ± SEM and analyzed using Student's t test. ***P<0.0001. (**C**) PDPN knockdown: primary LECs were transfected with control (mock) or two siRNA that targeted different regions of PDPN. Knockdown efficiency was assessed by Western blot using anti-PDPN and anti-GAPDH antibodies.

Figure 40.

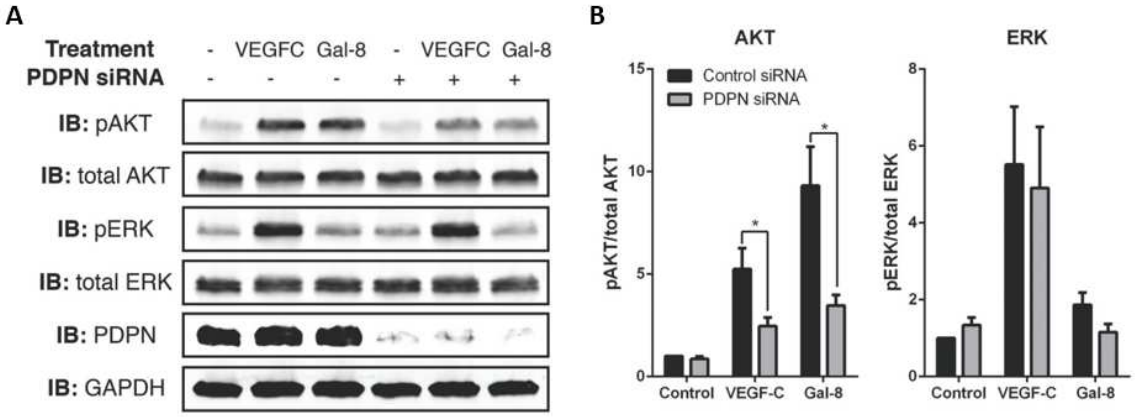

Figure 40. PDPN knockdown interferes with galectin-8- and VEGF-C-mediated signal. PDPN knockdown significantly decreases galectin-8-induced as well as VEGF-C-induced activation of AKT but not ERK. Primary LECs were transfected with control or PDPN siRNA. The cells were serum-starved and treated with galectin-8 (0.5 μM) or VEGF-C (50 ng/ml, positive control) for 30 min. Electrophoresis blots of cell lysates were probed with indicated antibodies (A). Quantification of fluorescence intensity of Western blots (N=5) is shown in right panels (B). Data are plotted as mean ± SEM and analyzed using Student's t test (c,e). *P<0.05 vs corresponding control.

Figure 41.

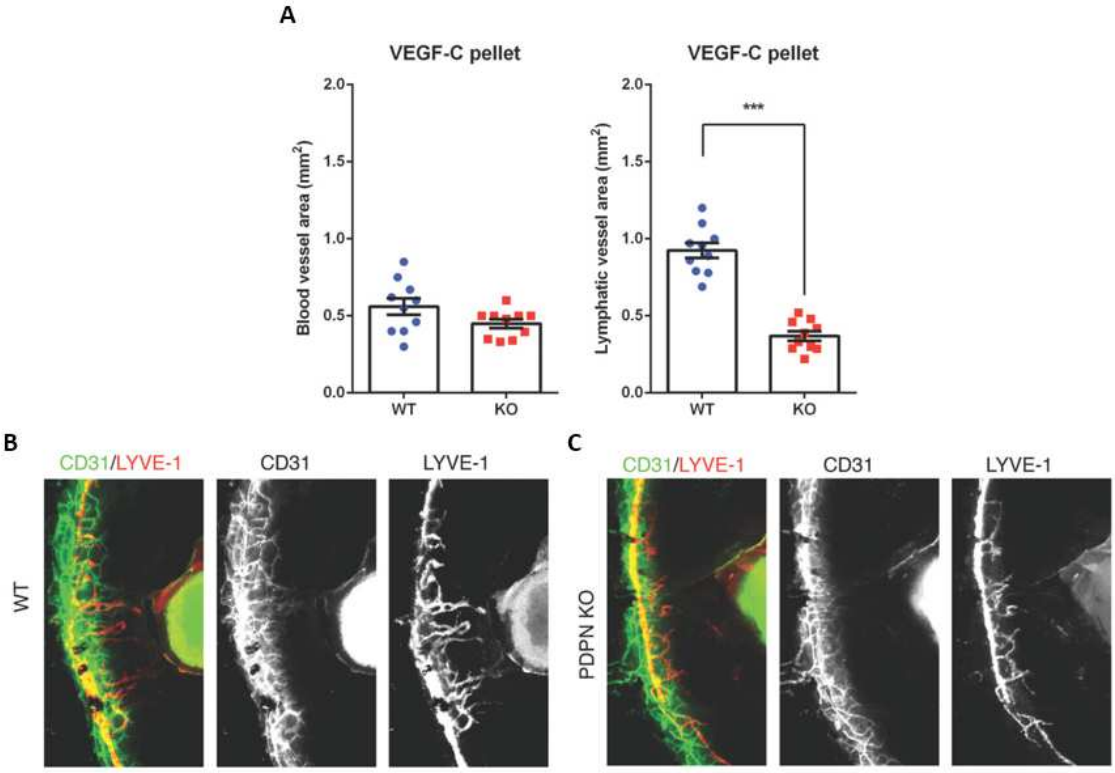

Figure 41. PDPN is required for VEGF-C-induced lymphangiogenesis in vivo. (**A** to **C**) VEGF-C pellets (160 ng) were implanted into wild type (WT) (B) and PDPN inducible KO (C) mice. After 7 day post implantation, the corneal flat mounts were stained with anti-CD31 and anti-LYVE-1 to visualize blood and lymphatic vessels, respectively. Blood vessel and lymphatic vessel areas were quantified (A). Representative fluorescence images from each group are shown in the bottom panels (B, C). N=10 for WT and KO mice. Data are plotted as mean ± SEM and analyzed using Student's t test. ****P*<0.001 vs WT. The results are representative of two independent experiments.

Figure 42.

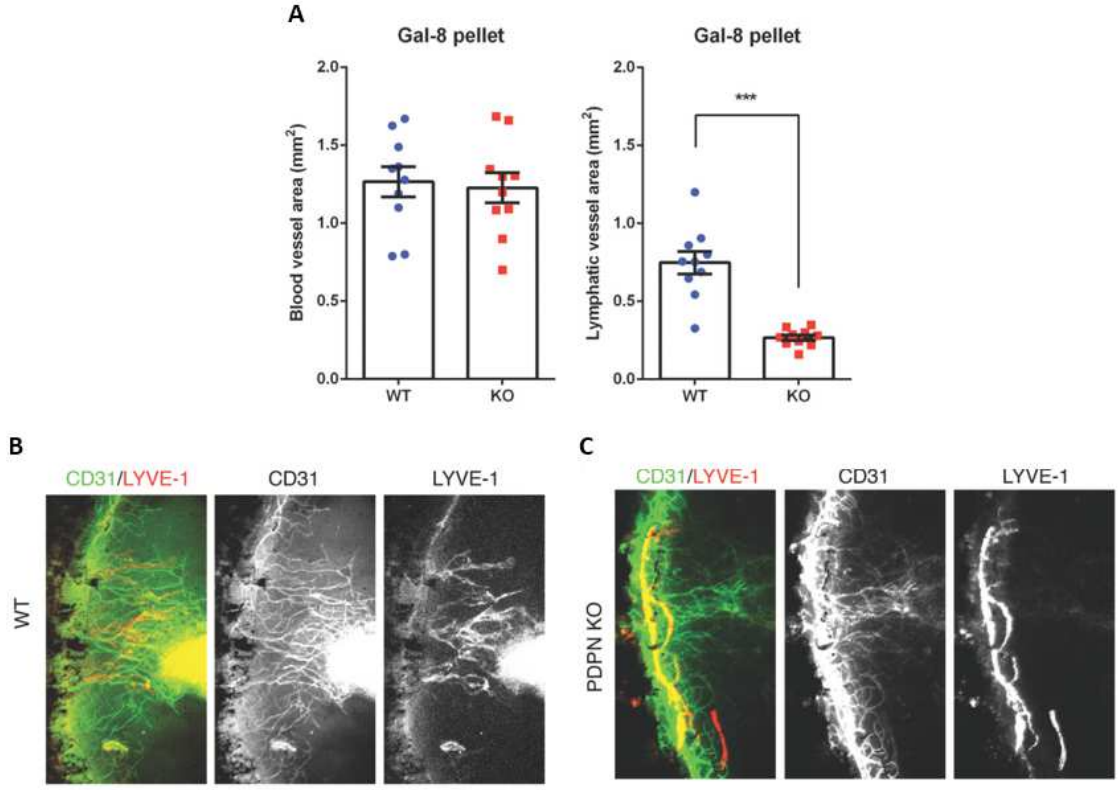

Figure 42. PDPN is required for galectin-8-induced lymphangiogenesis in vivo. (**A** to **C**) Galectin-8 pellets (160 ng) were implanted into wild type (WT) (B) and PDPN inducible KO (C) mice. After 7 day post implantation, the corneal flat mounts were stained with anti-CD31 and anti-LYVE-1 to visualize blood and lymphatic vessels, respectively. Blood vessel and lymphatic vessel areas were quantified (A). Representative fluorescence images from each group are shown in the bottom panels (B, C). N=9 for WT and KO mice. Data are plotted as mean ± SEM and analyzed using Student's t test. ****P*<0.001 vs WT. The results are representative of two independent experiments.

3.7 Integrins play a key role in galectin-8-mediated lymphangiogenesis.

In addition to α9β1 integrin, several other integrins including α1β1, α4β1 and α5β1 are involved in the process of lymphangiogenesis (reviewed in Chen et al[229]) and the interplay between integrin β1 and VEGFR-3 has been reported.[230,231] Therefore, to determine whether galectin-8-PDPN lymphangiogenic pathway involves specific integrins, first, LEC spheroids were treated with galectin-8 or VEGF-C in the presence or absence of blocking antibodies and peptides against a panel of integrins including anti-integrin α5 (clone NKI-SAM-1), anti-integrin αvβ3 (clone 23C6), anti-integrin β5 (clone KN52), Obtustatin (a blocking peptide against integrin α1β1) and BIO1211 (a blocking peptide against integrin α4β1). In this study, only blocking of integrins α1β1 (by Obtustatin) and α5β1 (by the neutralizing antibody) inhibited both VEGF-C- and galectin-8-induced LEC sprouting (**Fig. 43**). Secondly, to determine whether PDPN indirectly regulates the functions of VEGF-C/VEGFR-3 through controlling the function of integrins α1β1 and α5β1 in galectin-8-dependent manner, I performed studies to determine whether: (i) PDPN inhibition attenuates matrix mediated LEC migration, a process in which integrin-mediated cell-matrix interactions play a key role, (ii) PDPN interacts with integrins in a galectin-8-dependent manner, and (iii) knockdown PDPN impedes integrin-mediated signaling cascades. In this study, blocking the function of PDPN by antibodies as well as siRNA knockdown attenuated both fibronectin- and galectin-8- promoted cell migration (**Fig. 44**). These data in conjunction with a published study[118] showing that PDPN-Fc inhibits type I collagen-mediated cell migration suggest

that PDPN is involved not only in galectin-8 but also in fibronectin- and type I collagen-mediated LEC migration, a process in which integrins are well-known to play a key role. To assess the galectin-8-dependent interaction between integrins and PDPN, primary LECs were treated with galectin-8 for 15 minutes, fixed without permeabilization, stained with anti-integrin β1, PDPN and galectin-8 antibodies, and examined by confocal microscopy. In control cells, incubated with buffer only, both integrin β1 and PDPN were homogenously distributed all over the LECs; endogenous galectin-8 was detected all over the cells (**Fig. 45**) and in some cell-free areas presumably the extracellular matrix. Since I showed that galectin-8 was upregulated in inflamed human and mouse corneas, I added the exogenous galectin-8 to see whether galectin-8 changes the distribution of PDPN and/or integrin β1 on LECs. Addition of galectin-8 caused dramatic redistribution and clustering of PDPN and integrin β1 on LEC plasma membrane (**Fig. 45**). In addition, galectin-8, but not VEGF-C, treatment retain PDPN on cell surface (**Fig. 46**). To more directly assess the association between integrins and PDPN, lysates from untreated or galectin-8-treated LECs were incubated with anti-PDPN antibody, and immunoprecipitated proteins were examined by Western blotting using antibodies against integrins β1, α1, α5, galectin-8 and PDPN. In untreated cell lysates, immunoprecipitation with anti-PDPN co-immunoprecipitated endogenous galectin-8 and integrin α1β1, indicating that PDPN interacted with endogenous galectin-8 and the association between PDPN and integrin α1β1 was constitutive (**Fig. 47**). When cells were treated with exogenous galectin-8,

there was an increased association between PDPN and integrin α5β1, while the association between PDPN and integrin α1β1 remained similar (**Fig. 47**).

Next, to assess the role of PDPN on integrin-mediated signaling, LECs transfected with control or PDPN pooled siRNA were seeded on collagen I- or fibronectin-coated wells and allowed to adhere for 15 min at 37ºC. Unattached cells were removed and cell lysates from attached cells on collagen I or fibronectin were analyzed with Western blotting using phospho-specific integrin and focal adhesion kinase (FAK) antibodies. Phosphorylation of integrin β1 at residues Tyr783 and Thr788/789 was reduced in PDPN-knocked down cells compared to corresponding controls (**Fig. 48**), suggesting that the activation of integrin β1 is reduced in the absence of PDPN. Also, phosphorylation of FAK at the residue Tyr397 was decreased in the PDPN-knocked down cells seeded on collagen I- but not fibronectin-coated wells (**Fig. 48**). Additionally, phosphorylation of ERK at residues Thr202/Tyr204 was markedly reduced in the PDPN-knocked down cells seeded on both matrix proteins (**Fig. 48**). Taken together, these data lead us to conclude that PDPN regulates the functions of integrin β1 complexes, specifically of integrins α1β1 and α5β1 in LECs, and that this function is galectin-8 dependent.

Figure 43.

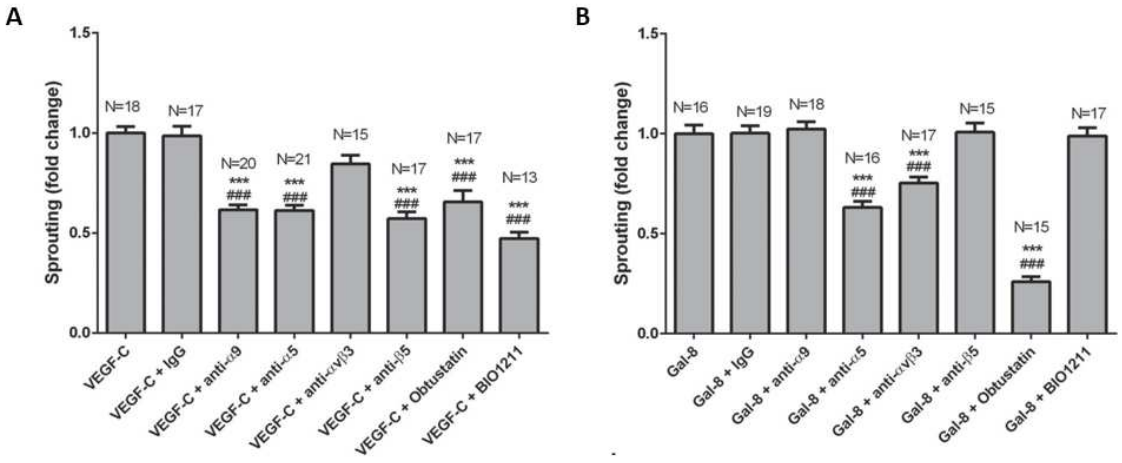

Figure 43. Inhibiting integrins α1β1 and α5β1 attenuates both VEGF-C- and galectin-8-mediated LEC sprouting. α1β1 and α5β1 inhibition reduces both VEGF-C- and galectin-8-induced LEC sprouting. LEC spheroids were stimulated with VEGF-C (50 ng/ml) (A) or galectin-8 (0.75μM) (B) in the presence or absence of control IgG, functional blocking antibodies (20 μg/ml) and peptides. The blocking peptides used in the assay were 4 μM of Obtustatin (specific for integrin α1β1) and 20 μM of BIO1211 (specific for integrin α4β1). After 24 hr, accumulated sprout lengths were quantified. A value of 1.0 was assigned to the sprout length of VEGF-C or galectin-8 treated LEC spheroids. The values for the inhibitor treated groups are expressed as a change in the sprout length with respect to VEGF-C or galectin-8 treated LEC spheroids. Data are plotted as mean ± SEM and analyzed using one-way ANOVA. ***P<0.001 vs VEGF-C or Gal-8; ###P<0.001 vs VEGF-C or Gal-8 + control IgG.

Figure 44.

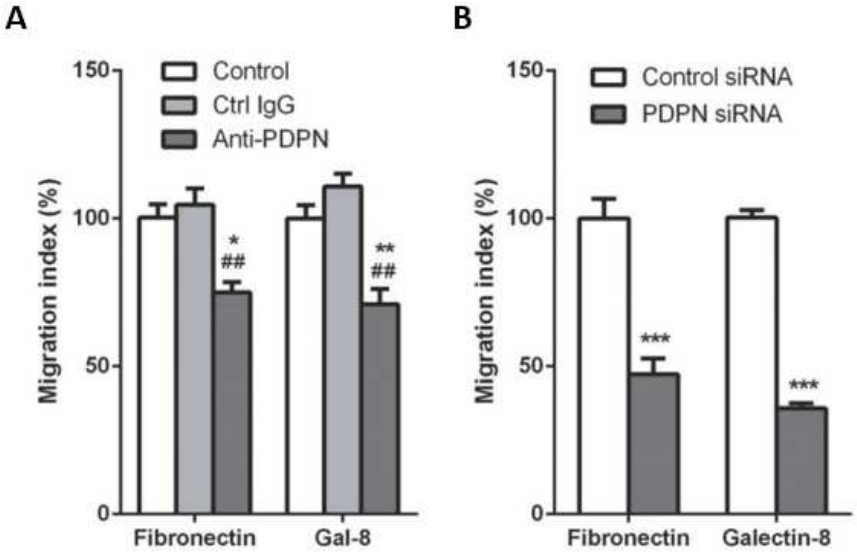

Figure 44. Knockdown and functional blocking of PDPN inhibit fibronectin-mediated LEC migration. (**A**) LECs were incubated with or without isotype control Ab or anti-PDPN Ab (10 μg/ml). (**B**) LECs were transfected with control siRNA or PDPN siRNA. The cells were seeded into the upper chamber of Transwell inserts. The lower-side of the insert membrane was coated with fibronectin (10 μg/ml) or galectin-8 (0.5 μM). After incubation for 2 hr at 37ºC, LECs that migrated to lower side of the membrane were counted. Results are expressed as % change where control is set as 100%. Data are plotted as mean ± SEM and analyzed using one-way ANOVA (A) and Student's t test (B). **P*<0.05, ***P*<0.01 vs control IgG (A); ****P*<0.001 vs control siRNA (B); $^{\#\#}$*P*<0.01 vs control IgG (A).

Figure 45.

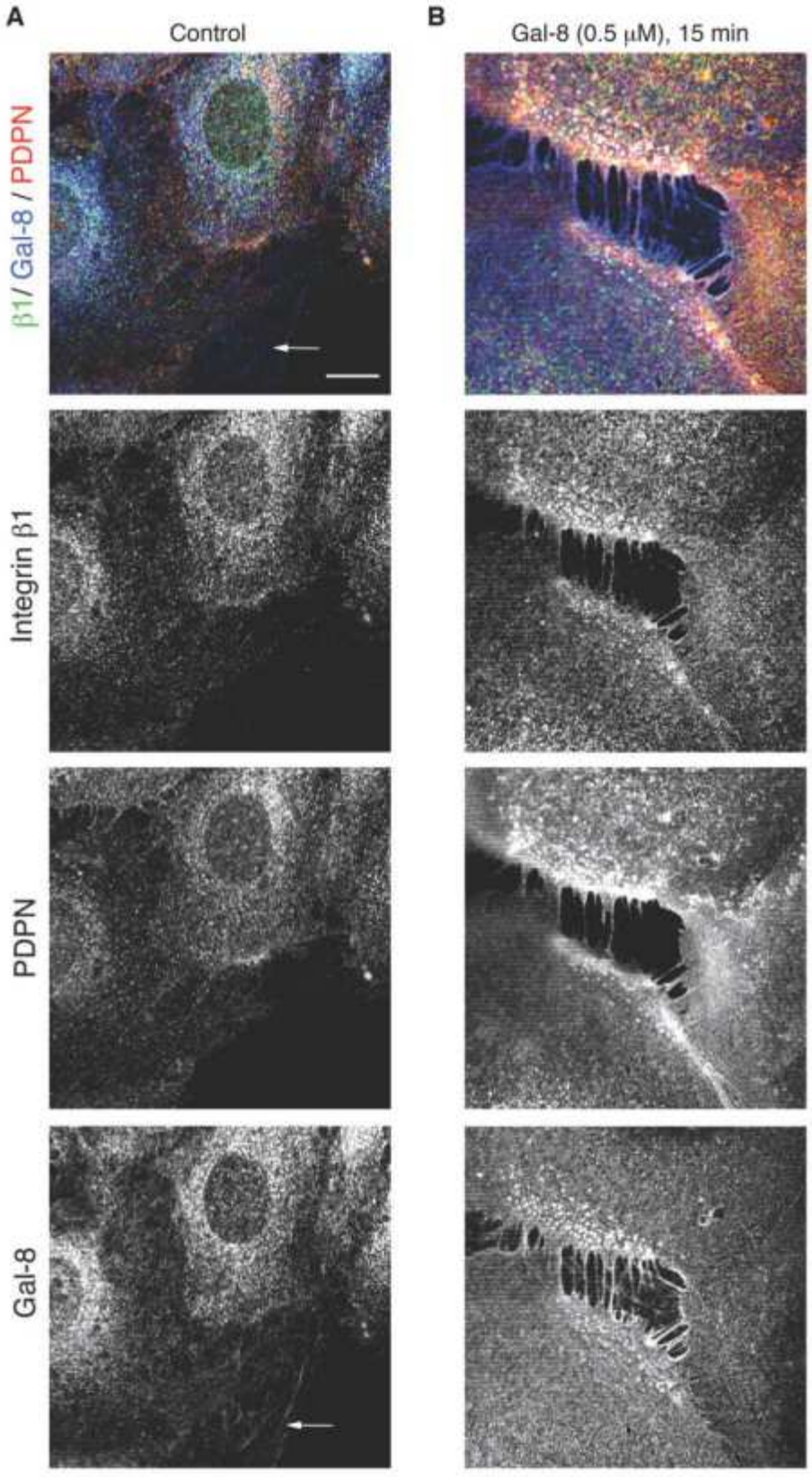
A
Control
B
Gal-8 (0.5 μM), 15 min
β1 / Gal-8 / PDPN
Integrin β1
PDPN
Gal-8

Figure 45. Galectin-8 treatment clusters PDPN and integrin β1. LECs were treated with or without galectin-8 for 15 min, fixed without permeabilization, stained with antibodies to anti-integrin β1 (green), PDPN (red) and galectin-8 (blue), and examined by confocal microscopy. Merged images are shown in the top panel. (**A**) In control LECs, no obvious colocalization of integrin β1, galectin-8 and PDPN. Note that galectin-8 also distributes at some cell-free area (arrow). (**B**) Exogenous galectin-8 sequesters integrin β1 and PDPN. PDPN and integrin β1 distribution reorganized and colocalized (white spots in the merged image) at cell borders after galectin-8 treatment. Scale bar: 10 μm.

Figure 46.

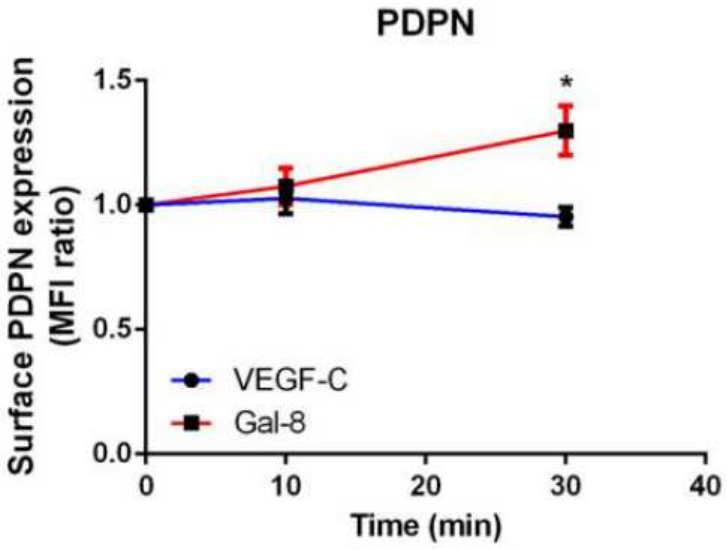

Figure 46. Galectin-8 treatment retains PDPN on cell surface. Gal-8 increases cell-surface residency PDPN. Primary LECs were treated with VEGF-C (50 ng/ml) or galectin-8 (0.2 μM) for 10 and 30 min. Cells were fixed and stained with anti-PDPN antibody. Cell surface expression of PDPN was analyzed with flow cytometry and quantified with FlowJo. Data are plotted as Mean ± SEM from three independent experiments and analyzed with Student's t test. *P<0.05, ***P<0.001 vs VEGF-C treatment. MFI: mean fluorescence intensity.

Figure 47.

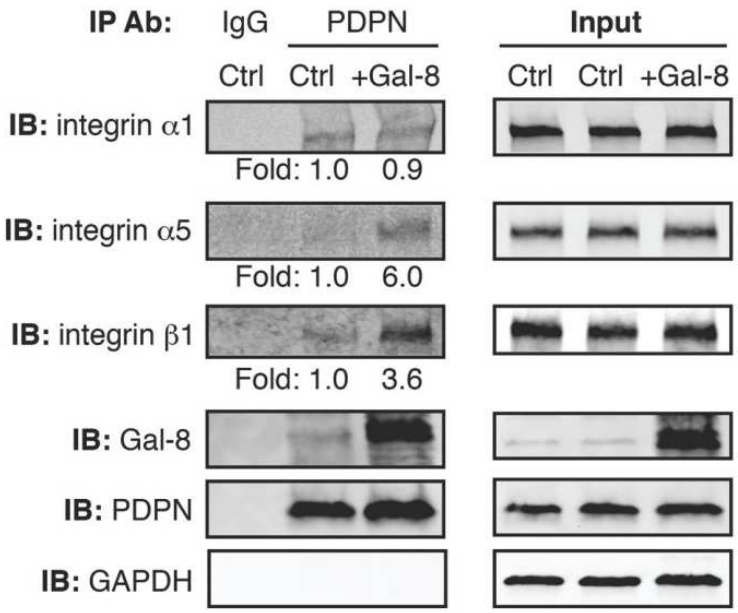

Figure 47. PDPN interacts with integrins in a galectin-8-dependent manner. Integrins α5 and β1 interact with PDPN in a galectin-8-dependent manner. LECs were incubated with or without galectin-8 (0.5 μM) for 15 min at 37ºC. Total cell lysates were immunoprecipitated with control antibody and anti-PDPN antibody, and were processed for Western blotting using antibodies indicated. Fold changes are normalized to PDPN.

Figure 48.

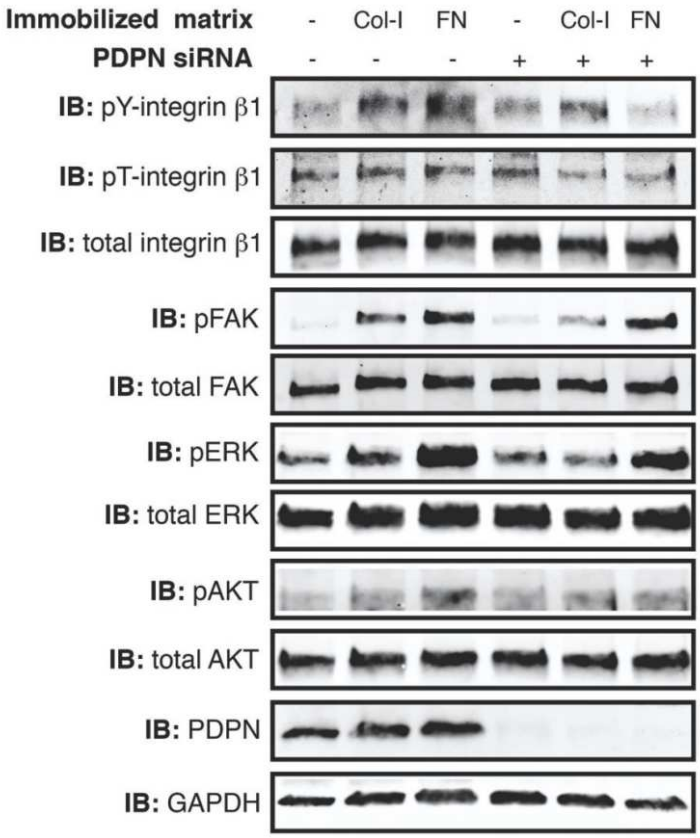

Figure 48. Knockdown of PDPN impedes extracellular matrix-induced signal. LECs were transfected with control or PDPN pooled siRNA. The cells were detached 48 hr post-transfection and stimulated with immobilized collagen I (4 μg/cm^2) or fibronectin (2 μg/cm^2), or left in suspension for 15 min at 37ºC. Cell lysates were subjected to Western blotting with antibodies indicated in methods.

3.8 Galectin-8 inhibitors significantly decrease inflammatory lymphangiogenesis in vivo.

To determine whether galectins can be targeted to control lymphangiogenesis, two in vivo models of lymphangiogenesis were used. After suture placement and $AgNO_3$ cauterization in the corneas of *Prox1*-EGFP reporter mice to induce inflammation, the mice were treated with TDG (200 mM, a pan inhibitor of galectins) or Gal-8N (15 μg, the dominant negative inhibitor of galectin-8) by subconjunctival injections on days 0, 2, 4 and 6 postsurgery. At the end of the treatment period, lymphatic vessel areas were quantified. Treatment with both TDG as well as Gal-8N significantly suppressed suture- and cautery-induced corneal lymphangiogenesis (**Fig. 49** and **Fig. 50**). These data suggest a promising new mechanism for the modulation of pathological lymphangiogenesis by targeting galectin-8.

Figure 49.

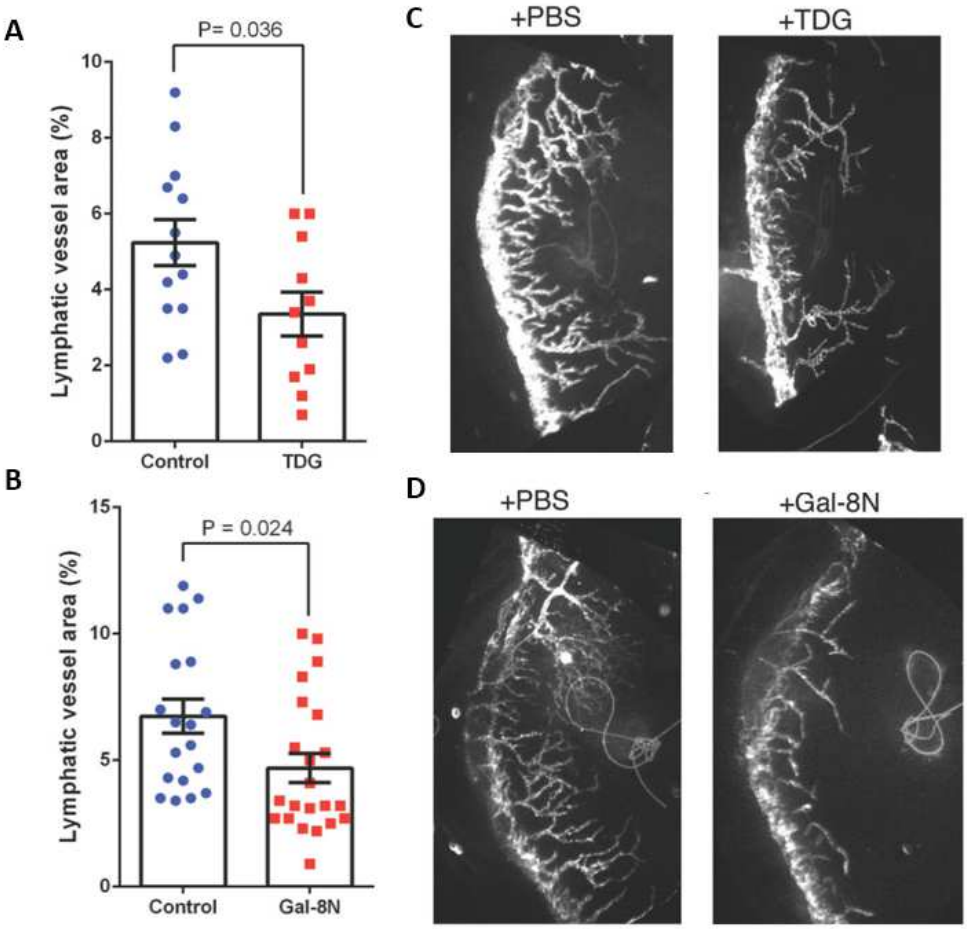

Figure 49. TDG and Gal-8N inhibit suture-induced lymphangiogenesis. Sutures were placed approximately 2 mm above the limbic vessel in the corneas of the *Prox1*-EGFP reporter mice. The animals were treated with TDG (200 mM in 10 µL, a pan inhibitor of galectins) (A, C), or Gal-8N (15 µg in 10 µL, a dominant negative inhibitor of galectin-8) (B, D) by local subconjunctival injections on days 0, 2, 4 and 6 post-surgery. At the end of the treatment period, lymphatic vessel areas were quantified (A, B). Representative images are shown in the right panels. Data are plotted as mean ± SEM and analyzed using Student's t test. The results are representative of two independent experiments.

Figure 50.

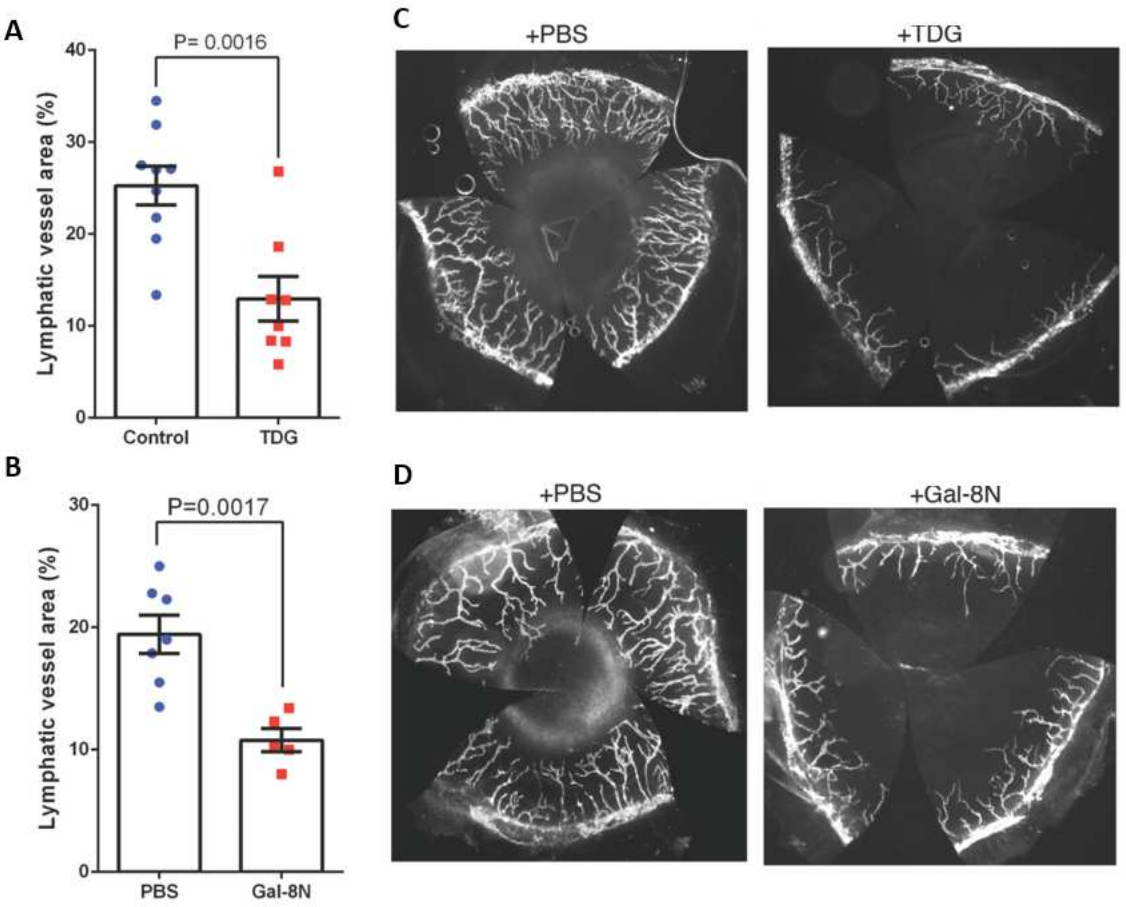

Figure 50. TDG and Gal-8N inhibit cautery-induced lymphangiogenesis. Silver nitrate cautery was introduced in the center of the corneas of the *Prox1*-EGFP reporter mice. The animals were treated with TDG (200 mM in 10 µL, a pan inhibitor of galectins) (A, C), or Gal-8N (15 µg in 10 µL, a dominant negative inhibitor of galectin-8) (B, D) by local subconjunctival injections on days 0, 2, 4 and 6 post-surgery. At the end of the treatment period, lymphatic vessel areas were quantified (A, B). Representative images are shown in the right panels. Data are plotted as mean ± SEM and analyzed using Student's t test. The results are representative of two independent experiments.

Discussion

4.1 Galectins as PAMPs and DAMPs in corneas.

We demonstrated here that galectins-1, -3, -7, -8, and -9, are expressed in normal mouse cornea, and under pathological conditions, expression levels and distribution of various galectins are drastically altered. In normal corneas, galectin-3 is mainly localized in epithelium, galectins-7, -8 and -9 are distributed in corneal epithelium and stroma, and galectin-1 is localized mainly in corneal stroma. All five galectins are highly upregulated in the insulted corneal stroma, whereas galectin-3 expression is markedly downregulated in insulted corneal epithelium. Source of galectins in the insulted corneal stroma can be infiltrating immune cells (reviewed in Liu FT et al.),[232] injured epithelium, activated tissue-resident macrophages, and endothelial cells of new blood vessels.

We used two different mouse models representing sterile and non-sterile inflammation. Antigen presenting cells recognize both pathogen-associated molecular patterns (PAMPs) from microbes (non-sterile inflammation, stranger model)[233] and damage-associated molecular patterns (DAMPs) from stressed, damaged and/or dying self-cells in the local tissue (sterile inflammation, danger model).[234] Both PAMPs and DAMPs induce inflammation by some shared receptors such as toll-like receptors and RAGE, as well as by distinct mechanisms. In this respect, a recent study has demonstrated that microRNA expression induced by DAMPs and PAMPs has a distinct signature; expression of miR-34c and miR-214 is increased in cells stimulated with DAMP, but not PAMP.[235] Galectins are considered DAMPs and receptors for PAMPs.[236]

We report here that changes in the expression levels of three of the five galectins tested (galectins-3, -8, and -9) were similar in both models. Overall, in both infected and cauterized corneas, galectin-3 expression was downregulated, whereas galectins-8 and -9 were upregulated. Changes in the expression level of galectins-1 and -7 were distinct in infected and cauterized corneas. Overall expression of these two galectins was downregulated in infected corneas but was either upregulated (galectin-7) or did not change (galectin-1) in cauterized corneas. Regardless of whether whole corneas were analyzed or corneal epithelial and stromal layers were analyzed separately, galectins-8 and -9 were upregulated in both infected and cauterized corneas. Decrease in galectin-3 expression in infected and cauterized corneas was largely due to the reduced expression of this lectin in corneal epithelium. Intriguingly, when epithelial and stromal layers were analyzed separately, galectins-1 and -7 expression was upregulated in both corneal epithelium and stroma, whereas when whole corneas were analyzed the expression of both these lectins was downregulated. Such a discrepancy, however, is readily explicable. Since galectins are soluble proteins and distributed in the extracellular matrix, tissue fluid, cell membrane and cytosol, it is possible that tissue fluid containing soluble galectins can leach out from inflamed corneas during incubation with EDTA and/or during separation of epithelial and stromal tissues. For galectins-1 and -7, the amounts of these two lectins in tissue fluid may be trace; therefore, the separation process of the tissue sheets may concentrate the two lectins.

Galectin-1 has been shown to suppress both *P. aeruginosa*- and HSV-induced corneal immunopathology by shifting the balance between effector T cells and regulatory T cells, and to inhibit pro-inflammatory cytokine production from innate immune cells.[196,237,238,239] Galectin-3 binds to the LPS of *P. aeruginosa* and may facilitate the invasion when the cornea gets infected.[240] Thus, in contrast to the protective effect of galectin-1 on immunopathology of Pseudomonas keratitis, it is possible that galectin-3 may exacerbate the infection. On the other hand, galectin-3 may also have protective effect due to its ability to accelerate re-epithelialization of corneal wounds.[162] Clearly, additional studies are needed to delineate the role of galectin-3 in the pathogenesis of Pseudomonas keratitis.

The role of galectins-7, -8 and -9 in *P. aeruginosa*-mediated corneal pathogenesis has thus far not been characterized. It has been reported that neutralizing galectin-9 abrogates the immune privilege status of the cornea and that local subconjunctival injections of galectin-9 diminishes the severity of HSV keratitis as well as the degree of corneal neovascularization in the mouse animal model.[241,242] Considering that galectin-9 deficiency aggravates several autoimmune diseases[242] and that exogenous galectin-9 increases effector T cell apoptosis and promotes regulatory T cell polarization,[243,244] it is possible that the upregulation of galectin-9 in the infected cornea may help dampen the corneal inflammation during *P. aeruginosa* infection.

As described above, changes in the expression level of galectins-7, -8 and -9 were distinct in the epithelium of infected and cauterized corneas. The

expression level of the three galectins was upregulated in infected corneas, but did not change in cauterized corneas. The significance of this observation is not clear at this time. However, the three galectins in infected corneas may function as receptors for PAMPs and the upregulation may be related to the defense mechanism in corneal epithelium.

4.2 Gal-8N as a dominant negative inhibitor for galectin-8.

Di/multivalent property of galectins allow them to cross-link many cell surface and extracellular matrix glycoproteins, such as integrins and growth factor receptors, to regulate signal transduction pathways.[245-248] In this respect, it is known that isolated CRDs of galectin-8 retain the carbohydrate binding activity but manifest impaired biological activity,[183,218] suggesting that the biological function of the lectin requires cooperative interactions of the two CRDs. In my studies, truncated galectin-8 containing only the N-CRD (Gal-8N) not only failed to induce lymphangiogenesis, but also effectively inhibited the lymphangiogenesis induced by full-length galectin-8. This suggests that Gal-8N effectively competes with full-length galectin-8 and thereby acts as a dominant negative inhibitor of galectin-8. In this respect, it has been reported that truncated galectin-3 containing a full CRD but lacking the N-terminal oligomerizing domain also serves as a dominant negative inhibitor of galectin-3.[155,217]

4.3 The interplay among galectin-8, integrins, PDPN and VEGFR-3.

A major finding of the current study is that galectin-8 modulates VEGF-C mediated lymphangiogenesis. My studies show that Gal-8N, the dominant-negative inhibitor of galectin-8, and 3'-SL (a competing disaccharide), but not 6'-SL (a noncompeting disaccharide) ameliorated VEGF-C-induced lymph-angiogenic activity in vitro. Furthermore, in the in vivo corneal micropocket assay, the extent of lymphangiogenesis induced by VEGF-C was significantly less in galectin-8 KO mice compared with the WT mice. To our knowledge, this is the first demonstration of a defect in lymphangiogenic response of galectin-8 knockout mice. Additionally, exogenous galectin-8 markedly enhanced VEGF-C-induced lymphangiogenesis in a carbohydrate-dependent manner. Together, these data conclusively establish that galectin-8 significantly influences VEGF-C-mediated lymphangiogenesis. Of note, the inhibitory effect of Gal-8N on VEGF-C-induced LEC sprouting is bell-shaped, which is similar to several other anti-(lymph)angiogenic molecules, such as RGD-mimetic integrin inhibitors, plasminogen activator-1, bortezomib, TGF-β1 and some HMG-CoA reductase inhibitors.[249,250] Not surprisingly, much higher concentration of galectin-8 (0.75 μM), compared to VEGF-C (2.38 nM), was required to produce equivalent LEC sprouting. This is because generally, the affinity of CRD of galectins towards their glycan ligands is lower (dissociation constant: ~ μM) compared to typical protein−protein interaction (dissociation constant: ~ 10 nM).[251] Despite the weak affinity of their CRD, galectins achieve a stable interaction with their ligands due to their multivalency that results in overall high avidity.[252,253] Therefore, even if

the affinity of one galectin-8 molecule for one PDPN molecule is weak, the overall high avidity is able to activate lymphangiogenesis pathway.

My findings that PDPN binds to galectin-8 in a carbohydrate-dependent manner, that it contains the high affinity glycans of galectin-8 (α2,3-sialylated glycans), that galectin-8 clusters PDPN on cell surface, and that unlike the knockdown of VEGFR-3, knockdown of PDPN abrogates galectin-8-induced lymphangiogenesis suggest that PDPN is a key player in the mechanism of galectin-8-induced lymphangiogenesis. Another major finding of the current study is that PDPN plays a critical role in VEGF-C-mediated lymphangiogenesis. Thus far, VEGF-C- and PDPN-mediated pathways have been independently shown to promote lymphangiogenesis, but the relationship in the molecular mechanism of the two pathways has not been demonstrated. My findings that PDPN knockdown in LECs only attenuated VEGF-C- induced AKT, but not ERK, phosphorylation, suggest that VEGF-C-induced AKT phosphorylation is PDPN-dependent. Interestingly, a previous study has shown that VEGF-C induces a strong AKT activation in LECs but not in blood ECs, whereas VEGF-C induces strong ERK activation in both cell types.[254] These data lead us to propose that AKT phosphorylation through PDPN may be essential for VEGF-C signaling in LECs. On the other hand, my findings that PDPN knockdown attenuates extracellular matrix protein-mediated activation of integrin pathway including phosphorylation of integrin β1, AKT and ERK, that integrin α5β1 binds to PDPN and galectin-8, and a published report showing that inhibiting integrin α5β1 curbs VEGF-C-mediated VEGFR-3 activation,[231] collectively suggest that PDPN

indirectly regulates VEGF-C-mediated signaling pathway by controlling the function of integrin α5β1, in which case one would expect the attenuation of both ERK and AKT activation in the PDPN knockdown cells. However, I observed that VEGF-C-mediated ERK activation is not significantly affected in the PDPN knockdown cells. I reason that VEGF-C-induced ERK, but not AKT, activation may be compensated by other integrins such as αvβ5 when the function of PDPN/galectin-8−associated integrin α5β1 is inhibited. This notion is supported by my observation that VEGF-C-, but not galectin-8-, induced LEC sprouting is inhibited by integrin αvβ5, as well as by a published study showing that VEGF-A-induced ERK activation is regulated by integrin αvβ5.[255] Together, my findings suggest that a galectin-8-dependent cross-talk among VEGF-C, PDPN, and integrin pathways plays a critical role in lymphangiogenesis. This is an important conceptual advance in the understanding of the molecular mechanism of a well-known VEGF-C lymphangiogenic pathway.

My studies revealed that VEGFR-3 is a galectin-8-binding protein, and galectin-8 clusters and retains VEGFR-3 on cell surface. Despite this, VEGFR-3 knockdown did not inhibit galectin-8-induced sprouting. This suggests that although VEGF-C-induced lymphangiogenesis is dependent on extracellular galectin-8, the lectin has the capacity to promote lymphangiogenesis independently of VEGFR-3, and VEGFR-3 may be a pseudoreceptor for galectin-8. I reason that inhibiting galectin-8 attenuates VEGF-C mediated signaling because the function of integrins α1β1 and α5β1, rather than VEGFR-3, is inhibited by galectin-8 inhibitors. I propose that galectin-8 has a unique dual-

faceted mechanism of action to promote lymphangiogenesis where galectin-8-mediated interactions between lymphangiogeneic integrins, α1β1/α5β1, and PDPN, are sufficient to activate the integrins and trigger the process of lymphangiogenesis without the involvement of VEGFR-3 (Model I, **Fig. 51Bi**), but in the presence of VEGFR-3, PDPN-galectin-8-integrin interactions substantially increase the magnitude of lymphangiogenic pathway by potentiating the VEGF-C/VEGFR-3 signaling (Model II, **Fig. 51Bii**). Accordingly, the resultant glycan-galectin lattice activates AKT, ERK and FAK to promote lymphangiogenesis. (**Fig. 51C**). Model I is supported by current studies showing that (i) VEGFR-3 is dispensable in galectin-8-mediated lymphangiogenesis, (ii) galectin-8-mediated lymphangiogenesis is dependent on PDPN and integrins α1β1/α5β1, and (iii) galectin-8 treatment increases the interaction of PDPN and integrin β1. This concept is further supported by published studies showing that (i) mouse embryonic fibroblasts lacking VEGFRs adhere and migrate on fully processed VEGF-C and D in an integrin α9β1-dependent manner,[225] suggesting that interaction between integrins with certain ligands can affect cell behavior in the absence of the growth factors' cognate receptor, VEGFR-3, (ii) extracellular matrix-induced LEC sprouting is independent of the intrinsic kinase activity of VEGFR-3,[256] (iii) galectins cross-link cell surface receptors including integrins by interacting with their glycans,[156,214,245,247] and (iv) galectin-mediated clustering of cell surface receptors leads to the activation of intracellular signaling.[245,246,248,257,258] Model II is supported by my findings that galectin-8 potentiates VEGF-C-induced lymphangiogenesis in vitro and in vivo, that

galectin-8 inhibitors attenuate VEGF-C-induced lymphangiogenesis in vitro as well as in vivo, and that galectin-8-induced lymphangiogenesis is reduced by α1β1 and α5β1 inhibitors. This concept is further reinforced by published studies showing that: (i) integrins associating with growth factor receptors regulate the capacity of the integrin/receptor complexes to propagate downstream signals,[33,259,260] and (ii) interaction between VEGFR-3 and integrin α5β1 is increased after VEGF-C stimulation.[231] (**Fig. 51A**)

Figure 51.

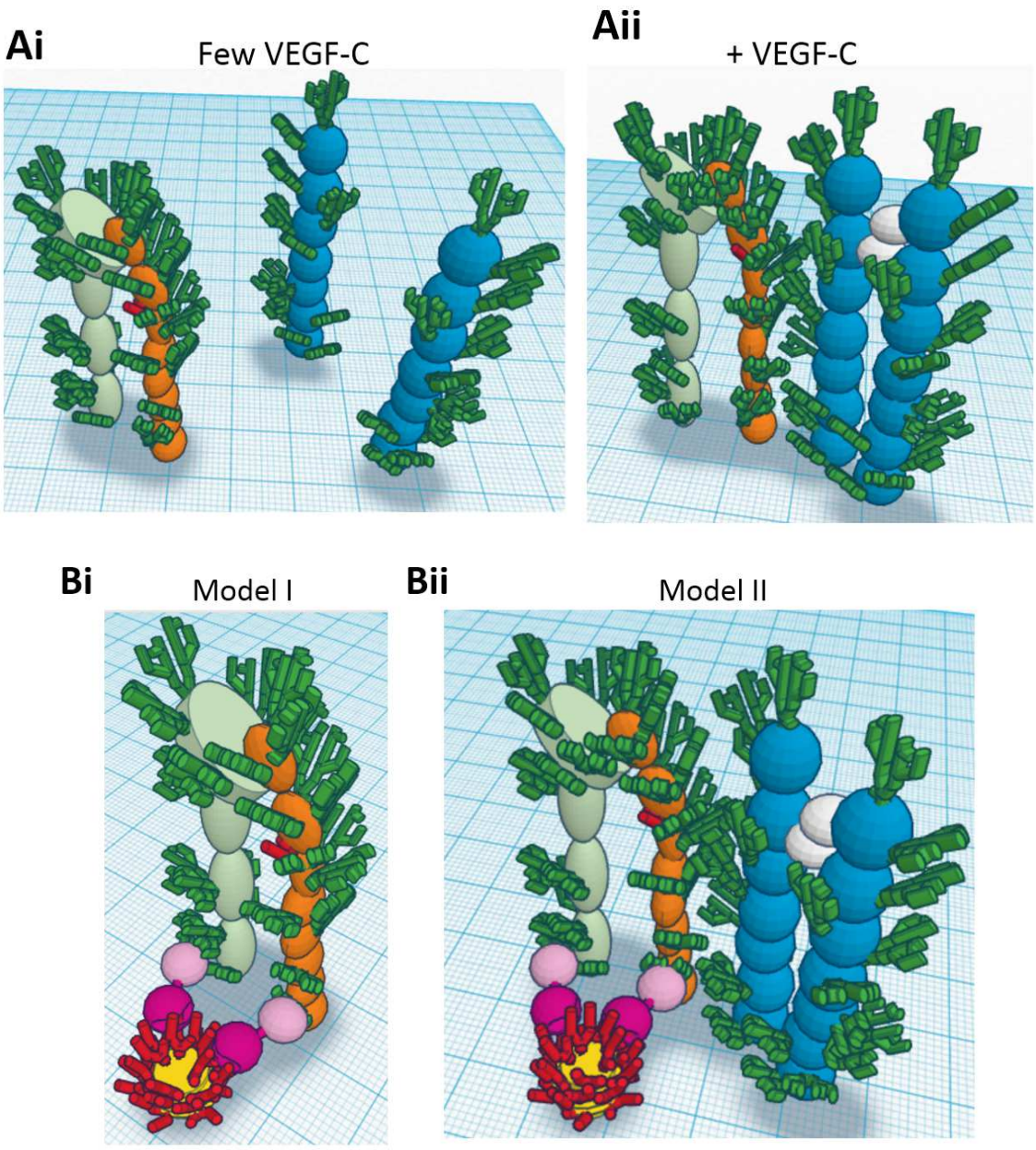

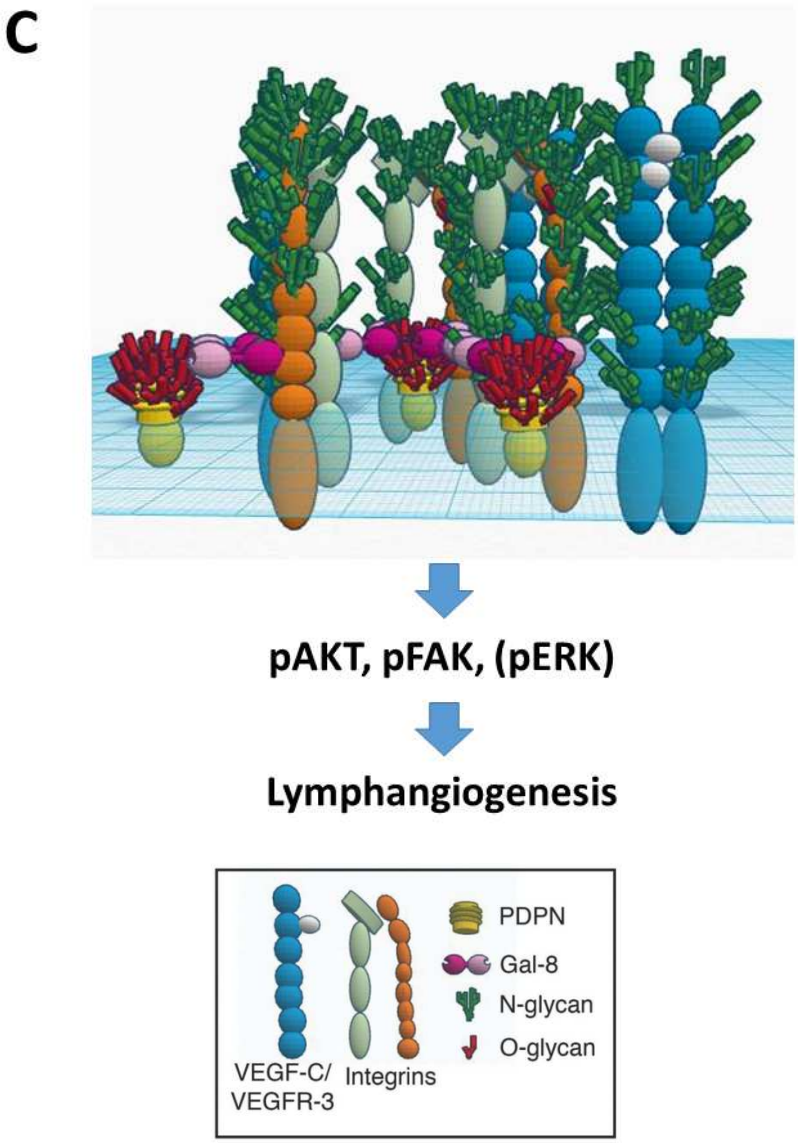

Figure 51. Proposed models of galectin-8-mediated lymphangiogenesis. (**A**) Interaction of VEGF-C/VEGFR-3 and integrins. (**i**) In the absence of VEGF-C, VEGFR-3 receptor is monomer and has few interaction with integrins. (**ii**) In the presence of VEGF-C, VEGFR-3 forms a dimer and associates with integrins. (**B**) (**i**) According to Model I, galectin-8 cross-links and clusters integrins α1β1/α5β1 and PDPN on the cell surface. The clustering activates lymphangiogenic signaling pathways that modulate events such as endothelial cell migration and sprouting without the involvement of VEGFR-3. This model is supported by current studies showing that (a) VEGFR-3 is dispensable in galectin-8-mediated lymph-angiogenesis, (b) galectin-8-mediated lymphangiogenesis is dependent on PDPN, and integrins α1β1/ α5β1, and (c) galectin-8 treatment increases the interaction of PDPN and integrin β1. (**ii**) In the presence of VEGFR-3 (Model II), PDPN−galectin-8−integrin interactions substantially increase the magnitude of lymphangiogenic pathway by potentiating the VEGF-C/VEGFR-3 signaling. This

model is supported by my findings that galectin-8 potentiates VEGF-C-induced lymphangiogenesis in vitro and in vivo, that galectin-8 inhibitors attenuate VEGF-C-induced lymphangiogenesis in vitro as well as in vivo, and that Gal-8-induced lymphangiogenesis is reduced by α1β1 and α5β1 inhibitors. Note that only extracellular domains of glycoproteins are shown. (**C**) Galectin-8-mediated lattice formation promotes lymphangiogenesis via activation of AKT and FAK signaling pathway. As galectin-8 treatment also activates ERK pathway, the lattice may indirectly activate ERK pathway.

Future Directions

5.1 Role of macrophages in galectin-8-mediated lymphangiogenesis.

Macrophages can directly and indirectly contribute to lymphangiogenesis. For direct mechanism, macrophages acquire LEC phenotype under inflammatory conditions and integrate into lymphatic vessels.[89,128,261] In addition, two VEGFR-3$^+$ cells in human blood (a small subpopulation of CD133$^+$VEGFR-3$^+$CD34$^+$ cells and a major subpopulation of CD14$^+$VEGFR-3$^+$CD31$^+$VEGFR-2$^-$ monocytes) have been identified as lymphatic progenitor cells and one or both types of the circulating progenitors contribute to *de novo* lymphangiogenesis.[89,262,263] For indirect mechanism, a subpopulation of macrophages was identified as the source of VEGF-C and thus induce lymphangiogenesis.[45,89,264,265]

It has been shown that macrophages subsets differentially regulate angiogenesis and/or lymphangiogenesis. M2 as well as M2-like macrophages, characterized as anti-inflammatory, are pro-angiogenic and pro-lymphangiogenic primarily through secreting pro-(lymph)angiogenic factors.[266-269] LPS-polarized M1-like macrophages acquire LEC phenotype and possibly contribute to *de novo* lymphangiogeneis.[90] In recent years, myeloid-derived suppressor cells (MDSCs), an emerging class of CD11b$^+$GR1$^+$ immune cells comprising a heterogeneous population of immature macrophages, granulocytes, and dendritic cells as well as other myeloid cells at early stages of differentiation,[270] have been shown to regulate tumor angiogenesis by secreting proangiogenic factors.[271] The impact of the MDSCs on regulating the process of (*de novo*) lymphangiogenesis has yet to be determined.

My preliminary data demonstrated that (i) macrophage depletion decreases galectin-8-mediated lymphangiogenesis in vivo (**Fig. 52**), and (ii) galectin-8 treatment transdifferentiates RAW264.7 cells into LEC-like cells (**Fig. 53**). These results lead us to hypothesize that galectin-8 may function as a chemoattractant for monocytes/macrophages and activate monocytes/ macrophages to acquire LEC phenotypes. Clearly, further studies are warranted to prove this hypothesis and to elaborate the molecular mechanism involved.

5.2 Targeting galectin-8 to treat inflammatory diseases.

Regardless of the mechanisms involved, my findings that the dominant negative inhibitor of galectin-8 as well as the pan inhibitor of galectin dampen lymphangiogenesis have broad implications for developing novel therapeutic strategies for conditions resulting from pathological lymphangiogenesis, such as tumor metastasis and transplant rejection. Anti-lymphangiogenic agents are also likely to be very useful for treatment of debilitating diseases of the eye. The growth of lymphatic vessels is the major reason of corneal graft rejection[41]. Penetrating keratoplasty is the most common form of solid tissue transplantation. Currently, approximately 40,000 corneal transplantations are performed each year in the United States. Success rate of penetrating keratoplasty is as high as 90% for uncomplicated first grafts performed in avascular low-risk beds. However, the rejection rate of the corneal grafts placed in high-risk vascularized host beds is extremely high (70% to 90%). Thus the development of safe and

targeted new regimens to inhibit lymphangiogenesis is a priority to promote graft survival. In this regard, targeting Gal-8 to inhibit lymphangiogenesis may lead to the development of novel strategies for preventing graft rejection. Anti-lymphangiogenesis drugs are also likely to be useful for treatment of dry eye disease. Significant upregulation of prolymphangiogenic factors (e.g. VEGF-C, VEGF-D, and VEGFR-3) and selective growth of lymphatic vessels without concurrent growth of blood vessels has been demonstrated in corneas with dry eye disease[272]. Dry eye disease is an immune-mediated disorder affecting about 5 million Americans. It severely impacts the vision-related quality of life and the symptoms can be debilitating. The current therapeutic options for dry eye disease are limited, mostly palliative, and expensive. Again targeting Gal-8 to inhibit lymphangiogenesis may be of therapeutic value for treatment of dry eye disease.

Moreover, there is unmet need of developing prolymphangiogenic therapy for disorders such as lymphedema, which affects approximately 140 million people worldwide[273]. The disease most frequently occurs after surgical removal of lymph nodes or radiation therapy, during the treatment of cancer. It is a progressive and lifelong complication of notably breast cancer for which no curative treatment exists[274,275]. Prolymphangiogenic property of galectin-8 may prove to be useful in this regard. Despite the well-established significance of lymphatics in the pathogenesis of numerous diseases, little is known about effective anti-lymphangiogenic agents compared to the abundance of anti-hemangiogenic

agents that have entered the clinical trials. It is our hope that with time our findings will lead to the development of strategies to manage the aspects of lymphangiogenesis for the benefits of patients. In conclusion, my study offers a new perspective on how glycans of the cell surface receptors can be exploited to understand and modulate the process of lymphangiogenesis.

Figure 52.

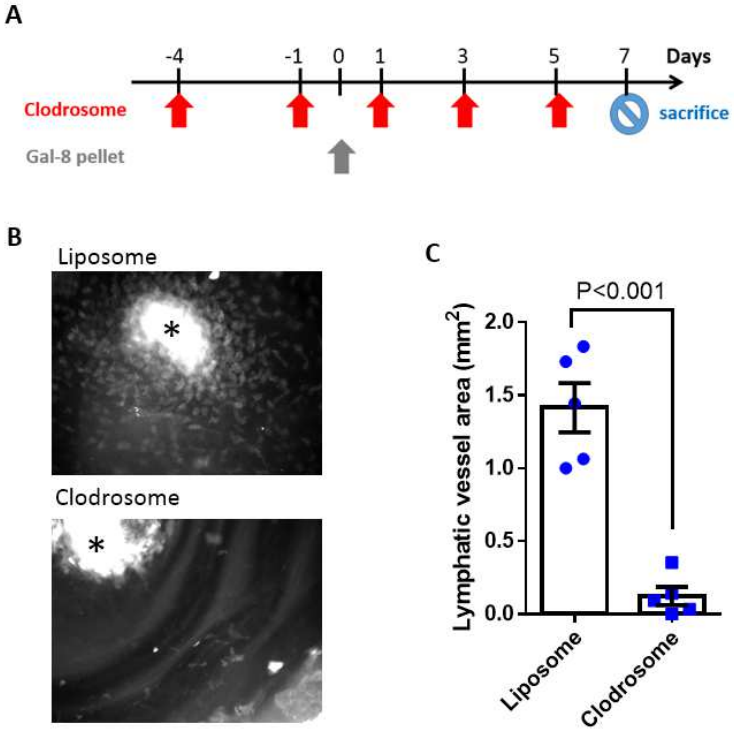

Figure 52. Macrophage depletion attenuates galectin-8-mediated lymphangiogenesis. (A) Depletion of macrophages in vivo was achieved with dichloromethylene diphosphonate-liposomes (clodronate liposomes, or clodrosome, EnCapsula NanoSciences). Systemic macrophage depletion was achieved by intraperitoneal injection of 200 µl (1 mg) clodrosome and local macrophage depletion was achieved by subconjunctival injection of 10 µl (50 µg) clodrosome at 4 days and 24 hours before galectin-8 pellet implantation and then at every 24 hours after implantation as depicted in A. As a control, empty liposomes (Encapsome, EnCapsula NanoSciences) were given at the same schedule. (**B**) Macrophage depletion after clodrosome injections. One week after galectin-8 pellet implantation, mouse corneas were harvested and stained with anti-F4/80 (a macrophage marker) antibody. Representative micrographs are shown. Black asterisks indicate the galectin-8 pellets. (**C**) Clodrosome treatment reduces galectin-8-mediated lymphangiogenesis. Lymphatic vessel areas of galectin-8-induced lymphangiogenesis in *Prox1*-EGFP reporter mice were quantified. Data are plotted as Mean ± SEM and analyzed using Student's t test.

Figure 53.

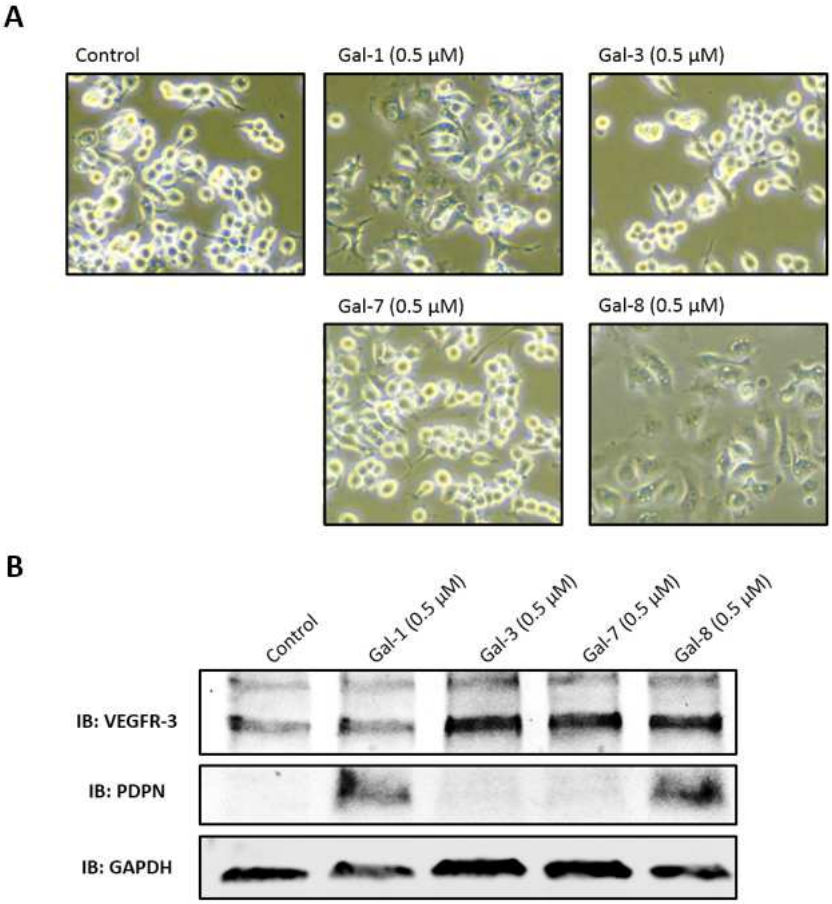

Figure 53. Galectin-8 transdifferentiates macrophages to lymphatic cell-like cells. RAW264.7 cells were treated with galectins (0.5 μM) in serum-free DMEM medium for 24 hr. (**A**) Representative cell morphology was shown in (A) at 24 hr after treatment. Note that galectin-8-treated RAW264.7 cells are flatten; some of the galectin-1-treated cells display similar morphology as galectin-8-treated cells. (**B**) Induced expression of PDPN in galectins-1 and -8 treated cells. After 24 hr-treatment, cell lysates were collected and subjected to Western blotting with anti-VEGFR-3, anti-PDPN and anti-GAPDH antibodies. While VEGFR-3 was detected in control and galectin-treated cells, PDPN was detected only in cells treated with galectins-1 and -8.

References

1 Brouillard, P., Boon, L. & Vikkula, M. Genetics of lymphatic anomalies. *J Clin Invest* **124**, 898-904, doi:10.1172/JCI71614 (2014).

2 Schulte-Merker, S., Sabine, A. & Petrova, T. V. Lymphatic vascular morphogenesis in development, physiology, and disease. *J Cell Biol* **193**, 607-618, doi:10.1083/jcb.201012094 (2011).

3 Smeltzer, D. M., Stickler, G. B. & Schirger, A. Primary lymphedema in children and adolescents: a follow-up study and review. *Pediatrics* **76**, 206-218 (1985).

4 International Society of, L. The diagnosis and treatment of peripheral lymphedema. 2009 Concensus Document of the International Society of Lymphology. *Lymphology* **42**, 51-60 (2009).

5 Beesley, V., Janda, M., Eakin, E., Obermair, A. & Battistutta, D. Lymphedema after gynecological cancer treatment : prevalence, correlates, and supportive care needs. *Cancer* **109**, 2607-2614, doi:10.1002/cncr.22684 (2007).

6 Petrek, J. A., Senie, R. T., Peters, M. & Rosen, P. P. Lymphedema in a cohort of breast carcinoma survivors 20 years after diagnosis. *Cancer* **92**, 1368-1377 (2001).

7 Jennbacken, K., Vallbo, C., Wang, W. & Damber, J. E. Expression of vascular endothelial growth factor C (VEGF-C) and VEGF receptor-3 in human prostate cancer is associated with regional lymph node metastasis. *Prostate* **65**, 110-116, doi:10.1002/pros.20276 (2005).

8 Dadras, S. S. *et al.* Tumor lymphangiogenesis predicts melanoma metastasis to sentinel lymph nodes. *Mod Pathol* **18**, 1232-1242, doi:10.1038/modpathol.3800410 (2005).

9 Bando, H. *et al.* The association between vascular endothelial growth factor-C, its corresponding receptor, VEGFR-3, and prognosis in primary breast cancer: a study with 193 cases. *Oncol Rep* **15**, 653-659 (2006).

10 Padera, T. P. *et al.* Lymphatic metastasis in the absence of functional intratumor lymphatics. *Science* **296**, 1883-1886, doi:10.1126/science.1071420 (2002).

11 Fukumura, D., Duda, D. G., Munn, L. L. & Jain, R. K. Tumor microvasculature and microenvironment: novel insights through intravital imaging in pre-clinical models. *Microcirculation* **17**, 206-225, doi:10.1111/j.1549-8719.2010.00029.x (2010).

12 Hirakawa, S. *et al.* VEGF-A induces tumor and sentinel lymph node lymphangiogenesis and promotes lymphatic metastasis. *J Exp Med* **201**, 1089-1099, doi:10.1084/jem.20041896 (2005).

13 Hirakawa, S. *et al.* VEGF-C-induced lymphangiogenesis in sentinel lymph nodes promotes tumor metastasis to distant sites. *Blood* **109**, 1010-1017, doi:10.1182/blood-2006-05-021758 (2007).

14 Harrell, M. I., Iritani, B. M. & Ruddell, A. Tumor-induced sentinel lymph node lymphangiogenesis and increased lymph flow precede melanoma metastasis. *Am J Pathol* **170**, 774-786, doi:10.2353/ajpath.2007.060761 (2007).

15 Garmy-Susini, B. *et al.* PI3Kalpha activates integrin alpha4beta1 to establish a metastatic niche in lymph nodes. *Proc Natl Acad Sci U S A* **110**, 9042-9047, doi:10.1073/pnas.1219603110 (2013).

16 Muller, A. *et al.* Involvement of chemokine receptors in breast cancer metastasis. *Nature* **410**, 50-56, doi:10.1038/35065016 (2001).

17 Kim, M. *et al.* CXCR4 signaling regulates metastasis of chemoresistant melanoma cells by a lymphatic metastatic niche. *Cancer Res* **70**, 10411-10421, doi:10.1158/0008-5472.CAN-10-2591 (2010).

18 Miteva, D. O. *et al.* Transmural flow modulates cell and fluid transport functions of lymphatic endothelium. *Circ Res* **106**, 920-931, doi:10.1161/CIRCRESAHA.109.207274 (2010).
19 Hirakawa, S. *et al.* Nodal lymphangiogenesis and metastasis: Role of tumor-induced lymphatic vessel activation in extramammary Paget's disease. *Am J Pathol* **175**, 2235-2248, doi:10.2353/ajpath.2009.090420 (2009).
20 Mendis, S. *et al. Global atlas on cardiovascular disease prevention and control*. (World Health Organization in collaboration with the World Heart Federation and the World Stroke Organization, 2011).
21 McGill, H. C., Jr., McMahan, C. A. & Gidding, S. S. Preventing heart disease in the 21st century: implications of the Pathobiological Determinants of Atherosclerosis in Youth (PDAY) study. *Circulation* **117**, 1216-1227, doi:10.1161/CIRCULATIONAHA.107.717033 (2008).
22 Small, D. M., Bond, M. G., Waugh, D., Prack, M. & Sawyer, J. K. Physicochemical and histological changes in the arterial wall of nonhuman primates during progression and regression of atherosclerosis. *J Clin Invest* **73**, 1590-1605, doi:10.1172/JCI111366 (1984).
23 Martel, C. *et al.* Lymphatic vasculature mediates macrophage reverse cholesterol transport in mice. *J Clin Invest* **123**, 1571-1579, doi:10.1172/JCI63685 (2013).
24 Kholova, I. *et al.* Lymphatic vasculature is increased in heart valves, ischaemic and inflamed hearts and in cholesterol-rich and calcified atherosclerotic lesions. *Eur J Clin Invest* **41**, 487-497, doi:10.1111/j.1365-2362.2010.02431.x (2011).
25 Vuorio, T. *et al.* Lymphatic vessel insufficiency in hypercholesterolemic mice alters lipoprotein levels and promotes atherogenesis. *Arterioscler Thromb Vasc Biol* **34**, 1162-1170, doi:10.1161/ATVBAHA.114.302528 (2014).
26 Campese, V. M. Salt sensitivity in hypertension. Renal and cardiovascular implications. *Hypertension* **23**, 531-550 (1994).
27 Weinberger, M. H. Salt sensitivity of blood pressure in humans. *Hypertension* **27**, 481-490 (1996).
28 Coleman, T. G., Granger, H. J. & Guyton, A. C. Whole-body circulatory autoregulation and hypertension. *Circ Res* **28**, Suppl 2:76-87 (1971).
29 Machnik, A. *et al.* Macrophages regulate salt-dependent volume and blood pressure by a vascular endothelial growth factor-C-dependent buffering mechanism. *Nat Med* **15**, 545-552, doi:10.1038/nm.1960 (2009).
30 Wiig, H. *et al.* Immune cells control skin lymphatic electrolyte homeostasis and blood pressure. *J Clin Invest* **123**, 2803-2815, doi:10.1172/JCI60113 (2013).
31 Titze, J. *et al.* Glycosaminoglycan polymerization may enable osmotically inactive Na+ storage in the skin. *Am J Physiol Heart Circ Physiol* **287**, H203-208, doi:10.1152/ajpheart.01237.2003 (2004).
32 Carlsson, S. *et al.* Affinity of galectin-8 and its carbohydrate recognition domains for ligands in solution and at the cell surface. *Glycobiology* **17**, 663-676, doi:10.1093/glycob/cwm026 (2007).
33 Kim, C., Ye, F. & Ginsberg, M. H. Regulation of integrin activation. *Annual review of cell and developmental biology* **27**, 321-345, doi:10.1146/annurev-cellbio-100109-104104 (2011).
34 Kopp, C. *et al.* 23Na magnetic resonance imaging-determined tissue sodium in healthy subjects and hypertensive patients. *Hypertension* **61**, 635-640, doi:10.1161/HYPERTENSIONAHA.111.00566 (2013).

35 Klotz, L. *et al.* Cardiac lymphatics are heterogeneous in origin and respond to injury. *Nature*, doi:10.1038/nature14483 (2015).
36 Kim, H., Kataru, R. P. & Koh, G. Y. Regulation and implications of inflammatory lymphangiogenesis. *Trends Immunol* **33**, 350-356, doi:10.1016/j.it.2012.03.006 (2012).
37 Alitalo, K. The lymphatic vasculature in disease. *Nat Med* **17**, 1371-1380, doi:10.1038/nm.2545 (2011).
38 Paupert, J., Sounni, N. E. & Noel, A. Lymphangiogenesis in post-natal tissue remodeling: lymphatic endothelial cell connection with its environment. *Mol Aspects Med* **32**, 146-158, doi:10.1016/j.mam.2011.04.002 (2011).
39 Yin, N. *et al.* Lymphangiogenesis is required for pancreatic islet inflammation and diabetes. *PLoS One* **6**, e28023, doi:10.1371/journal.pone.0028023 (2011).
40 Park, P. J. *et al.* Corneal lymphangiogenesis in herpetic stromal keratitis. *Surv Ophthalmol* **60**, 60-71, doi:10.1016/j.survophthal.2014.06.001 (2015).
41 Dietrich, T. *et al.* Cutting edge: lymphatic vessels, not blood vessels, primarily mediate immune rejections after transplantation. *Journal of immunology* **184**, 535-539, doi:10.4049/jimmunol.0903180 (2010).
42 Skobe, M. & Dana, R. Blocking the path of lymphatic vessels. *Nat Med* **15**, 993-994, doi:10.1038/nm0909-993 (2009).
43 Jurisic, G., Sundberg, J. P. & Detmar, M. Blockade of VEGF receptor-3 aggravates inflammatory bowel disease and lymphatic vessel enlargement. *Inflamm Bowel Dis* **19**, 1983-1989, doi:10.1097/MIB.0b013e31829292f7 (2013).
44 Kataru, R. P. *et al.* Critical role of CD11b+ macrophages and VEGF in inflammatory lymphangiogenesis, antigen clearance, and inflammation resolution. *Blood* **113**, 5650-5659, doi:10.1182/blood-2008-09-176776 (2009).
45 Baluk, P. *et al.* Pathogenesis of persistent lymphatic vessel hyperplasia in chronic airway inflammation. *J Clin Invest* **115**, 247-257, doi:10.1172/JCI22037 (2005).
46 Guo, R. *et al.* Inhibition of lymphangiogenesis and lymphatic drainage via vascular endothelial growth factor receptor 3 blockade increases the severity of inflammation in a mouse model of chronic inflammatory arthritis. *Arthritis Rheum* **60**, 2666-2676, doi:10.1002/art.24764 (2009).
47 Mortimer, P. S. & Rockson, S. G. New developments in clinical aspects of lymphatic disease. *J Clin Invest* **124**, 915-921, doi:10.1172/JCI71608 (2014).
48 Damstra, R. J., Voesten, H. G., Klinkert, P. & Brorson, H. Circumferential suction-assisted lipectomy for lymphoedema after surgery for breast cancer. *Br J Surg* **96**, 859-864, doi:10.1002/bjs.6658 (2009).
49 Brorson, H. & Svensson, H. Complete reduction of lymphoedema of the arm by liposuction after breast cancer. *Scand J Plast Reconstr Surg Hand Surg* **31**, 137-143 (1997).
50 Karkkainen, M. J. *et al.* A model for gene therapy of human hereditary lymphedema. *Proc Natl Acad Sci U S A* **98**, 12677-12682, doi:10.1073/pnas.221449198 (2001).
51 Harvey, N. L. *et al.* Lymphatic vascular defects promoted by Prox1 haploinsufficiency cause adult-onset obesity. *Nat Genet* **37**, 1072-1081, doi:10.1038/ng1642 (2005).
52 Wigle, J. T. & Oliver, G. Prox1 function is required for the development of the murine lymphatic system. *Cell* **98**, 769-778 (1999).
53 Nougues, J., Reyne, Y. & Dulor, J. P. Differentiation of rabbit adipocyte precursors in primary culture. *Int J Obes* **12**, 321-333 (1988).

54 Levi, B. *et al.* Molecular analysis and differentiation capacity of adipose-derived stem cells from lymphedema tissue. *Plast Reconstr Surg* **132**, 580-589, doi:10.1097/PRS.0b013e31829ace13 (2013).
55 Gomez-Ambrosi, J. *et al.* Involvement of serum vascular endothelial growth factor family members in the development of obesity in mice and humans. *J Nutr Biochem* **21**, 774-780, doi:10.1016/j.jnutbio.2009.05.004 (2010).
56 Silha, J. V., Krsek, M., Sucharda, P. & Murphy, L. J. Angiogenic factors are elevated in overweight and obese individuals. *Int J Obes (Lond)* **29**, 1308-1314, doi:10.1038/sj.ijo.0802987 (2005).
57 Wada, H. *et al.* Distinct characteristics of circulating vascular endothelial growth factor-a and C levels in human subjects. *PLoS One* **6**, e29351, doi:10.1371/journal.pone.0029351 (2011).
58 Karaman, S. *et al.* Blockade of VEGF-C and VEGF-D modulates adipose tissue inflammation and improves metabolic parameters under high-fat diet. *Mol Metab* **4**, 93-105, doi:10.1016/j.molmet.2014.11.006 (2015).
59 Resnikoff, S. *et al.* Global data on visual impairment in the year 2002. *Bull World Health Organ* **82**, 844-851, doi:/S0042-96862004001100009 (2004).
60 Quigley, H. A. & Broman, A. T. The number of people with glaucoma worldwide in 2010 and 2020. *Br J Ophthalmol* **90**, 262-267, doi:10.1136/bjo.2005.081224 (2006).
61 Rein, D. B. *et al.* The economic burden of major adult visual disorders in the United States. *Arch Ophthalmol* **124**, 1754-1760, doi:10.1001/archopht.124.12.1754 (2006).
62 Bill, A. Uveoscleral drainage of aqueous humor: physiology and pharmacology. *Prog Clin Biol Res* **312**, 417-427 (1989).
63 Aihara, M., Lindsey, J. D. & Weinreb, R. N. Aqueous humor dynamics in mice. *Invest Ophthalmol Vis Sci* **44**, 5168-5173 (2003).
64 Ramos, R. F., Hoying, J. B., Witte, M. H. & Daniel Stamer, W. Schlemm's canal endothelia, lymphatic, or blood vasculature? *J Glaucoma* **16**, 391-405, doi:10.1097/IJG.0b013e3180654ac6 (2007).
65 Kizhatil, K., Ryan, M., Marchant, J. K., Henrich, S. & John, S. W. Schlemm's canal is a unique vessel with a combination of blood vascular and lymphatic phenotypes that forms by a novel developmental process. *PLoS Biol* **12**, e1001912, doi:10.1371/journal.pbio.1001912 (2014).
66 Truong, T. N., Li, H., Hong, Y. K. & Chen, L. Novel characterization and live imaging of Schlemm's canal expressing Prox-1. *PLoS One* **9**, e98245, doi:10.1371/journal.pone.0098245 (2014).
67 Park, D. Y. *et al.* Lymphatic regulator PROX1 determines Schlemm's canal integrity and identity. *J Clin Invest* **124**, 3960-3974, doi:10.1172/JCI75392 (2014).
68 Aspelund, A. *et al.* The Schlemm's canal is a VEGF-C/VEGFR-3-responsive lymphatic-like vessel. *J Clin Invest* **124**, 3975-3986, doi:10.1172/JCI75395 (2014).
69 Thomson, B. R. *et al.* A lymphatic defect causes ocular hypertension and glaucoma in mice. *J Clin Invest* **124**, 4320-4324, doi:10.1172/JCI77162 (2014).
70 The definition and classification of dry eye disease: report of the Definition and Classification Subcommittee of the International Dry Eye WorkShop (2007). *Ocul Surf* **5**, 75-92 (2007).
71 Massingale, M. L. *et al.* Analysis of inflammatory cytokines in the tears of dry eye patients. *Cornea* **28**, 1023-1027, doi:10.1097/ICO.0b013e3181a16578 (2009).
72 De Paiva, C. S. *et al.* IL-17 disrupts corneal barrier following desiccating stress. *Mucosal Immunol* **2**, 243-253, doi:10.1038/mi.2009.5 (2009).

73 Stevenson, W., Chauhan, S. K. & Dana, R. Dry eye disease: an immune-mediated ocular surface disorder. *Arch Ophthalmol* **130**, 90-100, doi:10.1001/archophthalmol.2011.364 (2012).
74 Goyal, S. *et al.* Evidence of corneal lymphangiogenesis in dry eye disease: a potential link to adaptive immunity? *Arch Ophthalmol* **128**, 819-824, doi:10.1001/archophthalmol.2010.124 (2010).
75 Okanobo, A., Chauhan, S. K., Dastjerdi, M. H., Kodati, S. & Dana, R. Efficacy of topical blockade of interleukin-1 in experimental dry eye disease. *Am J Ophthalmol* **154**, 63-71, doi:10.1016/j.ajo.2012.01.034 (2012).
76 Saban, D. R. The chemokine receptor CCR7 expressed by dendritic cells: a key player in corneal and ocular surface inflammation. *Ocul Surf* **12**, 87-99, doi:10.1016/j.jtos.2013.10.007 (2014).
77 Saban, D. R. *et al.* New twists to an old story: novel concepts in the pathogenesis of allergic eye disease. *Curr Eye Res* **38**, 317-330, doi:10.3109/02713683.2012.747617 (2013).
78 Lee, H. S. *et al.* Involvement of corneal lymphangiogenesis in a mouse model of allergic eye disease. *Invest Ophthalmol Vis Sci* **56**, 3140-3148, doi:10.1167/iovs.14-16186 (2015).
79 Karkkainen, M. J. *et al.* Vascular endothelial growth factor C is required for sprouting of the first lymphatic vessels from embryonic veins. *Nature immunology* **5**, 74-80, doi:10.1038/ni1013 (2004).
80 Makinen, T. *et al.* Inhibition of lymphangiogenesis with resulting lymphedema in transgenic mice expressing soluble VEGF receptor-3. *Nat Med* **7**, 199-205, doi:10.1038/84651 (2001).
81 Dumont, D. J. *et al.* Cardiovascular failure in mouse embryos deficient in VEGF receptor-3. *Science* **282**, 946-949 (1998).
82 Kaipainen, A. *et al.* Expression of the fms-like tyrosine kinase 4 gene becomes restricted to lymphatic endothelium during development. *Proc Natl Acad Sci U S A* **92**, 3566-3570 (1995).
83 Partanen, T. A. *et al.* VEGF-C and VEGF-D expression in neuroendocrine cells and their receptor, VEGFR-3, in fenestrated blood vessels in human tissues. *FASEB J* **14**, 2087-2096, doi:10.1096/fj.99-1049com (2000).
84 Tammela, T. *et al.* Blocking VEGFR-3 suppresses angiogenic sprouting and vascular network formation. *Nature* **454**, 656-660, doi:10.1038/nature07083 (2008).
85 Valtola, R. *et al.* VEGFR-3 and its ligand VEGF-C are associated with angiogenesis in breast cancer. *Am J Pathol* **154**, 1381-1390, doi:10.1016/S0002-9440(10)65392-8 (1999).
86 Paavonen, K., Puolakkainen, P., Jussila, L., Jahkola, T. & Alitalo, K. Vascular endothelial growth factor receptor-3 in lymphangiogenesis in wound healing. *Am J Pathol* **156**, 1499-1504, doi:10.1016/S0002-9440(10)65021-3 (2000).
87 Chung, E. S. *et al.* Contribution of macrophages to angiogenesis induced by vascular endothelial growth factor receptor-3-specific ligands. *Am J Pathol* **175**, 1984-1992, doi:10.2353/ajpath.2009.080515 (2009).
88 Cursiefen, C. *et al.* Nonvascular VEGF receptor 3 expression by corneal epithelium maintains avascularity and vision. *Proc Natl Acad Sci U S A* **103**, 11405-11410, doi:10.1073/pnas.0506112103 (2006).
89 Schoppmann, S. F. *et al.* Tumor-associated macrophages express lymphatic endothelial growth factors and are related to peritumoral lymphangiogenesis. *Am J Pathol* **161**, 947-956, doi:10.1016/S0002-9440(10)64255-1 (2002).

90 Hall, K. L., Volk-Draper, L. D., Flister, M. J. & Ran, S. New model of macrophage acquisition of the lymphatic endothelial phenotype. *PLoS One* **7**, e31794, doi:10.1371/journal.pone.0031794 (2012).
91 Hamrah, P., Chen, L., Zhang, Q. & Dana, M. R. Novel expression of vascular endothelial growth factor receptor (VEGFR)-3 and VEGF-C on corneal dendritic cells. *Am J Pathol* **163**, 57-68, doi:10.1016/S0002-9440(10)63630-9 (2003).
92 Hamrah, P. *et al.* Expression of vascular endothelial growth factor receptor-3 (VEGFR-3) on monocytic bone marrow-derived cells in the conjunctiva. *Exp Eye Res* **79**, 553-561, doi:10.1016/j.exer.2004.06.028 (2004).
93 D'Alessio, S. *et al.* VEGF-C-dependent stimulation of lymphatic function ameliorates experimental inflammatory bowel disease. *J Clin Invest* **124**, 3863-3878, doi:10.1172/JCI72189 (2014).
94 Zhang, Y. *et al.* Activation of vascular endothelial growth factor receptor-3 in macrophages restrains TLR4-NF-kappaB signaling and protects against endotoxin shock. *Immunity* **40**, 501-514, doi:10.1016/j.immuni.2014.01.013 (2014).
95 Dellinger, M. T., Meadows, S. M., Wynne, K., Cleaver, O. & Brekken, R. A. Vascular endothelial growth factor receptor-2 promotes the development of the lymphatic vasculature. *PLoS One* **8**, e74686, doi:10.1371/journal.pone.0074686 (2013).
96 Wirzenius, M. *et al.* Distinct vascular endothelial growth factor signals for lymphatic vessel enlargement and sprouting. *J Exp Med* **204**, 1431-1440, doi:10.1084/jem.20062642 (2007).
97 Cursiefen, C. *et al.* VEGF-A stimulates lymphangiogenesis and hemangiogenesis in inflammatory neovascularization via macrophage recruitment. *The Journal of clinical investigation* **113**, 1040-1050, doi:10.1172/JCI20465 (2004).
98 Kerber, M. *et al.* Flt-1 signaling in macrophages promotes glioma growth in vivo. *Cancer Res* **68**, 7342-7351, doi:10.1158/0008-5472.CAN-07-6241 (2008).
99 Murakami, M. *et al.* VEGFR1 tyrosine kinase signaling promotes lymphangiogenesis as well as angiogenesis indirectly via macrophage recruitment. *Arterioscler Thromb Vasc Biol* **28**, 658-664, doi:10.1161/ATVBAHA.107.150433 (2008).
100 Hong, Y. K. *et al.* VEGF-A promotes tissue repair-associated lymphatic vessel formation via VEGFR-2 and the alpha1beta1 and alpha2beta1 integrins. *FASEB J* **18**, 1111-1113, doi:10.1096/fj.03-1179fje (2004).
101 Bjorndahl, M. A. *et al.* Vascular endothelial growth factor-a promotes peritumoral lymphangiogenesis and lymphatic metastasis. *Cancer Res* **65**, 9261-9268, doi:10.1158/0008-5472.CAN-04-2345 (2005).
102 Ivaska, J. & Heino, J. Interplay between cell adhesion and growth factor receptors: from the plasma membrane to the endosomes. *Cell Tissue Res* **339**, 111-120, doi:10.1007/s00441-009-0857-z (2010).
103 Chen, J., Alexander, J. S. & Orr, A. W. Integrins and their extracellular matrix ligands in lymphangiogenesis and lymph node metastasis. *Int J Cell Biol* **2012**, 853703, doi:10.1155/2012/853703 (2012).
104 Huang, X. Z. *et al.* Fatal bilateral chylothorax in mice lacking the integrin alpha9beta1. *Mol Cell Biol* **20**, 5208-5215 (2000).
105 Bazigou, E. *et al.* Integrin-alpha9 is required for fibronectin matrix assembly during lymphatic valve morphogenesis. *Dev Cell* **17**, 175-186, doi:10.1016/j.devcel.2009.06.017 (2009).

106 Ma, G. C. *et al.* A recurrent ITGA9 missense mutation in human fetuses with severe chylothorax: possible correlation with poor response to fetal therapy. *Prenat Diagn* **28**, 1057-1063, doi:10.1002/pd.2130 (2008).
107 Vlahakis, N. E., Young, B. A., Atakilit, A. & Sheppard, D. The lymphangiogenic vascular endothelial growth factors VEGF-C and -D are ligands for the integrin alpha9beta1. *J Biol Chem* **280**, 4544-4552, doi:10.1074/jbc.M412816200 (2005).
108 Vlahakis, N. E. *et al.* Integrin alpha9beta1 directly binds to vascular endothelial growth factor (VEGF)-A and contributes to VEGF-A-induced angiogenesis. *J Biol Chem* **282**, 15187-15196, doi:10.1074/jbc.M609323200 (2007).
109 Staniszewska, I. *et al.* Integrin alpha9 beta1 is a receptor for nerve growth factor and other neurotrophins. *J Cell Sci* **121**, 504-513, doi:10.1242/jcs.000232 (2008).
110 Grimaldo, S., Yuen, D., Ecoiffier, T. & Chen, L. Very late antigen-1 mediates corneal lymphangiogenesis. *Invest Ophthalmol Vis Sci* **52**, 4808-4812, doi:10.1167/iovs.10-6580 (2011).
111 Garmy-Susini, B. *et al.* Integrin alpha4beta1 signaling is required for lymphangiogenesis and tumor metastasis. *Cancer Res* **70**, 3042-3051, doi:10.1158/0008-5472.CAN-09-3761 (2010).
112 Dietrich, T. *et al.* Inhibition of inflammatory lymphangiogenesis by integrin alpha5 blockade. *Am J Pathol* **171**, 361-372 (2007).
113 Okazaki, T. *et al.* alpha5beta1 Integrin blockade inhibits lymphangiogenesis in airway inflammation. *Am J Pathol* **174**, 2378-2387, doi:10.2353/ajpath.2009.080942 (2009).
114 Schacht, V. *et al.* T1alpha/podoplanin deficiency disrupts normal lymphatic vasculature formation and causes lymphedema. *The EMBO journal* **22**, 3546-3556, doi:10.1093/emboj/cdg342 (2003).
115 Fu, J. *et al.* Endothelial cell O-glycan deficiency causes blood/lymphatic misconnections and consequent fatty liver disease in mice. *The Journal of clinical investigation* **118**, 3725-3737, doi:10.1172/JCI36077 (2008).
116 Navarro, A., Perez, R. E., Rezaiekhaligh, M., Mabry, S. M. & Ekekezie, II. T1alpha/podoplanin is essential for capillary morphogenesis in lymphatic endothelial cells. *American journal of physiology. Lung cellular and molecular physiology* **295**, L543-551, doi:10.1152/ajplung.90262.2008 (2008).
117 Navarro, A., Perez, R. E., Rezaiekhaligh, M. H., Mabry, S. M. & Ekekezie, II. Polarized migration of lymphatic endothelial cells is critically dependent on podoplanin regulation of Cdc42. *American journal of physiology. Lung cellular and molecular physiology* **300**, L32-42, doi:10.1152/ajplung.00171.2010 (2011).
118 Cueni, L. N. *et al.* Podoplanin-Fc reduces lymphatic vessel formation in vitro and in vivo and causes disseminated intravascular coagulation when transgenically expressed in the skin. *Blood* **116**, 4376-4384, doi:10.1182/blood-2010-04-278564 (2010).
119 Maruyama, Y. *et al.* The effect of podoplanin inhibition on lymphangiogenesis under pathological conditions. *Investigative ophthalmology & visual science* **55**, 4813-4822, doi:10.1167/iovs.13-13711 (2014).
120 Scholl, F. G., Gamallo, C., Vilaro, S. & Quintanilla, M. Identification of PA2.26 antigen as a novel cell-surface mucin-type glycoprotein that induces plasma membrane extensions and increased motility in keratinocytes. *J Cell Sci* **112 (Pt 24)**, 4601-4613 (1999).
121 Kaneko, M. K. *et al.* Functional glycosylation of human podoplanin: glycan structure of platelet aggregation-inducing factor. *FEBS letters* **581**, 331-336, doi:10.1016/j.febslet.2006.12.044 (2007).

122 Pan, Y. *et al.* Podoplanin requires sialylated O-glycans for stable expression on lymphatic endothelial cells and for interaction with platelets. *Blood* **124**, 3656-3665, doi:10.1182/blood-2014-04-572107 (2014).
123 Kolar, K. *et al.* Podoplanin: a marker for reactive gliosis in gliomas and brain injury. *J Neuropathol Exp Neurol* **74**, 64-74, doi:10.1097/NEN.0000000000000150 (2015).
124 Peters, A. *et al.* Th17 cells induce ectopic lymphoid follicles in central nervous system tissue inflammation. *Immunity* **35**, 986-996, doi:10.1016/j.immuni.2011.10.015 (2011).
125 Birke, K., Lutjen-Drecoll, E., Kerjaschki, D. & Birke, M. T. Expression of podoplanin and other lymphatic markers in the human anterior eye segment. *Invest Ophthalmol Vis Sci* **51**, 344-354, doi:10.1167/iovs.08-3307 (2010).
126 Grimaldo, S., Garcia, M., Zhang, H. & Chen, L. Specific role of lymphatic marker podoplanin in retinal pigment epithelial cells. *Lymphology* **43**, 128-134 (2010).
127 Astarita, J. L., Acton, S. E. & Turley, S. J. Podoplanin: emerging functions in development, the immune system, and cancer. *Front Immunol* **3**, 283, doi:10.3389/fimmu.2012.00283 (2012).
128 Kerrigan, A. M. *et al.* Podoplanin-expressing inflammatory macrophages activate murine platelets via CLEC-2. *J Thromb Haemost* **10**, 484-486, doi:10.1111/j.1538-7836.2011.04614.x (2012).
129 Yang, Y. & Oliver, G. Development of the mammalian lymphatic vasculature. *J Clin Invest* **124**, 888-897, doi:10.1172/JCI71609 (2014).
130 Wigle, J. T. *et al.* An essential role for Prox1 in the induction of the lymphatic endothelial cell phenotype. *EMBO J* **21**, 1505-1513, doi:10.1093/emboj/21.7.1505 (2002).
131 Johnson, N. C. *et al.* Lymphatic endothelial cell identity is reversible and its maintenance requires Prox1 activity. *Genes Dev* **22**, 3282-3291, doi:10.1101/gad.1727208 (2008).
132 Hong, Y. K. *et al.* Prox1 is a master control gene in the program specifying lymphatic endothelial cell fate. *Dev Dyn* **225**, 351-357, doi:10.1002/dvdy.10163 (2002).
133 Choi, I. *et al.* Visualization of lymphatic vessels by Prox1-promoter directed GFP reporter in a bacterial artificial chromosome-based transgenic mouse. *Blood* **117**, 362-365, doi:10.1182/blood-2010-07-298562 (2011).
134 Wigle, J. T., Chowdhury, K., Gruss, P. & Oliver, G. Prox1 function is crucial for mouse lens-fibre elongation. *Nat Genet* **21**, 318-322, doi:10.1038/6844 (1999).
135 Dyer, M. A., Livesey, F. J., Cepko, C. L. & Oliver, G. Prox1 function controls progenitor cell proliferation and horizontal cell genesis in the mammalian retina. *Nat Genet* **34**, 53-58, doi:10.1038/ng1144 (2003).
136 Cid, E. *et al.* Prox1 expression in rod precursors and Muller cells. *Exp Eye Res* **90**, 267-276, doi:10.1016/j.exer.2009.10.015 (2010).
137 Elsir, T., Smits, A., Lindstrom, M. S. & Nister, M. Transcription factor PROX1: its role in development and cancer. *Cancer Metastasis Rev* **31**, 793-805, doi:10.1007/s10555-012-9390-8 (2012).
138 Cooper, D. N. Galectinomics: finding themes in complexity. *Biochimica et biophysica acta* **1572**, 209-231 (2002).
139 Liu, F. T. & Rabinovich, G. A. Galectins as modulators of tumour progression. *Nature reviews. Cancer* **5**, 29-41, doi:10.1038/nrc1527 (2005).
140 Liu, F. T., Patterson, R. J. & Wang, J. L. Intracellular functions of galectins. *Biochimica et biophysica acta* **1572**, 263-273 (2002).
141 Hughes, R. C. Secretion of the galectin family of mammalian carbohydrate-binding proteins. *Biochimica et biophysica acta* **1473**, 172-185 (1999).

142 Gitt, M. A. *et al.* Sequence and mapping of galectin-5, a beta-galactoside-binding lectin, found in rat erythrocytes. *The Journal of biological chemistry* **270**, 5032-5038 (1995).
143 Wada, J. & Kanwar, Y. S. Identification and characterization of galectin-9, a novel beta-galactoside-binding mammalian lectin. *The Journal of biological chemistry* **272**, 6078-6086 (1997).
144 Gitt, M. A. *et al.* Galectin-4 and galectin-6 are two closely related lectins expressed in mouse gastrointestinal tract. *The Journal of biological chemistry* **273**, 2954-2960 (1998).
145 Leonidas, D. D. *et al.* Crystal structure of human Charcot-Leyden crystal protein, an eosinophil lysophospholipase, identifies it as a new member of the carbohydrate-binding family of galectins. *Structure* **3**, 1379-1393 (1995).
146 Dyer, K. D. & Rosenberg, H. F. Eosinophil Charcot-Leyden crystal protein binds to beta-galactoside sugars. *Life sciences* **58**, 2073-2082 (1996).
147 Dyer, K. D., Handen, J. S. & Rosenberg, H. F. The genomic structure of the human Charcot-Leyden crystal protein gene is analogous to those of the galectin genes. *Genomics* **40**, 217-221, doi:10.1006/geno.1996.4590 (1997).
148 Ogden, A. T. *et al.* GRIFIN, a novel lens-specific protein related to the galectin family. *The Journal of biological chemistry* **273**, 28889-28896 (1998).
149 Vasta, G. R. Roles of galectins in infection. *Nature reviews. Microbiology* **7**, 424-438, doi:10.1038/nrmicro2146 (2009).
150 Liu, F. T. Galectins: a new family of regulators of inflammation. *Clin Immunol* **97**, 79-88, doi:10.1006/clim.2000.4912 (2000).
151 Rabinovich, G. A. & Toscano, M. A. Turning 'sweet' on immunity: galectin-glycan interactions in immune tolerance and inflammation. *Nature reviews. Immunology* **9**, 338-352, doi:10.1038/nri2536 (2009).
152 Sato, S., Ouellet, M., St-Pierre, C. & Tremblay, M. J. Glycans, galectins, and HIV-1 infection. *Ann N Y Acad Sci* **1253**, 133-148, doi:10.1111/j.1749-6632.2012.06475.x (2012).
153 Croci, D. O. *et al.* Glycosylation-dependent lectin-receptor interactions preserve angiogenesis in anti-VEGF refractory tumors. *Cell* **156**, 744-758, doi:10.1016/j.cell.2014.01.043 (2014).
154 Hsieh, S. H. *et al.* Galectin-1, a novel ligand of neuropilin-1, activates VEGFR-2 signaling and modulates the migration of vascular endothelial cells. *Oncogene* **27**, 3746-3753, doi:10.1038/sj.onc.1211029 (2008).
155 Markowska, A. I., Liu, F. T. & Panjwani, N. Galectin-3 is an important mediator of VEGF- and bFGF-mediated angiogenic response. *The Journal of experimental medicine* **207**, 1981-1993, doi:10.1084/jem.20090121 (2010).
156 Markowska, A. I., Jefferies, K. C. & Panjwani, N. Galectin-3 protein modulates cell surface expression and activation of vascular endothelial growth factor receptor 2 in human endothelial cells. *The Journal of biological chemistry* **286**, 29913-29921, doi:10.1074/jbc.M111.226423 (2011).
157 Delgado, V. M. *et al.* Modulation of endothelial cell migration and angiogenesis: a novel function for the "tandem-repeat" lectin galectin-8. *FASEB journal : official publication of the Federation of American Societies for Experimental Biology* **25**, 242-254, doi:10.1096/fj.09-144907 (2011).
158 Heusschen, R., Schulkens, I. A., van Beijnum, J., Griffioen, A. W. & Thijssen, V. L. Endothelial LGALS9 splice variant expression in endothelial cell biology and angiogenesis. *Biochimica et biophysica acta* **1842**, 284-292, doi:10.1016/j.bbadis.2013.12.003 (2014).

159 Etulain, J. *et al.* Control of angiogenesis by galectins involves the release of platelet-derived proangiogenic factors. *PLoS One* **9**, e96402, doi:10.1371/journal.pone.0096402 (2014).
160 Cao, Z., Saravanan, C., Chen, W. S. & Panjwani, N. Examination of the Role of Galectins in Cell Migration and Re-epithelialization of Wounds. *Methods Mol Biol* **1207**, 317-326, doi:10.1007/978-1-4939-1396-1_21 (2015).
161 Argueso, P. *et al.* Association of cell surface mucins with galectin-3 contributes to the ocular surface epithelial barrier. *The Journal of biological chemistry* **284**, 23037-23045, doi:10.1074/jbc.M109.033332 (2009).
162 Cao, Z. *et al.* Galectins-3 and -7, but not galectin-1, play a role in re-epithelialization of wounds. *The Journal of biological chemistry* **277**, 42299-42305, doi:10.1074/jbc.M200981200 (2002).
163 Nishi, N., Itoh, A., Shoji, H., Miyanaka, H. & Nakamura, T. Galectin-8 and galectin-9 are novel substrates for thrombin. *Glycobiology* **16**, 15C-20C, doi:10.1093/glycob/cwl028 (2006).
164 Hadari, Y. R. *et al.* Galectin-8. A new rat lectin, related to galectin-4. *J Biol Chem* **270**, 3447-3453 (1995).
165 Reticker-Flynn, N. E. *et al.* A combinatorial extracellular matrix platform identifies cell-extracellular matrix interactions that correlate with metastasis. *Nature communications* **3**, 1122, doi:10.1038/ncomms2128 (2012).
166 Barrow, H. *et al.* Serum galectin-2, -4, and -8 are greatly increased in colon and breast cancer patients and promote cancer cell adhesion to blood vascular endothelium. *Clin Cancer Res* **17**, 7035-7046, doi:10.1158/1078-0432.CCR-11-1462 (2011).
167 Thijssen, V. L., Hulsmans, S. & Griffioen, A. W. The galectin profile of the endothelium: altered expression and localization in activated and tumor endothelial cells. *The American journal of pathology* **172**, 545-553, doi:10.2353/ajpath.2008.070938 (2008).
168 Romaniuk, M. A. *et al.* Human platelets express and are activated by galectin-8. *Biochem J* **432**, 535-547, doi:10.1042/BJ20100538 (2010).
169 Zappelli, C., van der Zwaan, C., Thijssen-Timmer, D. C., Mertens, K. & Meijer, A. B. Novel role for galectin-8 protein as mediator of coagulation factor V endocytosis by megakaryocytes. *J Biol Chem* **287**, 8327-8335, doi:10.1074/jbc.M111.305151 (2012).
170 Thurston, T. L., Wandel, M. P., von Muhlinen, N., Foeglein, A. & Randow, F. Galectin 8 targets damaged vesicles for autophagy to defend cells against bacterial invasion. *Nature* **482**, 414-418, doi:10.1038/nature10744 (2012).
171 Nikzad, H., Haddad Kashani, H., Kabir-Salmani, M., Akimoto, Y. & Iwashita, M. Expression of galectin-8 on human endometrium: Molecular and cellular aspects. *Iran J Reprod Med* **11**, 65-70 (2013).
172 Tsai, C. M. *et al.* Galectin-1 and galectin-8 have redundant roles in promoting plasma cell formation. *J Immunol* **187**, 1643-1652, doi:10.4049/jimmunol.1100297 (2011).
173 Thijssen, V. L., Hulsmans, S. & Griffioen, A. W. The galectin profile of the endothelium: altered expression and localization in activated and tumor endothelial cells. *The American journal of pathology* **172**, 545-553, doi:10.2353/ajpath.2008.070938 (2008).
174 Gopalkrishnan, R. V. *et al.* Molecular characterization of prostate carcinoma tumor antigen-1, PCTA-1, a human galectin-8 related gene. *Oncogene* **19**, 4405-4416, doi:10.1038/sj.onc.1203767 (2000).
175 Su, Z. Z. *et al.* Surface-epitope masking and expression cloning identifies the human prostate carcinoma tumor antigen gene PCTA-1 a member of the galectin gene family. *Proc Natl Acad Sci U S A* **93**, 7252-7257 (1996).

176 Bassen, R. *et al.* Expression of Po66-CBP, a type-8 galectin, in different healthy, tumoral and peritumoral tissues. *Anticancer Res* **19**, 5429-5433 (1999).
177 Bidon, N. *et al.* Two messenger RNAs and five isoforms for Po66-CBP, a galectin-8 homolog in a human lung carcinoma cell line. *Gene* **274**, 253-262 (2001).
178 Hadari, Y. R. *et al.* Galectin-8 binding to integrins inhibits cell adhesion and induces apoptosis. *J Cell Sci* **113 (Pt 13)**, 2385-2397 (2000).
179 Cattaneo, V. *et al.* Galectin-8 elicits pro-inflammatory activities in the endothelium. *Glycobiology* **24**, 966-973, doi:10.1093/glycob/cwu060 (2014).
180 Keller, M., Ruegg, A., Werner, S. & Beer, H. D. Active caspase-1 is a regulator of unconventional protein secretion. *Cell* **132**, 818-831, doi:10.1016/j.cell.2007.12.040 (2008).
181 Ideo, H., Seko, A., Ishizuka, I. & Yamashita, K. The N-terminal carbohydrate recognition domain of galectin-8 recognizes specific glycosphingolipids with high affinity. *Glycobiology* **13**, 713-723, doi:10.1093/glycob/cwg094 (2003).
182 Ideo, H., Matsuzaka, T., Nonaka, T., Seko, A. & Yamashita, K. Galectin-8-N-domain recognition mechanism for sialylated and sulfated glycans. *The Journal of biological chemistry* **286**, 11346-11355, doi:10.1074/jbc.M110.195925 (2011).
183 Carlsson, S., Carlsson, M. C. & Leffler, H. Intracellular sorting of galectin-8 based on carbohydrate fine specificity. *Glycobiology* **17**, 906-912, doi:10.1093/glycob/cwm059 (2007).
184 Patnaik, S. K. *et al.* Complex N-glycans are the major ligands for galectin-1, -3, and -8 on Chinese hamster ovary cells. *Glycobiology* **16**, 305-317, doi:10.1093/glycob/cwj063 (2006).
185 Hadari, Y. R. *et al.* Galectin-8 binding to integrins inhibits cell adhesion and induces apoptosis. *Journal of cell science* **113 (Pt 13)**, 2385-2397 (2000).
186 Levy, Y. *et al.* Galectin-8 functions as a matricellular modulator of cell adhesion. *The Journal of biological chemistry* **276**, 31285-31295, doi:10.1074/jbc.M100340200 (2001).
187 Nishi, N. *et al.* Galectin-8 modulates neutrophil function via interaction with integrin alphaM. *Glycobiology* **13**, 755-763, doi:10.1093/glycob/cwg102 (2003).
188 Carcamo, C. *et al.* Galectin-8 binds specific beta1 integrins and induces polarized spreading highlighted by asymmetric lamellipodia in Jurkat T cells. *Experimental cell research* **312**, 374-386, doi:10.1016/j.yexcr.2005.10.025 (2006).
189 Eshkar Sebban, L. *et al.* The involvement of CD44 and its novel ligand galectin-8 in apoptotic regulation of autoimmune inflammation. *J Immunol* **179**, 1225-1235 (2007).
190 Zick, Y. *et al.* Role of galectin-8 as a modulator of cell adhesion and cell growth. *Glycoconj J* **19**, 517-526, doi:10.1023/B:GLYC.0000014081.55445.af (2004).
191 Tribulatti, M. V., Cattaneo, V., Hellman, U., Mucci, J. & Campetella, O. Galectin-8 provides costimulatory and proliferative signals to T lymphocytes. *J Leukoc Biol* **86**, 371-380, doi:10.1189/jlb.0908529 (2009).
192 Cueni, L. N. & Detmar, M. Galectin-8 interacts with podoplanin and modulates lymphatic endothelial cell functions. *Experimental cell research* **315**, 1715-1723, doi:10.1016/j.yexcr.2009.02.021 (2009).
193 Rundhaug, J. E. Matrix metalloproteinases and angiogenesis. *J Cell Mol Med* **9**, 267-285 (2005).
194 Diskin, S., Cao, Z., Leffler, H. & Panjwani, N. The role of integrin glycosylation in galectin-8-mediated trabecular meshwork cell adhesion and spreading. *Glycobiology* **19**, 29-37, doi:10.1093/glycob/cwn100 (2009).

195 Kuwabara, I. *et al.* Galectin-7 (PIG1) exhibits pro-apoptotic function through JNK activation and mitochondrial cytochrome c release. *The Journal of biological chemistry* **277**, 3487-3497, doi:10.1074/jbc.M109360200 (2002).
196 Suryawanshi, A., Cao, Z., Thitiprasert, T., Zaidi, T. S. & Panjwani, N. Galectin-1-mediated suppression of Pseudomonas aeruginosa-induced corneal immunopathology. *Journal of immunology* **190**, 6397-6409, doi:10.4049/jimmunol.1203501 (2013).
197 Hsu, D. K., Zuberi, R. I. & Liu, F. T. Biochemical and biophysical characterization of human recombinant IgE-binding protein, an S-type animal lectin. *J Biol Chem* **267**, 14167-14174 (1992).
198 Levi, G. & Teichberg, V. I. Isolation and physicochemical characterization of electrolectin, a beta-D-galactoside binding lectin from the electric organ of Electrophorus electricus. *The Journal of biological chemistry* **256**, 5735-5740 (1981).
199 Cao, R. *et al.* Mouse corneal lymphangiogenesis model. *Nature protocols* **6**, 817-826, doi:10.1038/nprot.2011.359 (2011).
200 Rogers, M. S., Birsner, A. E. & D'Amato, R. J. The mouse cornea micropocket angiogenesis assay. *Nature protocols* **2**, 2545-2550, doi:10.1038/nprot.2007.368 (2007).
201 Cho, Y. K. *et al.* Vascular endothelial growth factor receptor 1 morpholino decreases angiogenesis in a murine corneal suture model. *Investigative ophthalmology & visual science* **53**, 685-692, doi:10.1167/iovs.11-8391 (2012).
202 Cursiefen, C. *et al.* Roles of thrombospondin-1 and -2 in regulating corneal and iris angiogenesis. *Investigative ophthalmology & visual science* **45**, 1117-1124 (2004).
203 Herzog, B. H. *et al.* Podoplanin maintains high endothelial venule integrity by interacting with platelet CLEC-2. *Nature* **502**, 105-109, doi:10.1038/nature12501 (2013).
204 Valenzuela, D. M. *et al.* High-throughput engineering of the mouse genome coupled with high-resolution expression analysis. *Nature biotechnology* **21**, 652-659, doi:10.1038/nbt822 (2003).
205 Tsuboi, Y. *et al.* Galectin-9 protects mice from the Shwartzman reaction by attracting prostaglandin E2-producing polymorphonuclear leukocytes. *Clinical immunology* **124**, 221-233, doi:10.1016/j.clim.2007.04.015 (2007).
206 Sehrawat, S. *et al.* Galectin-9/TIM-3 interaction regulates virus-specific primary and memory CD8 T cell response. *PLoS pathogens* **6**, e1000882, doi:10.1371/journal.ppat.1000882 (2010).
207 Oomizu, S. *et al.* Cell surface galectin-9 expressing Th cells regulate Th17 and Foxp3+ Treg development by galectin-9 secretion. *PloS one* **7**, e48574, doi:10.1371/journal.pone.0048574 (2012).
208 Fontenot, J. D., Gavin, M. A. & Rudensky, A. Y. Foxp3 programs the development and function of CD4+CD25+ regulatory T cells. *Nature immunology* **4**, 330-336, doi:10.1038/ni904 (2003).
209 Levy, A. P., Levy, N. S. & Goldberg, M. A. Post-transcriptional regulation of vascular endothelial growth factor by hypoxia. *The Journal of biological chemistry* **271**, 2746-2753 (1996).
210 Czyzyk-Krzeska, M. F., Dominski, Z., Kole, R. & Millhorn, D. E. Hypoxia stimulates binding of a cytoplasmic protein to a pyrimidine-rich sequence in the 3'-untranslated region of rat tyrosine hydroxylase mRNA. *The Journal of biological chemistry* **269**, 9940-9945 (1994).
211 McGary, E. C., Rondon, I. J. & Beckman, B. S. Post-transcriptional regulation of erythropoietin mRNA stability by erythropoietin mRNA-binding protein. *The Journal of biological chemistry* **272**, 8628-8634 (1997).

212 Shih, S. C. & Claffey, K. P. Hypoxia-mediated regulation of gene expression in mammalian cells. *International journal of experimental pathology* **79**, 347-357 (1998).
213 Chiariotti, L., Salvatore, P., Frunzio, R. & Bruni, C. B. Galectin genes: regulation of expression. *Glycoconj J* **19**, 441-449, doi:10.1023/B:GLYC.0000014073.23096.3a (2004).
214 Diskin, S. *et al.* Galectin-8 promotes cytoskeletal rearrangement in trabecular meshwork cells through activation of Rho signaling. *PloS one* **7**, e44400, doi:10.1371/journal.pone.0044400 (2012).
215 Lau, K. S. *et al.* Complex N-glycan number and degree of branching cooperate to regulate cell proliferation and differentiation. *Cell* **129**, 123-134, doi:10.1016/j.cell.2007.01.049 (2007).
216 Yang, R. Y., Hill, P. N., Hsu, D. K. & Liu, F. T. Role of the carboxyl-terminal lectin domain in self-association of galectin-3. *Biochemistry* **37**, 4086-4092, doi:10.1021/bi971409c (1998).
217 John, C. M., Leffler, H., Kahl-Knutsson, B., Svensson, I. & Jarvis, G. A. Truncated galectin-3 inhibits tumor growth and metastasis in orthotopic nude mouse model of human breast cancer. *Clinical cancer research : an official journal of the American Association for Cancer Research* **9**, 2374-2383 (2003).
218 Levy, Y. *et al.* It depends on the hinge: a structure-functional analysis of galectin-8, a tandem-repeat type lectin. *Glycobiology* **16**, 463-476, doi:10.1093/glycob/cwj097 (2006).
219 Deng, Y., Atri, D., Eichmann, A. & Simons, M. Endothelial ERK signaling controls lymphatic fate specification. *The Journal of clinical investigation* **123**, 1202-1215, doi:10.1172/JCI63034 (2013).
220 Zhou, F. *et al.* Akt/Protein kinase B is required for lymphatic network formation, remodeling, and valve development. *The American journal of pathology* **177**, 2124-2133, doi:10.2353/ajpath.2010.091301 (2010).
221 Garner, O. B. & Baum, L. G. Galectin-glycan lattices regulate cell-surface glycoprotein organization and signalling. *Biochemical Society transactions* **36**, 1472-1477, doi:10.1042/BST0361472 (2008).
222 Rabinovich, G. A., Toscano, M. A., Jackson, S. S. & Vasta, G. R. Functions of cell surface galectin-glycoprotein lattices. *Current opinion in structural biology* **17**, 513-520, doi:10.1016/j.sbi.2007.09.002 (2007).
223 Joukov, V. *et al.* Proteolytic processing regulates receptor specificity and activity of VEGF-C. *The EMBO journal* **16**, 3898-3911, doi:10.1093/emboj/16.13.3898 (1997).
224 Wirzenius, M. *et al.* Distinct vascular endothelial growth factor signals for lymphatic vessel enlargement and sprouting. *The Journal of experimental medicine* **204**, 1431-1440, doi:10.1084/jem.20062642 (2007).
225 Vlahakis, N. E., Young, B. A., Atakilit, A. & Sheppard, D. The lymphangiogenic vascular endothelial growth factors VEGF-C and -D are ligands for the integrin alpha9beta1. *The Journal of biological chemistry* **280**, 4544-4552, doi:10.1074/jbc.M412816200 (2005).
226 Favier, B. *et al.* Neuropilin-2 interacts with VEGFR-2 and VEGFR-3 and promotes human endothelial cell survival and migration. *Blood* **108**, 1243-1250, doi:10.1182/blood-2005-11-4447 (2006).
227 Karpanen, T. *et al.* Functional interaction of VEGF-C and VEGF-D with neuropilin receptors. *FASEB journal : official publication of the Federation of American Societies for Experimental Biology* **20**, 1462-1472, doi:10.1096/fj.05-5646com (2006).
228 Caunt, M. *et al.* Blocking neuropilin-2 function inhibits tumor cell metastasis. *Cancer cell* **13**, 331-342, doi:10.1016/j.ccr.2008.01.029 (2008).

229 Chen, J., Alexander, J. S. & Orr, A. W. Integrins and their extracellular matrix ligands in lymphangiogenesis and lymph node metastasis. *International journal of cell biology* **2012**, 853703, doi:10.1155/2012/853703 (2012).
230 Wang, J. F., Zhang, X. F. & Groopman, J. E. Stimulation of beta 1 integrin induces tyrosine phosphorylation of vascular endothelial growth factor receptor-3 and modulates cell migration. *The Journal of biological chemistry* **276**, 41950-41957, doi:10.1074/jbc.M101370200 (2001).
231 Zhang, X., Groopman, J. E. & Wang, J. F. Extracellular matrix regulates endothelial functions through interaction of VEGFR-3 and integrin alpha5beta1. *Journal of cellular physiology* **202**, 205-214, doi:10.1002/jcp.20106 (2005).
232 Liu, F. T. & Rabinovich, G. A. Galectins: regulators of acute and chronic inflammation. *Ann N Y Acad Sci* **1183**, 158-182, doi:10.1111/j.1749-6632.2009.05131.x (2010).
233 Janeway, C. A., Jr. Approaching the asymptote? Evolution and revolution in immunology. *Cold Spring Harbor symposia on quantitative biology* **54 Pt 1**, 1-13 (1989).
234 Matzinger, P. Tolerance, danger, and the extended family. *Annual review of immunology* **12**, 991-1045, doi:10.1146/annurev.iy.12.040194.005015 (1994).
235 Unlu, S. *et al.* Damage associated molecular pattern molecule-induced microRNAs (DAMPmiRs) in human peripheral blood mononuclear cells. *PloS one* **7**, e38899, doi:10.1371/journal.pone.0038899 (2012).
236 Sato, S., St-Pierre, C., Bhaumik, P. & Nieminen, J. Galectins in innate immunity: dual functions of host soluble beta-galactoside-binding lectins as damage-associated molecular patterns (DAMPs) and as receptors for pathogen-associated molecular patterns (PAMPs). *Immunological reviews* **230**, 172-187, doi:10.1111/j.1600-065X.2009.00790.x (2009).
237 Rajasagi, N. K. *et al.* Galectin-1 reduces the severity of herpes simplex virus-induced ocular immunopathological lesions. *Journal of immunology* **188**, 4631-4643, doi:10.4049/jimmunol.1103063 (2012).
238 Garin, M. I. *et al.* Galectin-1: a key effector of regulation mediated by CD4+CD25+ T cells. *Blood* **109**, 2058-2065, doi:10.1182/blood-2006-04-016451 (2007).
239 Rabinovich, G. A. & Gruppi, A. Galectins as immunoregulators during infectious processes: from microbial invasion to the resolution of the disease. *Parasite immunology* **27**, 103-114, doi:10.1111/j.1365-3024.2005.00749.x (2005).
240 Gupta, S. K., Masinick, S., Garrett, M. & Hazlett, L. D. Pseudomonas aeruginosa lipopolysaccharide binds galectin-3 and other human corneal epithelial proteins. *Infection and immunity* **65**, 2747-2753 (1997).
241 Reddy, P. B. *et al.* Influence of galectin-9/Tim-3 interaction on herpes simplex virus-1 latency. *Journal of immunology* **187**, 5745-5755, doi:10.4049/jimmunol.1102105 (2011).
242 Shimmura-Tomita, M. *et al.* Galectin-9-mediated protection from allo-specific T cells as a mechanism of immune privilege of corneal allografts. *PloS one* **8**, e63620, doi:10.1371/journal.pone.0063620 (2013).
243 Matsumoto, R. *et al.* Human ecalectin, a variant of human galectin-9, is a novel eosinophil chemoattractant produced by T lymphocytes. *The Journal of biological chemistry* **273**, 16976-16984 (1998).
244 Kashio, Y. *et al.* Galectin-9 induces apoptosis through the calcium-calpain-caspase-1 pathway. *Journal of immunology* **170**, 3631-3636 (2003).
245 Partridge, E. A. *et al.* Regulation of cytokine receptors by Golgi N-glycan processing and endocytosis. *Science* **306**, 120-124, doi:10.1126/science.1102109 (2004).

246 Saravanan, C., Liu, F. T., Gipson, I. K. & Panjwani, N. Galectin-3 promotes lamellipodia formation in epithelial cells by interacting with complex N-glycans on alpha3beta1 integrin. *Journal of cell science* **122**, 3684-3693, doi:10.1242/jcs.045674 (2009).
247 Seguin, L. *et al.* An integrin beta3-KRAS-RalB complex drives tumour stemness and resistance to EGFR inhibition. *Nature cell biology* **16**, 457-468, doi:10.1038/ncb2953 (2014).
248 Stillman, B. N. *et al.* Galectin-3 and galectin-1 bind distinct cell surface glycoprotein receptors to induce T cell death. *Journal of immunology* **176**, 778-789 (2006).
249 Schulz, M. M. *et al.* Phenotype-based high-content chemical library screening identifies statins as inhibitors of in vivo lymphangiogenesis. *Proc Natl Acad Sci U S A* **109**, E2665-2674, doi:10.1073/pnas.1206036109 (2012).
250 Reynolds, A. R. Potential relevance of bell-shaped and u-shaped dose-responses for the therapeutic targeting of angiogenesis in cancer. *Dose-response : a publication of International Hormesis Society* **8**, 253-284, doi:10.2203/dose-response.09-049.Reynolds (2009).
251 Hirabayashi, J. *et al.* Oligosaccharide specificity of galectins: a search by frontal affinity chromatography. *Biochim Biophys Acta* **1572**, 232-254 (2002).
252 Ahmad, N. *et al.* Galectin-3 precipitates as a pentamer with synthetic multivalent carbohydrates and forms heterogeneous cross-linked complexes. *J Biol Chem* **279**, 10841-10847, doi:10.1074/jbc.M312834200 (2004).
253 Brewer, C. F., Miceli, M. C. & Baum, L. G. Clusters, bundles, arrays and lattices: novel mechanisms for lectin-saccharide-mediated cellular interactions. *Curr Opin Struct Biol* **12**, 616-623 (2002).
254 Tvorogov, D. *et al.* Effective suppression of vascular network formation by combination of antibodies blocking VEGFR ligand binding and receptor dimerization. *Cancer cell* **18**, 630-640, doi:10.1016/j.ccr.2010.11.001 (2010).
255 Hood, J. D., Frausto, R., Kiosses, W. B., Schwartz, M. A. & Cheresh, D. A. Differential alphav integrin-mediated Ras-ERK signaling during two pathways of angiogenesis. *J Cell Biol* **162**, 933-943, doi:10.1083/jcb.200304105 (2003).
256 Galvagni, F. *et al.* Endothelial cell adhesion to the extracellular matrix induces c-Src-dependent VEGFR-3 phosphorylation without the activation of the receptor intrinsic kinase activity. *Circulation research* **106**, 1839-1848, doi:10.1161/CIRCRESAHA.109.206326 (2010).
257 Nieminen, J., Kuno, A., Hirabayashi, J. & Sato, S. Visualization of galectin-3 oligomerization on the surface of neutrophils and endothelial cells using fluorescence resonance energy transfer. *The Journal of biological chemistry* **282**, 1374-1383, doi:10.1074/jbc.M604506200 (2007).
258 Seguin, L. *et al.* An integrin beta-KRAS-RalB complex drives tumour stemness and resistance to EGFR inhibition. *Nat Cell Biol*, doi:10.1038/ncb2953 (2014).
259 Brunton, V. G., MacPherson, I. R. & Frame, M. C. Cell adhesion receptors, tyrosine kinases and actin modulators: a complex three-way circuitry. *Biochimica et biophysica acta* **1692**, 121-144, doi:10.1016/j.bbamcr.2004.04.010 (2004).
260 Kim, S. H., Turnbull, J. & Guimond, S. Extracellular matrix and cell signalling: the dynamic cooperation of integrin, proteoglycan and growth factor receptor. *The Journal of endocrinology* **209**, 139-151, doi:10.1530/JOE-10-0377 (2011).
261 Maruyama, K. *et al.* Inflammation-induced lymphangiogenesis in the cornea arises from CD11b-positive macrophages. *The Journal of clinical investigation* **115**, 2363-2372, doi:10.1172/JCI23874 (2005).

262 Kerjaschki, D. *et al.* Lymphatic endothelial progenitor cells contribute to de novo lymphangiogenesis in human renal transplants. *Nat Med* **12**, 230-234, doi:10.1038/nm1340 (2006).
263 Salven, P., Mustjoki, S., Alitalo, R., Alitalo, K. & Rafii, S. VEGFR-3 and CD133 identify a population of CD34+ lymphatic/vascular endothelial precursor cells. *Blood* **101**, 168-172, doi:10.1182/blood-2002-03-0755 (2003).
264 Kerjaschki, D. *et al.* Lymphatic neoangiogenesis in human kidney transplants is associated with immunologically active lymphocytic infiltrates. *J Am Soc Nephrol* **15**, 603-612 (2004).
265 Skobe, M. *et al.* Concurrent induction of lymphangiogenesis, angiogenesis, and macrophage recruitment by vascular endothelial growth factor-C in melanoma. *Am J Pathol* **159**, 893-903, doi:10.1016/S0002-9440(10)61765-8 (2001).
266 Zhang, B. *et al.* M2-polarized macrophages promote metastatic behavior of Lewis lung carcinoma cells by inducing vascular endothelial growth factor-C expression. *Clinics (Sao Paulo)* **67**, 901-906 (2012).
267 Mantovani, A. *et al.* The chemokine system in diverse forms of macrophage activation and polarization. *Trends Immunol* **25**, 677-686, doi:10.1016/j.it.2004.09.015 (2004).
268 Jetten, N. *et al.* Anti-inflammatory M2, but not pro-inflammatory M1 macrophages promote angiogenesis in vivo. *Angiogenesis* **17**, 109-118, doi:10.1007/s10456-013-9381-6 (2014).
269 Nakao, S. *et al.* VAP-1-mediated M2 macrophage infiltration underlies IL-1beta- but not VEGF-A-induced lymph- and angiogenesis. *Am J Pathol* **178**, 1913-1921, doi:10.1016/j.ajpath.2011.01.011 (2011).
270 Ostrand-Rosenberg, S., Sinha, P., Beury, D. W. & Clements, V. K. Cross-talk between myeloid-derived suppressor cells (MDSC), macrophages, and dendritic cells enhances tumor-induced immune suppression. *Semin Cancer Biol* **22**, 275-281, doi:10.1016/j.semcancer.2012.01.011 (2012).
271 Gabrilovich, D. I., Ostrand-Rosenberg, S. & Bronte, V. Coordinated regulation of myeloid cells by tumours. *Nat Rev Immunol* **12**, 253-268, doi:10.1038/nri3175 (2012).
272 Goyal, S. *et al.* Evidence of corneal lymphangiogenesis in dry eye disease: a potential link to adaptive immunity? *Archives of ophthalmology* **128**, 819-824, doi:10.1001/archophthalmol.2010.124 (2010).
273 Brorson, H., Ohlin, K., Olsson, G., Svensson, B. & Svensson, H. Controlled compression and liposuction treatment for lower extremity lymphedema. *Lymphology* **41**, 52-63 (2008).
274 Witte, M. H. *et al.* Lymphangiogenesis and hemangiogenesis: potential targets for therapy. *Journal of surgical oncology* **103**, 489-500, doi:10.1002/jso.21714 (2011).
275 Szuba, A. & Rockson, S. G. Lymphedema: classification, diagnosis and therapy. *Vascular medicine* **3**, 145-156 (1998).